ARCADIS

THE WATER INSTITUTE OF THE GULF

US Army Corps of Engineers ®
New Orleans District

CPRA
Coastal Protection and Restoration Authority of Louisiana

Hydrodynamic and Sediment Transport Modeling using *FLOW-3D* for Siting and Optimization of the LCA Medium Diversion at White Ditch

Technical Report

December 2013

Hydrodynamic and Sediment Transport Modeling using *FLOW-3D* for Siting and Optimization of the LCA Medium Diversion at White Ditch

Technical Report

Prepared for:
USACE, New Orleans District, and CPRA

Prepared by:
Hugh Roberts, P.E.,
John Richardson, Ph.D., P.E.,
Randy Lagumbay, Ph.D.
ARCADIS U.S., Inc.
4999 Pearl East Circle, Suite 200
Boulder, CO 80301

Ehab Meselhe, Ph.D., P.E.,
Yanxia Ma, Ph.D.
The Water Institute of the Gulf
301 N. Main Street, Suite 2000
Baton Rouge, LA 70825

Our Ref.:
NL500025.0000

Date:
December 2013

Tables

Figures

Appendix A

EXECUTIVE SUMMARY

The U.S. Army Corps of Engineers (USACE) New Orleans District (MVN) and the Coastal Protection and Restoration Authority (CPRA) of Louisiana are in the process of evaluating intake structure and outfall channel design alternatives for the LCA Medium Diversion at White Ditch. The diversion will deliver sediment to a receiving basin, contributing to the LCA systematic approach to coastal restoration. The project area extends south from Belair, Louisiana, to the Louisiana Coastline and extends east from the Mississippi River to Oak River (also known as River aux Chenes) in southeastern Louisiana.

The purpose of this study was to identify the most promising location for the diversion, evaluate the best alignment for the outfall channel, and investigate how variations in the structure's design could affect its ability to capture sediment. In these analyses, the location and design that maximized sediment concentrations in the outfall channel were considered to be the most favorable. This study focused on Lower Mississippi River hydraulics and sediment supply. Sediment distribution in the receiving delta, including delivery via the outfall channel, was addressed in a parallel study completed by the USACE Engineering Research and Development Center. Engineering design, cost estimation, and other factors critical to overall project decisions were completed by USACE MVN, CPRA, and other partners.

The following conclusions were reached based on the results of this study:

1. A diversion at Location 1 (River Mile 68.6 above Head of Passes) or Location 4 (River Mile 57.5) would capture the greatest amount of sediment, with Location 1 demonstrating the greatest project benefit;
2. Location 1 is positioned in a river bend where flow patterns carry sediment into the entrance of the diversion structure; and
3. At Location 1, particularly for larger material, Sediment Water Ratios (SWRs) are calculated to be greater than 1.0.

Based on these findings and discussions with the USACE, CPRA, and others, it was recommended that the diversion structure be positioned at Location 1 and that additional design improvements be considered in the final design of the structure. Location 1 was selected rather than Location 4 primarily due to considerations beyond those evaluated in this study, including cost considerations. Further, the outfall for Location 1 is positioned in the upper reaches of the receiving basin allowing for a greater chance to retain even fine size sediment material, thereby maximizing the land-building potential of the diversion.

The study was carried out using a comprehensive three-dimensional numerical model of the adjacent reach of the Mississippi River, the diversion structure, and the outfall channel. The model of choice is known as ***FLOW-3D***, which is a general purpose Computational Fluid Dynamics computer program designed especially for the simulation of combined free surface and closed conduit flow. Model studies were carried out in two steps. Steady-flow patterns were simulated and then the movement of sediment in the river and through the diversion was calculated. The model results of both steps were then used to compute a SWR or a ratio of sediment concentration passing through the diversion compared to a cross-sectional average sediment concentration in the adjacent reach of the Mississippi River. Sediment capture has been quantified in the form of SWRs for seven different size classes of particles ranging from clay to sand (2, 8, 32, 63, 96, 125, and 250 microns), as well as an aggregated value for all classes.

The model was calibrated and validated prior to being used to evaluate design alternatives. Flow conditions and sediment transport trends were calibrated and validated using Mississippi River observational data from events in 2009 and 2011. The calibration was performed using vessel-based Acoustic Doppler Current Profiler measurements from April 2009 when the flow rate of the Lower Mississippi River was approximately 700,000 cubic feet per second (cfs) at the measurement locations. The models were then validated against an independent dataset collected in March 2011, at a time that the Mississippi River discharge at Belle Chasse was

approximately 970,000 cfs. This field survey was selected because higher river flows could occur during diversion operation.

The design optimization portion of the study was completed in three phases. The first was the evaluation of design alternatives near Phoenix, Louisiana, which was the preferred site identified during the previously completed feasibility study. The diversion location near Phoenix is referred to as Location 3 in both the feasibility study and this study. Location 1 and Location 2 are up river from Phoenix, while Location 4 and Location 5 are down river. All simulations in the first design evaluation phase were completed using the ***FLOW-3D*** model developed as part of an earlier Myrtle Grove Diversion analysis.

The first suite of design optimization simulations evaluated the recommended diversion dimensions from the 2010 feasibility study. The feasibility recommended design consisted of a series of box culverts at an elevation of -16 feet North American Vertical Datum of 1988 (NAVD88), which were capable of passing 35,000 cfs at peak Lower Mississippi River flows and less than 35,000 cfs for lower river flows. In addition to the feasibility study proposed design, multiple design alternatives at Location 3 and the nearby Location 4 were evaluated in order to optimize the diversion SWR at the general location identified in the feasibility study. The conclusions of the first phase were that:

- Location 3 is positioned at the beginning of a river bend where secondary flow patterns that would carry sediment into the diversion are not present. This makes it difficult for the structure to capture sediment;
- A -16-foot NAVD88 sill elevation was not sufficiently deep to capture coarse materials and thus divert the necessary sediment load to meet the project land building targets at Location 3 and most likely other locations;
- A -40-foot NAVD88 sill elevation notably improved sediment capture;
- Flow separation occurs for the diversion geometry and alignment proposed by the feasibility study;

- Design modifications to the intake structure geometry can improve the performance of the diversion and resulting SWR, while reducing flow separation;
- Given the diversion has been evaluated to convey a maximum of 35,000 cfs during its operation period, it was recommended to divert 35,000 cfs for all river flow rates of 600,000 cfs and greater in order to maximize the sediment output from the diversion;
- Location 4 should be further evaluated because it is located on an established sandbar and the discharge basin is close by. Therefore, the length of the discharge channel could be minimized;
- Open channel diversion designs appear to render similar SWRs as box culvert designs; thus, in coordination with USACE cost estimations, the team determined that all designs moving forward would incorporate an open channel layout rather than box culverts due to cost and constructability considerations; and
- Locations for the diversion structure upstream and downstream of Location 3 should be considered, particularly to improve the sediment capture of coarse material.

A second phase of the diversion optimization analysis focused on the determination of optimal diversion locations ranging from Location 1 (River Mile 68.6 above Head of Passes) through Location 4 (River Mile 57.5) in the feasibility study. This phase required an extension to the model domain applied in the initial evaluation simulations in order to incorporate Location 1 and Location 2 in the study domain. The model was calibrated and validated using the same approach as the model developed by Meselhe et al. 2011. Following validation, simulations for Locations 1, 2, 2.5 (between Locations 2 and 3), 3, and 4 were completed using consistent model geometries. Diversion geometries were selected based on lessons learned during the first phase of the analysis. Each location was evaluated with an open channel diversion, a sill elevation of -40 feet NAVD88, and an effective width intended to divert approximately 35,000 cfs for a Mississippi River flow rate of 700,000 cfs.

In the final phase of the design optimization study, some additional analyses were carried out and used to identify design features that improve the ability to divert sediment from the Mississippi River. Diversion performance for various diversion elevations including -25, -30, and -40 feet NAVD88 was examined. The geometry of the leading (upstream) edge of the diversion was also examined to optimize the balance between SWRs and flow separation in the diversion entrance. Lastly, a sloped bottom from the diversion entrance into the river was considered, although the results were ultimately excluded from consideration due to maintenance and constructability concerns raised by USACE MVN. According to these results, the intake channel at Location 1 (29°45'40.59"N, 90°01'08.53"W) should be oriented at a 90-degree angle to the riverbank at an invert elevation of -40 feet NAVD88 with a flat bottom. An effective width of 72 feet (e.g., two tainter gates approximately 36 feet wide) and an approach channel length of 360 feet were considered. In addition to this, the leading edge of the entrance to the intake channel should be rounded to minimize flow separations and to reduce the likelihood of sedimentation in the channel during periods of time when the structure is not in operation.

These design recommendations represent the most favorable design configuration based on the analyses described within. Many of the analyses serve as lessons learned for diversion structure design optimization, which can be considered in future design iterations and adaptive management strategies.

1. INTRODUCTION

The U.S. Army Corps of Engineer (USACE) New Orleans District (MVN) and the Coastal Protection and Restoration Authority (CPRA) of Louisiana are in the process of designing a diversion intake structure and diversion outfall channel that will deliver sediment to a receiving basin. As shown in Figure 1-1, the project area extends south from Belair, Louisiana, to the Louisiana Coastline and extends east from the Mississippi River to Oak River (also known as River aux Chenes) in southeastern Louisiana. The area's hydrologic boundary includes the River aux Chenes sub-basin and nearby portions of the upper Breton Sound Basin.

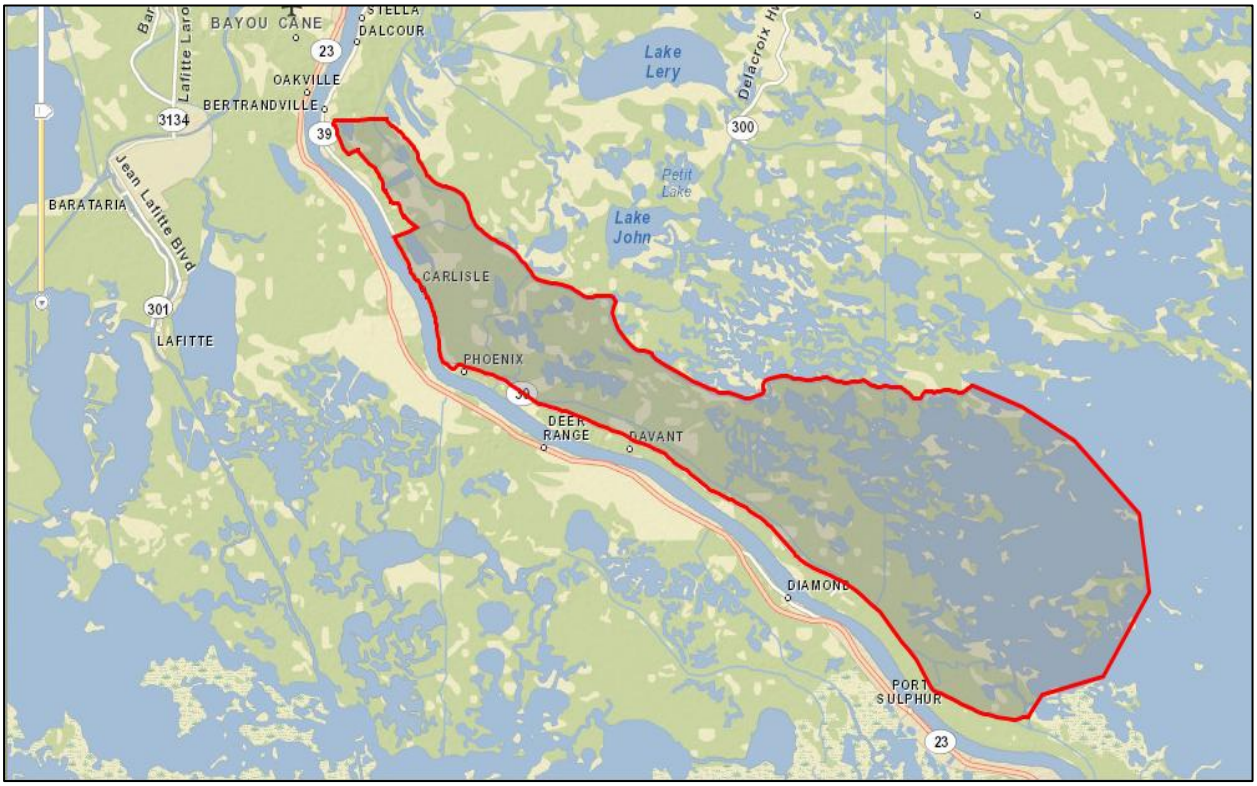

Figure 1-1. Project Area (adapted from www.lca.gov/Map/Map.aspx?ProjectID=9)

Tentative intake locations identified in the feasibility study are shown in Figure 1-2 (USACE and CPRA 2010). Of the five locations shown, the LCA Medium Diversion at White Ditch structure was recommended for construction at Location 3. Thus, the feasibility level design at Location 3 was used to produce baseline modeling results that served as the foundation for this work. The results from the baseline study provide a point of reference to further evaluate the performance of the diversion at Location 3 and other locations. Locations 1, 2, 3, and 4 and a site between Location 2 and Location 3 (referred to as Location 2.5) were evaluated in this analysis.

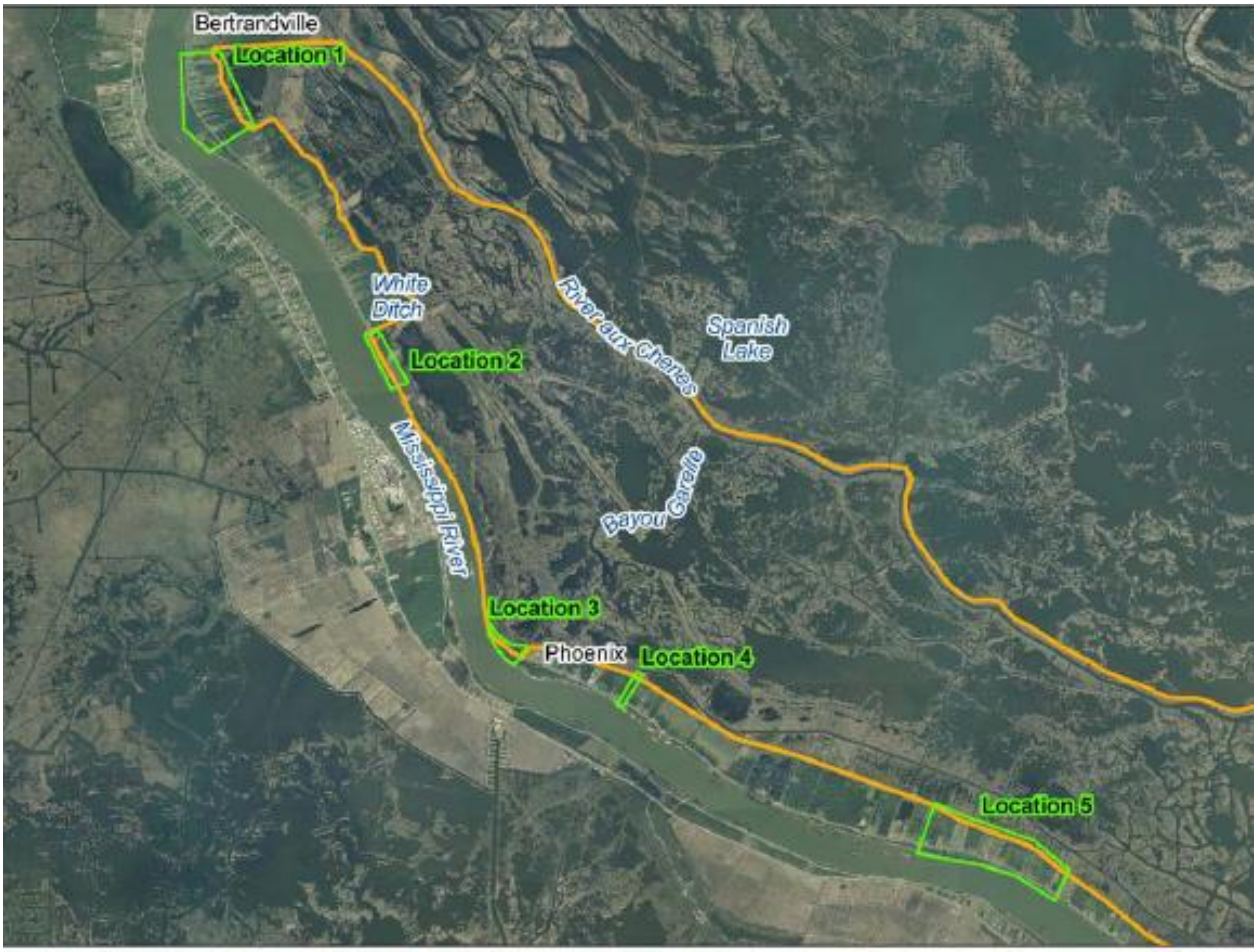

Figure 1-2. Sediment Intake Locations Identified in the Feasibility Study (adapted from LCA Ecosystem Restoration Study).

The domain of the numerical model used in this study includes a portion of the Mississippi River, the diversion intake structure, and the outfall channel (designed and supplied by the USACE). The design flow rate through the diversion structure is 35,000 cubic feet per second (cfs).

The numerical model was used to identify the most promising location for the diversion, evaluate the best alignment for the diversion, and investigate how variations in the structure's design could affect its ability to capture sediment. Model studies were carried out in two steps. Steady-flow patterns, for design conditions, were simulated and then the movement of sediment in the river and through the diversion was calculated. Using these data, the ratio between sediment concentrations entering the diversion and sediment concentrations in the river was computed. In these analyses, the location and design that maximized sediment concentrations in the outfall channel were considered to be the most favorable.

At the conclusion of the study, recommendations for the placement and optimum design of the structure were made. Location 1 is the recommended location, based on the relatively high total sediment water ratio for all sediment size classes (notably high sediment water ratios for coarse silts and sand). This location diverts water and sediment to the upper portion of the receiving basin allowing for a greater chance to retain even fine size sediment material, thereby maximizing land-building potential. Details are further discussed in Section 4.

2. APPROACH

A three-dimensional, Computational Fluid Dynamics (CFD), model was constructed and used to simulate flow and sediment transport in a portion of the Mississippi River. In its entirety, the completed model extends from River Mile (RM) 56, above the Head of Passes, to RM 76 at Belle Chasse.[1] The model was constructed within the framework of the commercially available CFD program known as ***FLOW-3D*** (Flow Science 2010). This program was selected for use because it is designed for the simulation of free surface and closed conduit flow (e.g., flow in the Mississippi River and through the proposed diversion structure), it has particle tracking capabilities (e.g., to simulate sediment movement), and the model produces results that can be easily compared to field observations.

FLOW-3D solves the Reynolds Averaged Navier-Stokes equations and uses various closure schemes to simulate the creation, transport, and dissipation of turbulent kinetic energy. The program also has the ability to calculate the movement of individual sediment particles that are carried by the flow. The governing equations of fluid motion are formulated using non-linear transient, second-order differential equations. The system of differential equations is solved numerically using algebraic expressions. Solutions to these equations provide numerical approximations of all flow variables within a staggered grid, and these numerical approximations approach their analytical values as the grid is refined. In this study several computations, each based on different grid resolutions, were carried out so that an appropriate level of refinement could be established (e.g., a level of grid refined that produced accurate results but was not overly demanding on available computer resources).

2.1 Hydrodynamics

The numerical algorithms in ***FLOW-3D*** are based on finite volume methods formulated within a structured mesh. Structured meshes are known for their computational efficiency, and the finite volume methods used in ***FLOW-3D*** are conservative because they are derived directly from the integral form of the conservation laws for fluid motion.

FLOW-3D is capable of simulating flow through complex geometries using a method called Fractional Area/Volume Obstacle Representation, or FAVOR (Hirt and Sicilian 1985). With FAVOR, complex shapes can be incorporated into a structured mesh without resorting to “stair stepping” and the resulting

[1] *NOTE:* Two different numerical models were used in this study: one that extended from RM 56 to RM 76: and one that covered a smaller portion of this distance. In the course of the analysis, the river model’s domain was made larger so that the operation of the diversion structure could be analyzed in some upstream locations.

computational scheme is accurate and efficient.[2] This is an essential feature because the river bottom is rippled, shallow bars exist, and bank boundaries are irregular.

For problems with a variable free surface, ***FLOW-3D*** uses the Volume of Fluid method (Hirt and Nichols 1981) to determine the location of fluid within the computational mesh. This technique consists of three parts: a scheme to describe the shape and location of the fluid surface; a method to track the movement of the fluid surface; and a means for applying boundary conditions at the fluid surface. In this analysis, the movement of air above the water was not computed; instead, it was assumed that the movement of air has no significant effect on the water's motion, and a condition of zero shear stress and constant pressure was applied at the fluid free surface. Neglecting the effect of air from analyses of this kind is a typical assumption and applicable to the solution of this problem (it is analogous to a condition with no wind).

A summary of the governing equations used in ***FLOW-3D*** appears below. For more details, the interested reader is referred to the ***FLOW-3D*** Users' Manual (Flow Science 2010).

Mass Continuity Equation:

$$V_F \frac{\partial \rho}{\partial t} + \frac{\partial}{\partial x}(\rho u A_x) + R\frac{\partial}{\partial y}(\rho v A_y) + \frac{\partial}{\partial z}(\rho w A_z) = R_{DIF} + R_{SOR} \qquad \textbf{Equation 2-1}$$

Momentum Equation:

$$\frac{\partial u}{\partial t} + \frac{1}{V_F}\left\{u A_x \frac{\partial u}{\partial x} + v A_y R\frac{\partial u}{\partial y} + w A_z \frac{\partial u}{\partial z}\right\} = -\frac{1}{\rho}\frac{\partial p}{\partial x} + G_x + f_x - b_x - \frac{R_{SOR}}{\rho V_F}(u - u_w - \delta u_s) \qquad \textbf{Equation 2-2a}$$

$$\frac{\partial v}{\partial t} + \frac{1}{V_F}\left\{u A_x \frac{\partial v}{\partial x} + v A_y R\frac{\partial v}{\partial y} + w A_z \frac{\partial v}{\partial z}\right\} = -\frac{1}{\rho}\frac{\partial p}{\partial y} + G_y + f_y - b_y - \frac{R_{SOR}}{\rho V_F}(v - v_w - \delta v_s) \qquad \textbf{Equation 2-2b}$$

$$\frac{\partial w}{\partial t} + \frac{1}{V_F}\left\{u A_x \frac{\partial w}{\partial x} + v A_y R\frac{\partial w}{\partial y} + w A_z \frac{\partial w}{\partial z}\right\} = -\frac{1}{\rho}\frac{\partial p}{\partial z} + G_z + f_z - b_z - \frac{R_{SOR}}{\rho V_F}(w - w_w - \delta w_s) \qquad \textbf{Equation 2-2c}$$

Where V_F is the fluid volume fraction, ρ is the fluid density, u, v, and w are velocities in the three primary directions (x, y, and z), R_{DIF} is a turbulent diffusion term, and R_{SOR} is a mass source; A_x, A_y, and A_z are the flow area fractions (at cell faces) in the x, y, and z directions, respectively. The terms (x, y, and z) for G are body accelerations, f are viscous accelerations, b are flow losses across porous media, and ρ is water density. The last term in the right-hand side of Equations 2-2a, 2-2b, and 2-2c is the mass injected into

[2] In ***FLOW-3D***, multiple mesh blocks can be used to construct continuous meshes through rangy areas and grid nesting can be used to resolve small-scale details. Both of these approaches were used to compute flow in the Mississippi River and to resolve details associated with the diversion's design.

the flow field through general moving objects, where u_w, v_w, and w_w are velocities of the source component, and u_s, v_s, and w_s are velocities of the fluid at the surface of the moving object, whereas δ defines the pressure type of the source.

A critical factor, determining the ability of a numerical model to simulate complex flow patterns, is the closure scheme used to simulate turbulence. ***FLOW-3D*** includes several turbulence closure schemes, namely Prandtl mixing length, one-equation transport, two-equation k-ε transport, Renormalized-Group (RNG) theory, and Large Eddy Simulation.

Within the framework of ***FLOW-3D,*** turbulent kinetic energy is defined as follows:

$$k_T = \frac{1}{2}\left(\overline{u'^2} + \overline{v'^2} + \overline{w'^2}\right) \qquad \textbf{Equation 2-3}$$

where ***u', v', w'*** are turbulent fluctuations in the ***x, y, z*** directions. Two-equation turbulent closure schemes are widely used due to their relative computational efficiency and adequate performance for a wide-range of practical applications. The transport equations for turbulent kinetic energy and its dissipation are expressed below (Harlow and Nakayama 1967):

$$\frac{\partial k_T}{\partial t} + \frac{1}{V_F}\left\{uA_x\frac{\partial k_T}{\partial x} + vA_yR\frac{\partial k_T}{\partial y} + wA_z\frac{\partial k_T}{\partial z}\right\} = P_T + G_T + Diff_{k_T} - \varepsilon_T \qquad \textbf{Equation 2-4}$$

$$\frac{\partial \epsilon_T}{\partial t} + \frac{1}{V_F}\left\{uA_x\frac{\partial \epsilon_T}{\partial x} + vA_yR\frac{\partial \epsilon_T}{\partial y} + wA_z\frac{\partial \epsilon_T}{\partial z}\right\} = \frac{CDIS1\cdot\varepsilon_T}{k_T}(P_T + CDIS3\cdot G_T) + Diff_\varepsilon - CDIS2\frac{\varepsilon_T^2}{k_T} \qquad \textbf{Equation 2-5}$$

Where P_T is the turbulent kinetic energy production, G_T is the buoyancy production term, ***Diff*** is the diffusion term, and ***CDIS1***, ***CDIS2,*** and ***CDIS3*** are dimensionless calibration parameters.

In this study, the RNG method (Yakhot and Orszag 1986; Yakhot and Smith 1992) was used for turbulent closure. The RNG model applies statistical methods to the derivation of turbulent kinetic energy and its dissipation rate. The main difference between the RNG method and the standard *k*-ε model is that the constants (appearing in the governing equations of the turbulence model) are found empirically in the *k*-ε model whereas they are derived explicitly in the RNG model. The RNG approach appears to have wider applicability than the standard k-ε model, and the RNG model is more adequate for riverine applications where strong shear regions may be present.

2.2 Sediment Transport

FLOW-3D can be used to simulate sediment transport using Lagrangian particle tracking. With this approach the movement of each particle is considered individually, particles are released at the upstream

end of the model, and their trajectories are calculated. Particle transport is governed by advection and diffusion with a diffusion coefficient of $D = k\mu + \text{NUP}$ (where: μ is mass diffusivity; *k* is the Schmidt number; and NUP is a particle diffusion coefficient). If NUP is non-zero, then each particle is given an additional increment in position. The underlying theory is briefly described below.

After being released, particles diffuse in all directions forming a cloud, within which the particle distribution is similar to a Gaussian distribution in each direction. Inside the cloud, however, each particle remains a discrete entity in the numerical simulation. The new position of a particle is determined from calculated flow patterns, and the local diffusion of each particle is then computed using a Monte Carlo technique where three random numbers are selected for each particle and then used to compute random shifts in each of the three coordinate directions.

The fundamental equation used to model mass particles is shown below:

$$\frac{d\boldsymbol{u}_p}{dt} = -\frac{1}{\rho_p}\nabla P + \boldsymbol{g} + + \alpha(\boldsymbol{u} - \boldsymbol{u}') + \beta(\boldsymbol{u} - \boldsymbol{u}')|\boldsymbol{u} - \boldsymbol{u}'| \cdot \frac{\rho}{\rho_p}. \qquad \textbf{Equation 2-6}$$

Where ρ and ρ_p are fluid and particle density, respectively; g is gravity; *u* and *P* are fluid velocity and pressure, respectively; α and *β* are the drag coefficients divided by the particle's mass; $u' = u_p + u_{diff}$, in which u_p and u_{diff} are the particle mean velocity and diffusion velocity, respectively. u_{diff} is evaluated according to the Monte Carlo technique mentioned above.

In this analysis, particle transport was calculated for material in seven different size classes ranging from 2 to 250 microns in size. Each of the seven sediment classes included material made up from a range of sizes, which are listed in Table 2-1. This approach is capable of estimating the spatial distribution of sediments in the model domain, by tracking the movement individual mass particles as they move.

Table 2-1. Sediment Size Class and Size Range

Sediment Classification (microns)	Size Range in Computations (microns)	Descriptor
2	1 - 3	Clay
8	4 - 15	Silt
32	16 - 63	Silt
64	64 - 78	Very Fine Sand
96	79 - 113	Very Fine Sand
125	114 - 187	Very Fine / Fine Sand
250	188 - 250	Fine Sand

Sediment/fluid interaction is also considered in ***FLOW-3D*** – the two primary interaction mechanisms between suspended sediment and the surrounding fluid being momentum exchange and volume displacement. In this project, assuming that sediment concentrations were relatively small, the volume displacement and the effect of particles on the fluid flow were ignored. The impact of fluid flow on the particles motion was, however, reflected by a drag force. For a spherical particle, the drag coefficient is given by an empirical relation:

$$C_D = \frac{4d}{3}\beta = (\frac{24}{Re} + \frac{6}{1+\sqrt{Re}} + 0.4). \qquad \textbf{Equation 2-7}$$

Where Re is the Reynolds number with an expression of $Re = d \cdot \rho \cdot U/\mu$, in which d is the particle diameter, $U = |u - u'|$; β is a Reynolds number dependent drag coefficient.

For applications where the relative difference between particle density and fluid density is not large, as is the case with sediment and water in this project, it is important to calculate the drag resistance of the particles as they move through the fluid. The total loss of momentum by this mechanism, however, is too small to be transferred back to the fluid. As such, it is possible and desirable to compute fluid motion and then use the flow field to move the particles.

2.3 Model Domain and Setup

During the course of this study, two model domains were used. The first model domain was identical to that used in the Myrtle Grove Diversion study conducted by Meselhe et al. (2011). This domain is referred to as the initial domain throughout this report. The initial domain extends from RM 56.0 to RM 62.7. All river miles referenced are relative to the Head of Passes. As shown in Figure 2-1, this area has been surveyed using high-resolution multi-beam techniques (Allison 2011). The initial domain includes potential sediment diversion sites at Location 3 and Location 4. This domain was initially used in this study due to the availability of a previously calibrated and validated model in the area from the 2011 Myrtle Grove analysis. Additionally, at the outset of the project, Location 3 was the primary location of concern, thus a larger domain was not required.

A single mesh block was used to define the computational domain. A grid resolution of 330 feet (horizontal) and 8 feet (vertical) was initially used to establish a general flow field for modeled discharges. Then, the grid was successively refined to resolve flow features of interest (e.g., recirculating flow patterns) in the river. The grid was further refined to approximately 164 feet (horizontal) and 8 feet (vertical) down to a final grid of 50 feet (horizontal) and 8 feet (vertical) to capture details of the complex flow pattern observed in the field data.

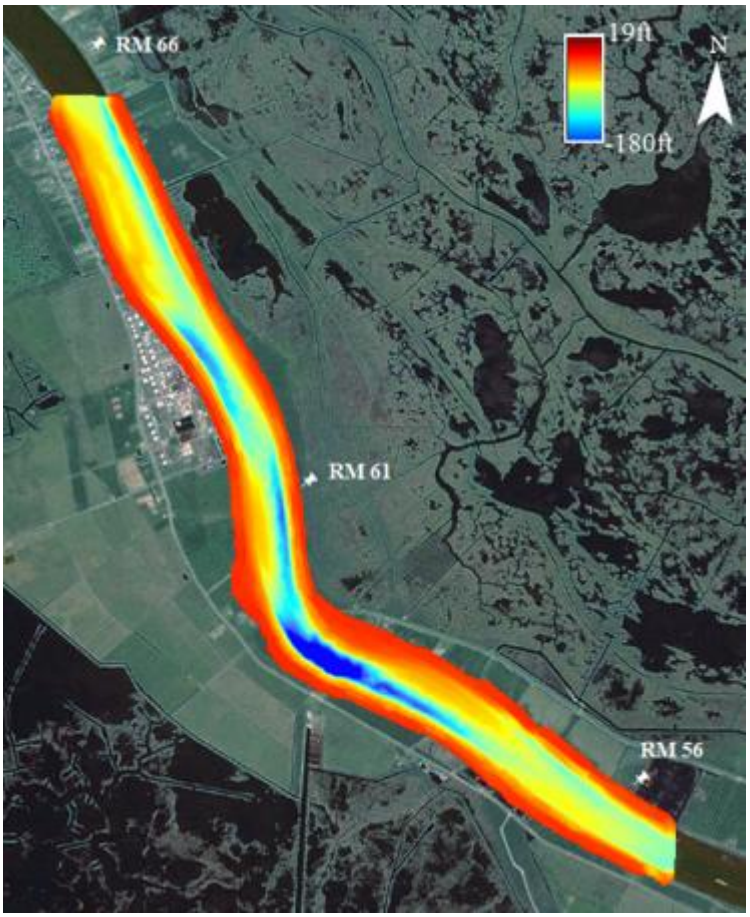

Figure 2-1. The Initial FLOW-3D Model Domain and River Bathymetry (multi beam). The domain extends from RM 56 above the Head of Passes to RM 62.7.

As the project evolved, the modeling team, in coordination with the USACE and CPRA, determined that it was necessary to study the operation of the diversion at other locations, which were located beyond the upstream boundary of the initial model domain. These locations are referred to as Locations 1, 2, and 2.5 (Location 1 and Location 2 are shown in Figure 1-2, and Location 2.5 was positioned about half-way between Locations 2 and 3, along a narrow sand bar).

A revised model, referred to as the extended domain model, was developed so that the operation of the diversion structure at Locations 1, 2, and 2.5 could be simulated. This model extends from RM 56, above the Head of Passes, to RM 76 at Belle Chasse. Because multi-beam data were not available for the entire reach, the single beam survey from 2003 completed by the USACE was used throughout to ensure consistency in survey approach, datum, and data processing. Figure 2-2 shows the extended model domain as well as the river bathymetry. This domain was selected because the upstream boundary is far removed from the northernmost study location (Location 1). The model's setup also permits the flow and particle transport to fully develop before reaching the proposed diversion locations.

Figure 2-2. **The Extended *FLOW-3D* Model Domain and River Bathymetry (single beam). The domain extends from RM 56 above the Head of Passes to RM 76 at Belle Chasse. Pushpin markers represent every 5 RM from the upstream model domain.**

Similar to the initial domain, a coarse grid resolution of 330 feet (horizontal) and 8 feet (vertical) was used to establish a general flow field for the observed water discharges. Once a model simulation had reached steady state, the grid resolution was gradually refined to 82 feet (horizontal) and 8 feet (vertical) throughout the entire domain. Finally, the model grid was further refined to 16.4 feet (horizontal) and 3.3 feet (vertical) locally around the Myrtle Grove meander bend. The refined area extends from RM 56 to RM 62, covering almost the entire initial model domain. This strategy was designed to resolve the complicated river circulation (especially at river meanders) and to capture the complex geometry of the diversion structure.

The following sections describe the calibration and validation of the extended model domain. In these sections, coarse (whole domain) and refined (local domain) grids refer to resolutions of 82 feet (horizontal) and 8 feet (vertical) and 16.4 feet (horizontal) and 3.3 feet (vertical), respectively.

3. CALIBRATION AND VALIDATION

Model calibration and validation were completed for both the initial model domain and extended model domain. As discussed later, final simulations comparing performance at all locations as well as optimization studies at Location 1 were carried out using the extended domain model. Additionally, the calibration and validation of the initial model domain are documented as part of the Myrtle Grove diversion project (Meselhe et al 2011), which covers the same river reach as the initial White Ditch model domain. In order to focus on the calibration and validation details most pertinent to the analysis, this section summarizes the calibration and validation of the initial domain and describes and quantifies the extended model calibration and validation in greater detail. The summary of the initial domain calibration and validation is intended to supply background information on previous analyses with the model and to outline the approach used in the extended domain analysis.

The calibration of both models was performed using vessel-based Acoustic Doppler Current Profiler (ADCP) measurements from April 2009 (these data were collected by Allison [2011] and are previously discussed by Meselhe et al. [2011]). In April 2009, the flow rate of the Lower Mississippi River was approximately 700,000 cfs at the measurement locations. Measurement locations for velocities and sediment concentrations for the April 2009 event are shown in Figure 3-1 and Figure 3-2, respectively.

The models were validated against an independent dataset collected in March 2011. At this time, the Mississippi River discharge at Belle Chasse was approximately 970,000 cfs. This field survey was selected because higher river flows, such as this, could occur during when the diversion is operating.

The March 2011 dataset includes ADCP velocity and suspended sediment measurements as shown in Figure 3-3 and Figure 3-4, respectively. Because the field survey was only conducted at MGup (ref. Figures 3-3 and 3-4), comparisons with observations were limited to that location. During the validation, no adjustments to any of the parameters discussed in the calibration section were made.

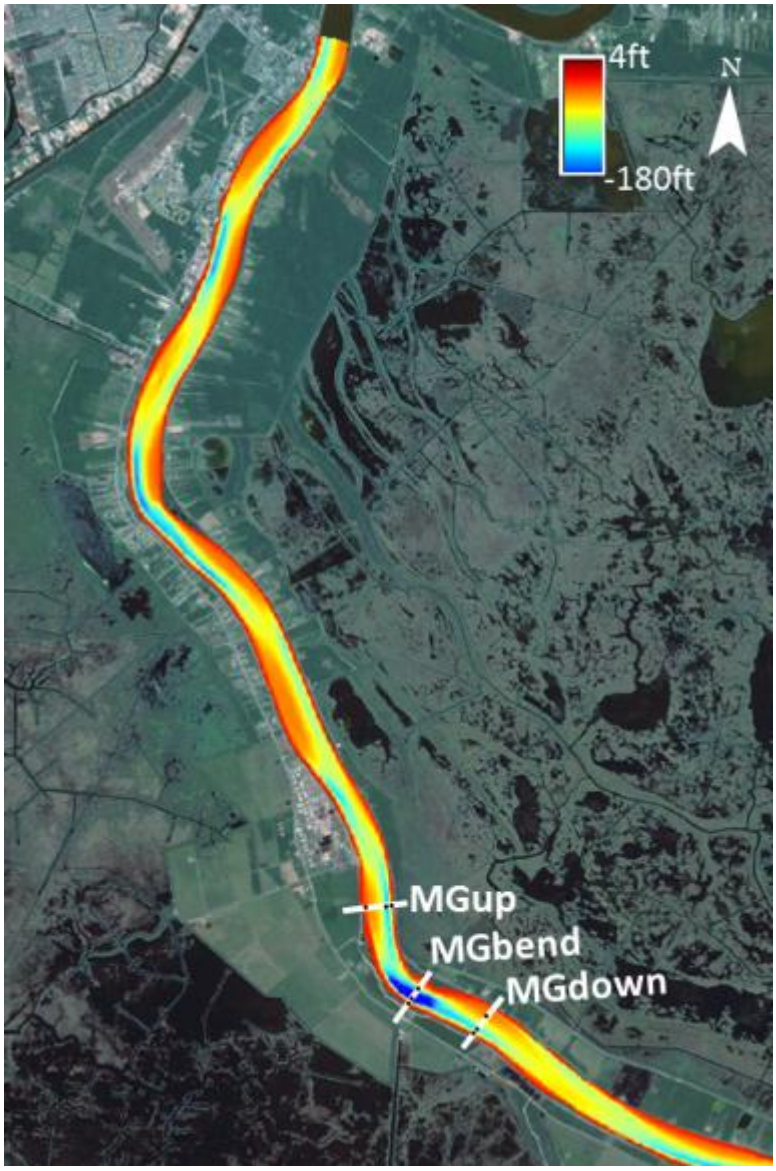

Figure 3-1. **Model Calibration Locations for Velocity Field during April 2009.**

White lines indicate locations of depth-averaged velocity transects. Black dots along each transect indicate locations of vertical velocity profiles. From west to east bank, the three locations are referred to as RDB, Thalweg, and LDB.

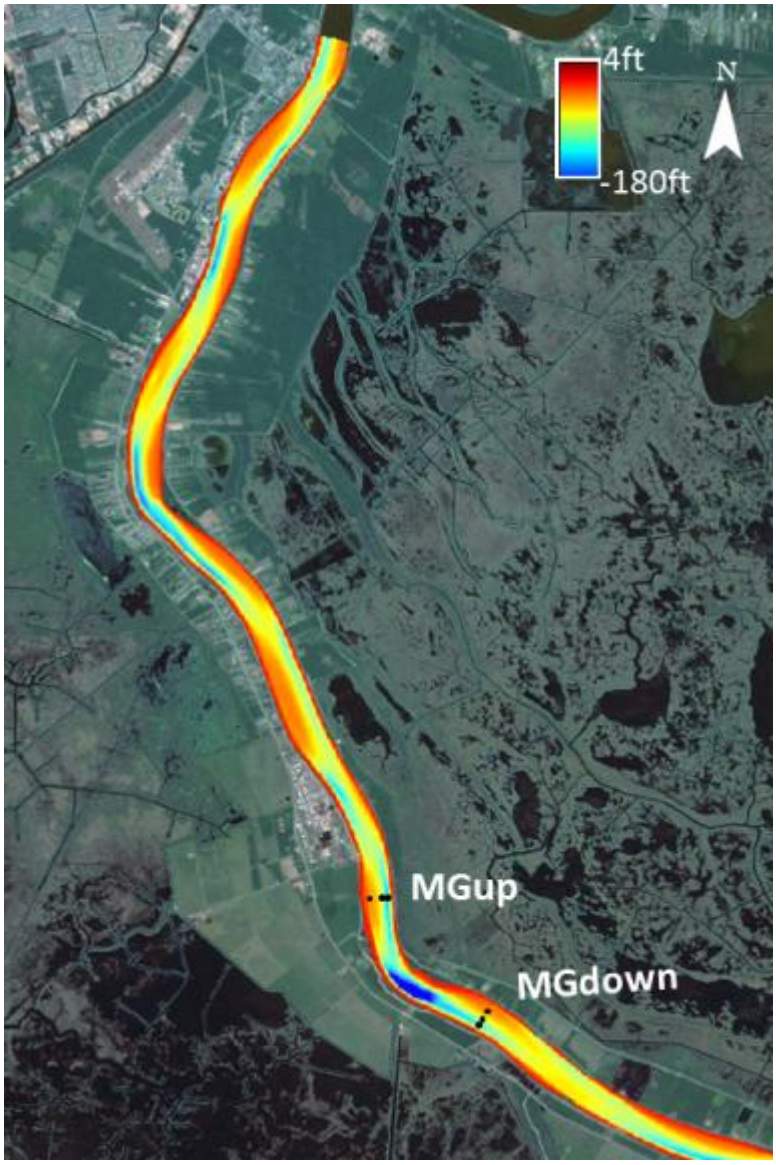

Figure 3-2. **Model Calibration Locations for Suspended Concentrations during April 2009. From west to east bank, three dots represent RDB, middle, and LDB (black dots).**

Figure 3-3. **Model Validation Locations for Velocity Field during March 2011.**

White lines indicate locations of depth-averaged velocity transects. Black dots along each transect indicate locations of vertical velocity profiles. From west to east bank, the three locations are referred to as RDB, Thalweg, and LDB.

Figure 3-4. Model Validation Locations for Suspended Concentrations during March 2011. From west to east bank, three dots represent RDB, middle, and LDB (black dots).

3.1 Initial Domain Model Calibration and Validation

3.1.1 Initial Domain Hydrodynamics Calibration

Boundary roughness, associated with the resistance of riverbanks and bed form, is a critical parameter in the hydrodynamic calculations carried out by ***FLOW-3D***. Boundary roughness is typically caused by form drag and skin friction. Form drag is associated with bed forms such as sand ripples and dunes, which are imbedded in river bathymetry. Skin friction is approached by using a wall function in ***FLOW-3D***. The wall

roughness coefficient in ***FLOW-3D*** is used as a calibration parameter (Flow Science 2010). For a water flow of 700,000 cfs, as modeled for the April 2009 event, a wall roughness value of 0.06 provided a head drop of 0.7 foot across the length of the river reach within the initial mode domain (RM 62.7 to RM 56). This value was successfully used and calibrated in the Myrtle Grove diversion project (Meselhe et al. 2011), which covers the same river reach as the White Ditch diversion project initial domain.

Once appropriate water surface elevations were calculated, the model's ability to reproduce circulation patterns or features within the river was evaluated based on velocity profiles measured with the ADCP (Allison 2011). These features are re-circulation eddies, near the inside of the meander bend, and secondary circulation, typically along the meander. At the river bend, immediately downstream of Location 3, approximately RM 59.5, a cross-section of the surface velocity profile was extracted from ***FLOW-3D***. It shows downstream river flow speeds reaching as high as 5 feet per second (ft/s) at the location of deepest river depth. This flow speed decreased gradually toward the bank lines on both sides of the cross section. However, near the left descending bank (inside the bend), a flow reversal occurs. The same feature was captured by the ADCP (Allison 2011) and documented in Meselhe et al. (2011). To evaluate the model's ability to capture the spatial variations, both horizontal and vertical velocity profiles were extracted and compared to the ADCP measurements. Figure 3-1 shows field measurements located upstream of the meander in the vicinity of a point bar (MGup); near the meander in the vicinity of a deep hole (MGbend); and downstream of the meander and the deep hole (MGdown), as described in Allison (2011) and Meselhe et al. (2011). With the observer looking downstream, velocity vectors at these three locations all exhibited fully developed clockwise eddies (e.g., secondary circulation).

Velocity calibration was performed at the MGup and MGdown locations shown in Figure 3-1. At each location, a near-surface horizontal transect (7-foot depth) as well as vertical velocity magnitudes were compared using output from ***FLOW-3D*** and the ADCP measurements performed from April 4 through April 9, 2009. At MGup, model results compared well with field measurements, with a maximum velocity of 5 ft/s occurring in the middle of the river channel near the water surface. At MGdown, there was a relatively large scatter in the field observations. This can be attributed to the high level of turbulence and secondary motion resulting from the deep hole in the outside bend of the channel and the bend curvature. Overall, considering the standard error resulting from fluctuations in the measured data, the model results and field data compared well.

3.1.2 Initial Domain Sediment Calibration

In ***FLOW-3D***, particles are treated individually and are weakly coupled to the flow. Particles and flow interact with each other through momentum exchange. Thus, the model produces a realistic representation of the particle density and spatial distribution, especially in regions with a complex flow field. The process used to convert the spatial distribution of discrete mass particles into sediment concentration has been reviewed in Meselhe et al. (2011) and is quoted below.

For a given number of particles in the domain (P_n), among a number of size classes (m), the sediment reference concentration within the domain is a function of the total volume of particles (V_p) and the particle density such that

$$C^m{}_{ref} = P_n V_p \rho_p \qquad \textbf{Equation 3-1}$$

Where $C^m{}_{ref}$ is the reference concentration for a number of size classes (m), P_n is the number of particles, V_p is the volume of particles, and ρ_p is the particle density. To obtain the reference sand concentration, $C^s{}_{ref}$, Equation 3-2 has been used for m classes of sand size particles.

$$C_{ref}{}^s = \sum_{i=1}^{m} (C_{ref}) \qquad \textbf{Equation 3-2}$$

Hence, the normalized concentration is

$$Cs = \frac{C_{ref}}{V_w} = X \qquad \textbf{Equation 3-3}$$

Where C_s is the sand concentration, C_{ref} is the reference concentration, and V_w is the domain water volume. The term X is used to derive a conversion factor to transform the model output into concentration directly.

The final conversion factor is proportional to the measured sediment load in the flow event under consideration. As such, because the sediment load and total water flow have been measured for the calibration and validation events used here, the term X can be easily calculated. The sediment load was calculated based on the detailed isokinetic measurements at MGup. A cross-section and depth averaged concentration for each size class observed in the isokinetic samples was estimated for each grain size fraction using laboratory techniques.

For the sediment load used in the calibration, X is equal to 56.7. It is largely derived by a conversion of the total sediment load to the model domain from metric tons per day to milligrams per liter. Following

these steps, the resulting conversion factor is then used to convert the model-derived particle density to a sediment concentration. The ***FLOW-3D*** code was modified by Meselhe et al. (2011) to complete this computation.

In the initial domain model used in this analysis, particles are released at the upstream boundary into a steady-state flow field. The Lagrangian particle tracking method, used to predict sediment transport, makes use of a diffusion coefficient (*D*), which is often used to simulate the dispersive nature of individual particles in natural systems. Considered to be a calibration parameter, an appropriate value for this coefficient was chosen so that a good agreement between model output and observed data was produced. A value of 0.05 was obtained during calibration by Meselhe et al. (2011) for the same model domain and flow conditions as in this project. Therefore, the same value was applied here for particle class sizes 32 microns and greater. For particles in size classes 2 and 8 microns, selection of the diffusion coefficient was not as important because very small particles, such as these, tend to be well distributed in the water column and their movement is governed primarily by the movement of the water (e.g., the movement of particles in this size range tends to be dominated by the movement of the carrying fluid). As such, additional diffusion of particles in these smaller size classes was not modeled.

Particle interaction with the river bed (*i.e.,* deposition and erosion) was handled through a coefficient of restitution. In these calculations, the coefficient value was set to 1.0 so that the momentum of particles calculated to hit bottom was conserved. Visually, these particles would appear to saltate. They would come to rest in locations where flow speeds were negligible, and they would be suspended in more vigorous flows. This ad hoc way to handle erosion and deposition is not strictly correct. However, the method provided good agreement with available field data (ref. sections 3.2.3 and 3.2.5) and was easy to implement. In the future, this approach to sediment deposition and erosion could be refined if desired.[3]

The model was validated against an independent dataset collected in March 2011. The dataset included suspended sediment and ADCP velocity measurements as shown in Figure 3-3 and Figure 3-4.

3.1.3 Initial Domain Hydrodynamics Validation

During the March 2011 survey, vessel-based ADCP measurements were made at MGup. For comparison with field measurements, a horizontal velocity profile near the water surface and vertical velocity profiles throughout the water column at three locations at the MGup transect were extracted from

[3] This would, however, require the collection of additional field data.

FLOW-3D model results. The vertical velocity profiles output from the model exhibited the typical exponential shape versus depth (similar to the ADCP measurements). Compared to the field observations, the model output for the vertical profiles tended to (1) slightly underestimate the near-bed velocity; (2) agree very well in the middle of the water column; and (3) slightly overestimate the velocities near the water surface. For the horizontal velocity profile, the model results generally followed the same trend as the observations. Model velocities agreed well with field observations in the shallow water area near the inside bank, but the model overestimated flow speeds in the deep water near the right descending bank. Overall, modeled velocity profiles matched the field ADCP measurements. The standard deviation between modeling results and observations ranged from 0.6 to 1.3 ft/s, which is not significant compared to the velocity range of 0 to 6.6 ft/s.

3.1.4 Initial Domain Sediment Validation

The field survey in March 2011 included measurements of vertical sand concentration at three locations along MGup (Allison 2011). Sand concentration profiles at the same locations were extracted from ***FLOW-3D***. The model's ability to reproduce observed concentrations appears satisfactory, with good agreement throughout 90 percent of the water column at all three sites. Small disagreement occurred at two of the vertical casts at the 30 percent depth. This is potentially due to a higher uncertainty in the field observations, as shown by a sudden increase in sand concentration at the 30 percent depth. It is important to mention that there are no duplicates of isokinetic sampling or multiple samples at any locations; therefore, it is difficult to assess the field uncertainty. However, according to Allison (2011), the expected uncertainty is proportional to the river turbulence, flow depth, and other parameters and can be on the order of 5 percent to 10 percent of the measured concentrations near the surface and as much as 50 percent of the measured concentration near the bed at high discharges.

3.2 Extended Domain Model Calibration and Validation

The extended domain model was calibrated using the same data and approach as was used with the initial domain model. Details of revised boundary conditions, hydrodynamic calibration, and sediment calibration are provided below.

3.2.1 Extended Domain Boundary Conditions

The discharge and tail water elevation for the April 2009 event were used as upstream and downstream boundary conditions, respectively. The discharge during the April 2009 survey period was equal to 700,000 cfs; hence, this value was used for the upstream boundary at RM 76. Unfortunately, there were no tailwater data available at the downstream end of the model domain. As a result, numerical

simulations from HEC-RAS (Davis 2010) were used to estimate the tailwater elevation, and measurements at the Conoco-Phillips station (RM 63.2) were used for confirmation. The value obtained was 6.2 feet referenced to the North American Vertical Datum of 1988 (NAVD88; Meselhe et al. 2011).

For model validation, field data from March 31 to April 1, 2011, were used. During this period of time the river discharge was equal to about approximately 970,000 cfs. The tailwater at the downstream boundary was estimated using the same method mentioned above, and the value was 7 feet NAVD88.

3.2.2 Extended Domain Hydrodynamics Calibration

As discussed in Section 2.1, the RNG model was used for turbulence closure. With this scheme, surface roughness is incorporated through boundary conditions and used to determine turbulence quantities, such as turbulent kinetic energy and its rate of dissipation. A wall roughness coefficient of 0.6 was selected based on previous numerical experimentations (Meselhe et al. 2011) and the results of the initial domain model calibration. For a river flow of 700,000 cfs, this roughness provided a water stage of 7.8 feet NAVD88 at Belle Chasse, which is consistent with recorded data ranging from 7 to 8 feet by the U.S. Geological Survey.[4]

The field dataset used for the extended model calibration was the same as that used for the local model calibration. The field events were conducted in April 2009 (Allison 2011). Three locations: MGup, MGbend, and MGdown were selected. At each location, one depth-averaged velocity, horizontal, profile (Figure 3-1, white lines), and three vertical velocity profiles (Figure 3-1, black dots) were used for model calibration. From the right-descending riverbank to the left-descending riverbank, the three profiles are labeled as right-descending bank (RDB), mid-thalweg (Thalweg), and left-descending bank (LDB). Numerical results for MGup and MGdown were extracted from the model results with a coarse grid resolution of 82 feet (horizontal) and 8 feet (vertical). In the case of MGbend, a locally refined grid of 16.4 feet (horizontal) and 3.3 feet (vertical) was used to capture strong re-circulation eddies and secondary circulation patterns. Panels (a) and (c) in Figure 3-5 show bank-to-bank transects of depth-averaged velocity for MGup and MGdown. In each transect, red dots indicate field measurements; the black line shows the ***FLOW-3D*** model results; and the three vertical lines correspond to the locations of vertical velocity profiles. Depth-averaged flow speed velocities are faster in the deep area, reaching 5 ft/s, and are slower in the shallow areas close to the sand bars (RDB at MGup; LDB at MGdown). From these results, it is apparent that, even with the coarse grid, the model reproduced overall flow patterns at MGup and MGdown that are in good agreement with the observed data. Panel b in Figure 3-5 shows the

[4] http://waterdata.usgs.gov/usa/nwis/uv?07374525

velocity calibration at MGbend. With the coarse grid (black line), the modeled velocities are in good agreement with observations at the outside of the meander, but they disagree on the inside, where strong re-circulation occurs. The locally refined grid produced better results, as shown by the blue line.

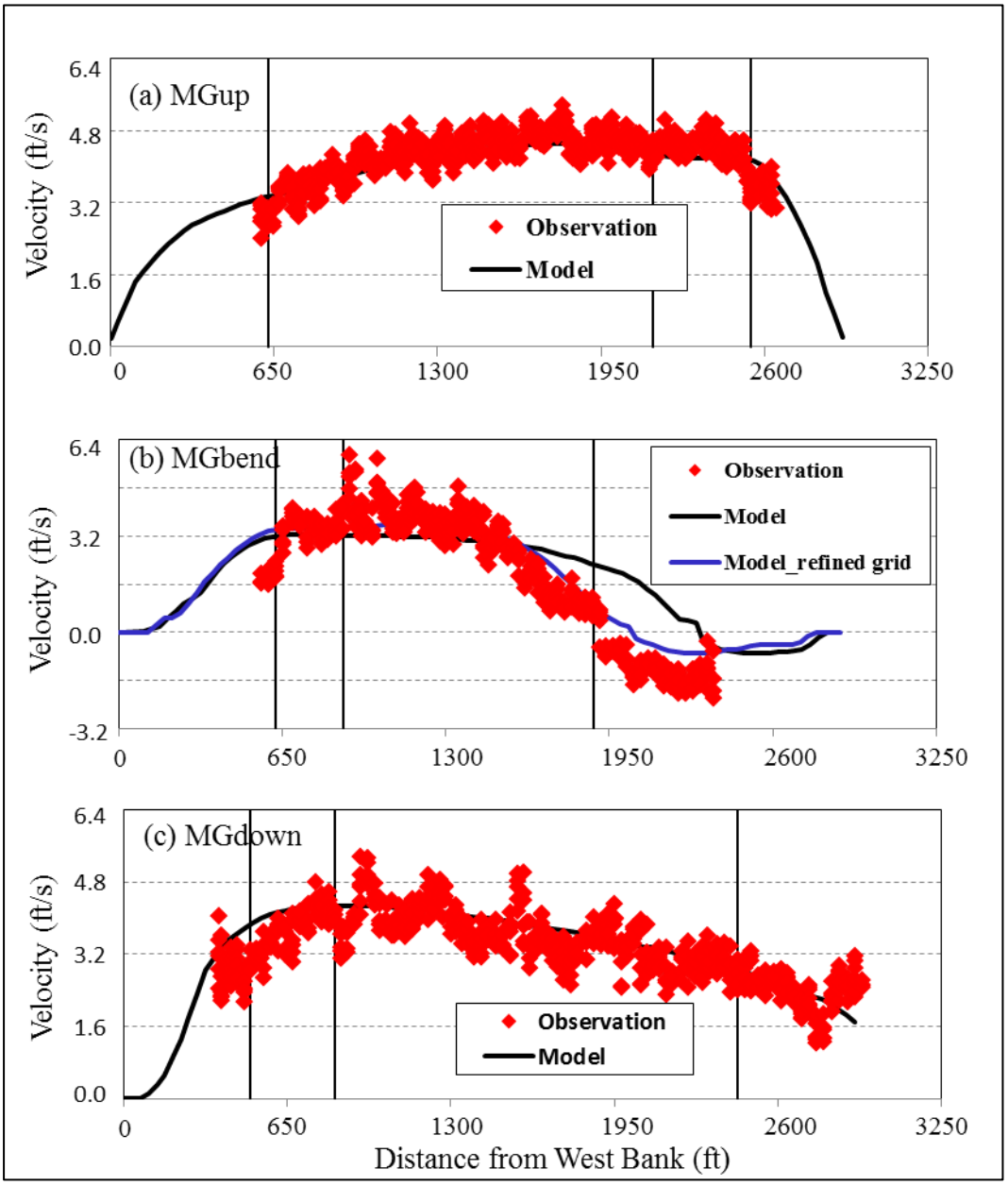

Figure 3-5. **Velocity Transects at (a) MGup, (b) MGbend, and (c) MGdown.**
Red dots are field measurements in April 2009, and black thick lines are FLOW-3D results obtained using the coarse grid. The vertical lines indicate locations of three vertical velocity profiles along each transect. In panel (b), the blue line is the FLOW-3D result obtained using the locally refined grid.

The meander bend at Myrtle Grove is characterized by strong secondary circulation and re-circulation eddies. These features can only be captured using a finer grid resolution, such as the locally refined grid. Figure 3-6 shows an extensive re-circulation eddy at the left descending bank, with reverse flow speeds exceeding 1 ft/s. Figure 3-7 shows the evolution of a secondary circulation pattern at MGbend. White dashed lines in the right panel indicate the location of three cross sections, and the right panels show the vertical velocity magnitude and vectors along each cross section. Note that the vertical scale in the cross-sectional plot is highly exaggerated. At the upstream end of the re-circulation eddy (panel b), secondary circulation starts to develop near the bottom of the water column. At the second cross section (Panel c in Figure 3-7), the secondary motion becomes stronger and covers nearly the entire water column. Then it gradually diminishes as it reaches the downstream cross section (panel d),

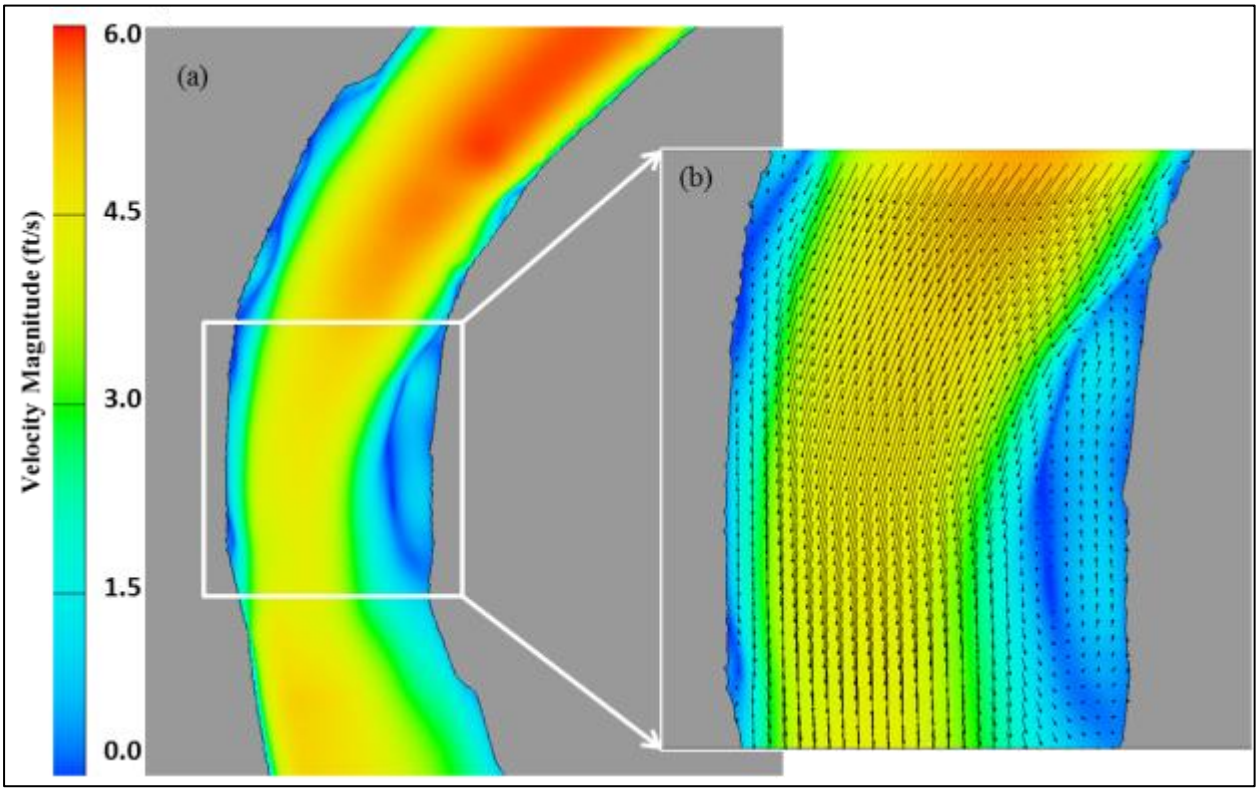

Figure 3-6. **(a) Model Estimated Velocity Magnitude; (b) Velocity Vectors at the Meander Bend near Myrtle Grove.**
This figure is showing strong recirculation at the left descending bank.

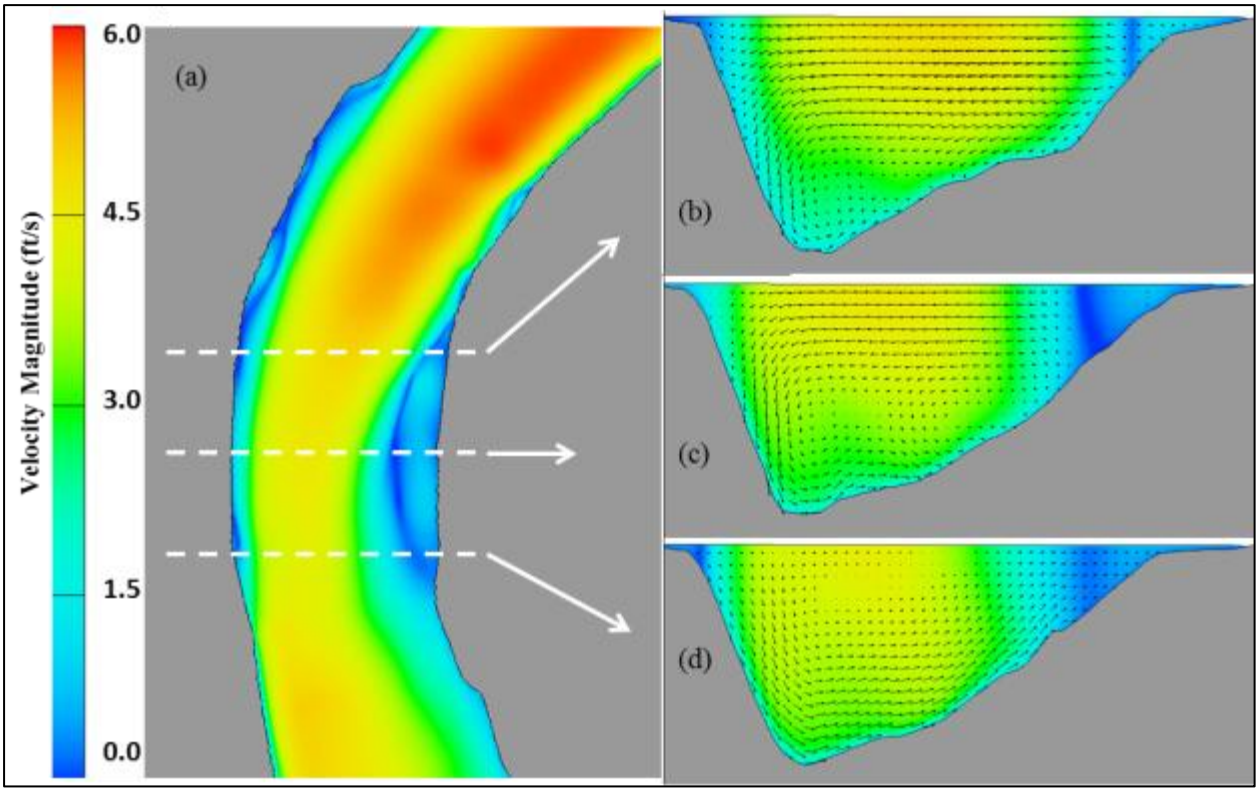

Figure 3-7. **(a) Model Estimated Velocity Magnitude (the same as in Figure 3-4); (b), (c), (d) Cross-Section Velocity Magnitude and Direction, Showing Secondary Circulation at the Meander Bend near Myrtle Grove.**
White dashed lines indicate location of those three cross sections. In panels (b), (c), and (d), vertical and horizontal directions are not to scale.

Figure 3-8, Figure 3-9, and Figure 3-10 summarize velocity profile comparisons between field observations and model results. In each figure, open and solid circles represent field observations and the uncertainty of the observations, respectively; whereas the red line represents the model results. Similar to the velocity transect calibration, the model results with the coarse grid match the measured data at MGup and MGdown, while the locally refined model produced better agreement at MGbend (blue lines in Figure 3-9). Note that the lack of agreement near the bottom may result from the downward-looking ADCP receiving excessive strong acoustic signals reflected by the river bed.

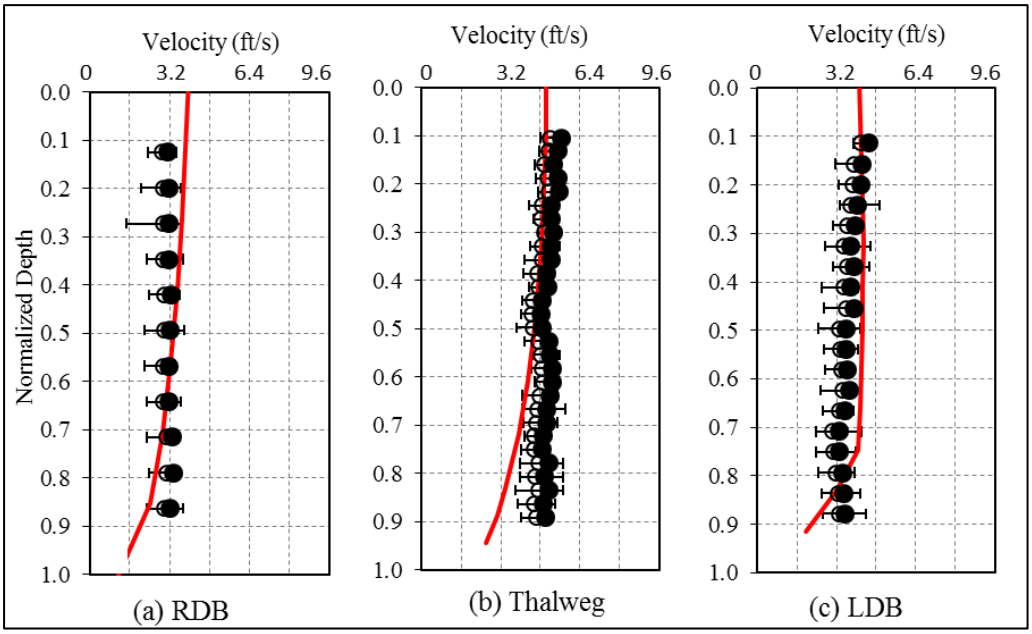

Figure 3-8. **Velocity Profile Calibration Results at MGup.**

In each panel, open and solid circles represent field observation and observation uncertainty, respectively; red line shows modeling velocity.

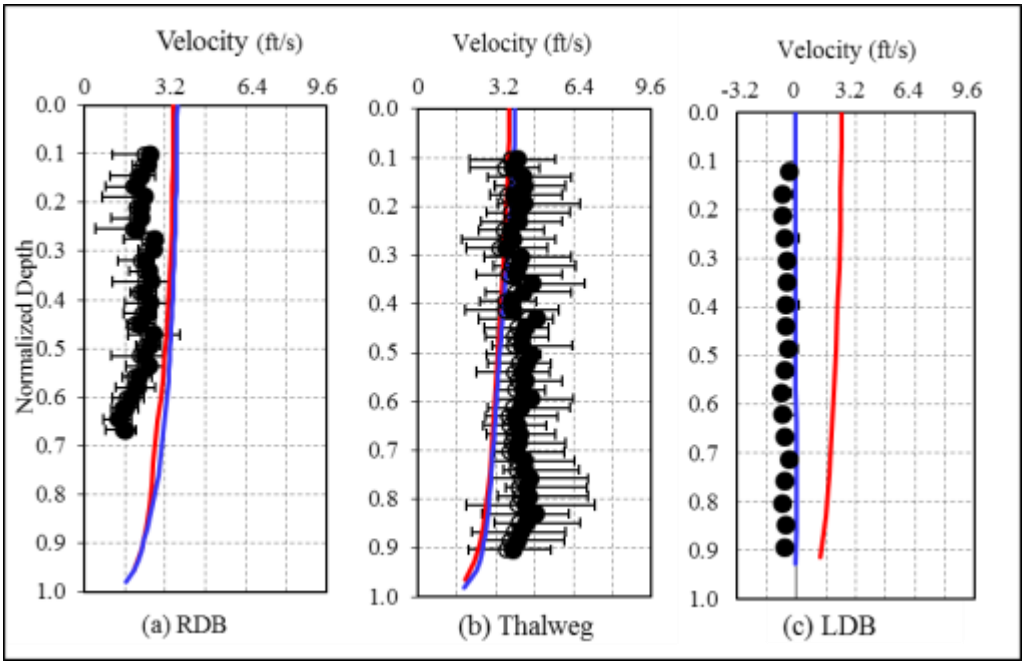

Figure 3-9. **Velocity Profile Calibration Results at MGbend.**

In each panel, open and solid circles represent field observation and observation uncertainty, respectively; red line shows modeling velocity from coarse grid; blue line shows modeled result from locally refined grid.

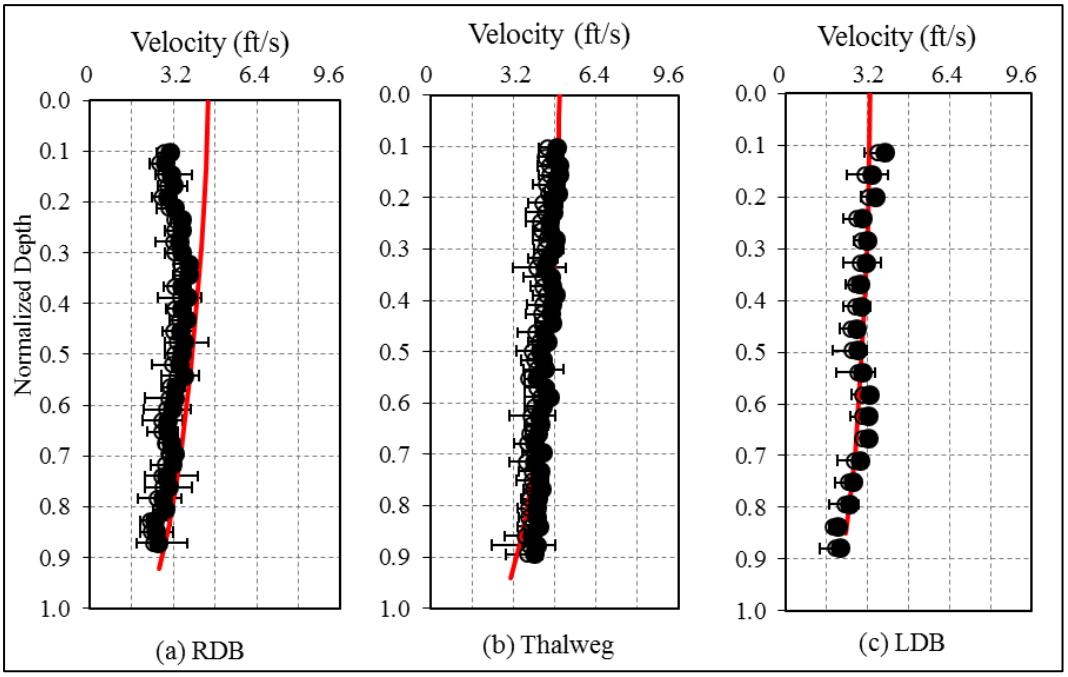

Figure 3-10. Velocity Profile Calibration Results at MGdown.

In each panel, open and solid circles represent field observation and observation uncertainty, respectively; red line shows modeling velocity.

3.2.3 Extended Domain Sediment Calibration

The sediment calibration coeficients, as discussed in Section 2.2, include Schmidt number *k*, particle diffusion coefficient (NUP), and drag coefficient β. During the sediment calibration, these variables were set with *k* equal to 1, NUP equal to 0.05, and β equal to 1. It is also assumed that no enegy loss occurs when mass particles collide with the river bed. In the model, particles were released uniformly across the entire cross section of the upstream boundary. Therefore no biases were associated with the source at the start point. Driven by a fully developed steady river flow, the particles moved and were redistributed through the entire model domain.

Suspended sand concentration (C_s) data were collected at three cast locations along each MGup, MGbend, and MGdown transect with an isokinetic sampler during a field survey in April 2009 (Allison 2011). For each cast, the sampling was done at five depths (e.g., 0.1, 0.3, 0.5, 0.7, and 0.9 of the total water depth). However, ***FLOW-3D*** only provides particle count within each grid cell instead of sediment concentration. The procedure described in Section 3.1.2 was used to convert particle count to sediment concentration. Specifically, the following steps were performed:

1. Five vertical control volumes were set up centering the location of each sampling cast. The depths of these control volumes correspond respectively to 0.1, 0.3, 0.5, 0.7, 0.9 of total water depth estimated by ***FLOW-3D***, consistent with the filed measurement.
2. Conversion was done from sediment counts to sand concentrations in each control volume based on the procedure described in Section 3.1.2.
3. Sand concentrations, estimated in step 2 (above), were corrected by the factor *X*, described in Section 3.1.2.

The model results were compared to field measurements at MGup and MGdown. A similar comparison at MGbend was not excuted due to the high uncertainty in field observations (Allison, pers. comm. 2013). Figure 3-2 shows the locations of field observations. At both MGup and MGdown, three suspended sand profiles were measured. They are referred to as RDB, middle, and LDB, respectively (black dots).

Figure 3-11 shows the results of the sediment calibration. Red dots and lines indicate ***FLOW-3D*** results, and black dots show field observations. Overall, the model estimates of sand concentration were satisfactory, proving the ability of ***FLOW-3D*** to reproduce the hydrodynamics and sediment transport dynamics in the river. Disagreements between measured and modeled data are probably caused by:

1. scatters in observations, e.g., sudden changes of C_s in the middle water column (panels e and f);
2. uncertainties in observations near the river bed caused by high turbulent fluctuation of bedload materials;
3. uncertainties in the boundary conditions and / or the bathymetric data used; and
4. deficiencies associated with the ***FLOW-3D*** sediment transport method.

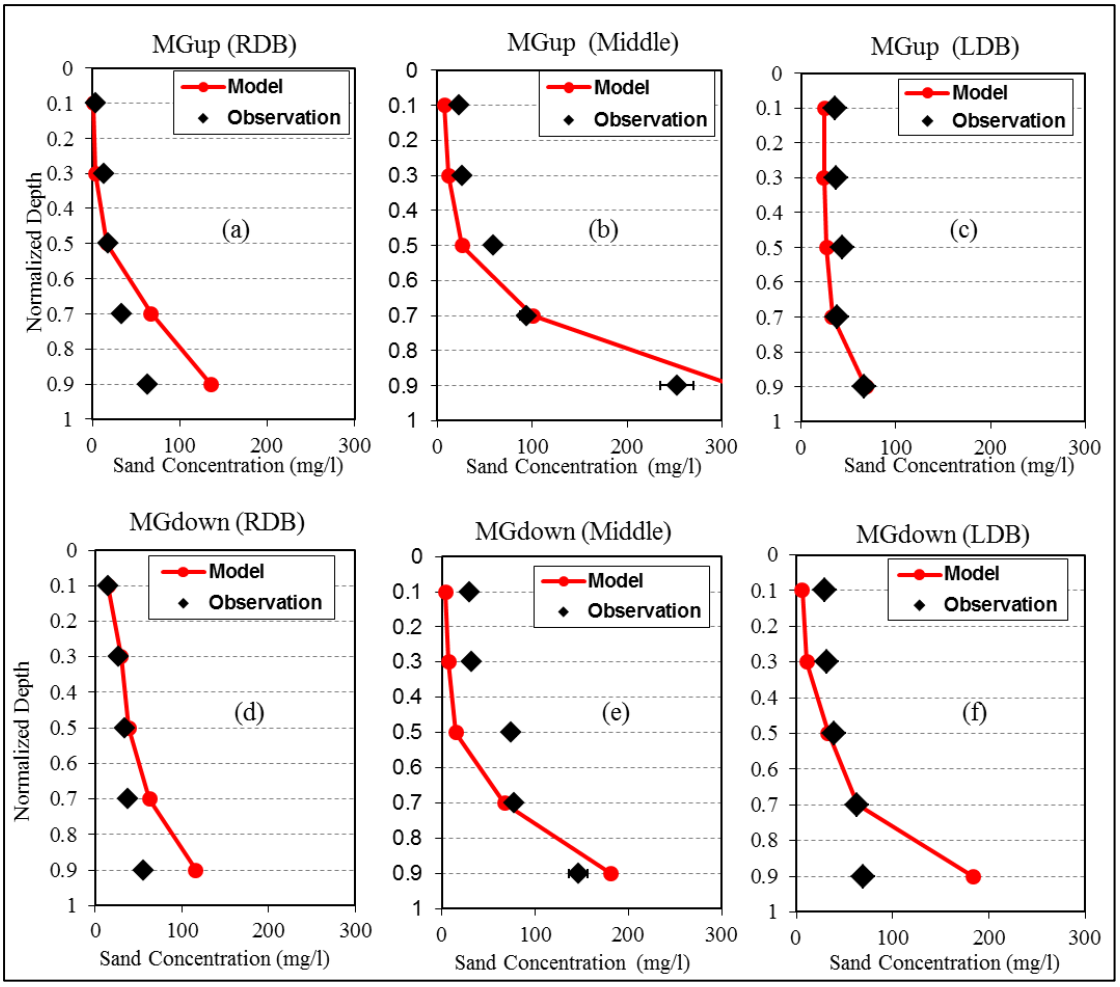

Figure 3-11. **Suspended Sand Calibration Results at MGup and MGdown, April 2009 Flow Used During Model Calibration.**

Red dots and lines indicate FLOW-3D results, and black dots show field observations.

3.2.4 Extended Domain Hydrodynamics Validation

Figure 3-3 shows the location of velocity measurements at MGup in March 2011. Figure 3-12 shows the comparison between the model results and observed data. Red dots represent depth-averaged velocity measurements and the thick black line represents the corresponding model results. The vertical lines indicate locations of the three vertical velocity profiles as shown in Figure 3-13. It is clear that both the horizontal and vertical velocity profiles estimated by ***FLOW-3D*** agree well with the field observations. The results show the ability of the model to simulate different flow conditions. Note that velocities presented in the figures are from ***FLOW-3D*** using the coarse grid. The model was refined in subsequent simulations that included details of the diversion intake structure and outfall channel's design.

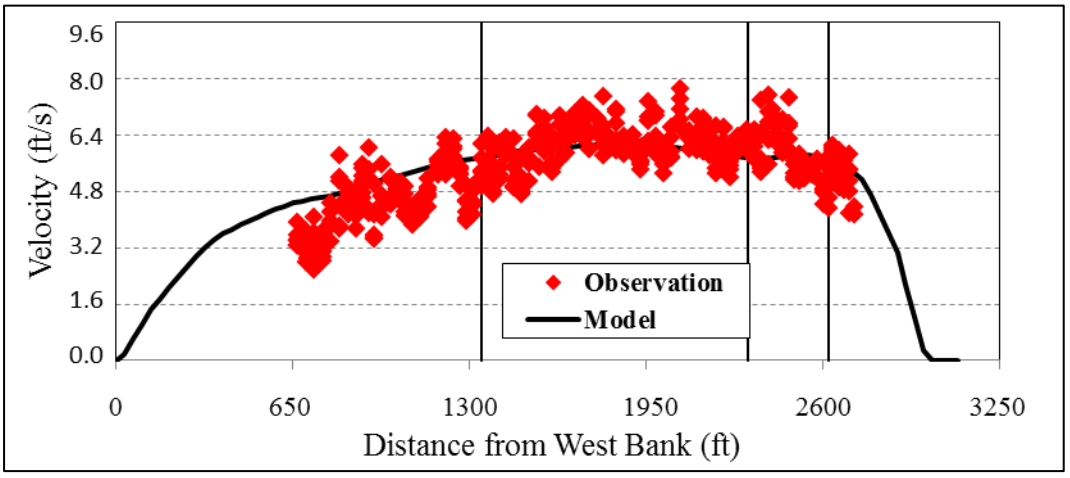

Figure 3-12. Velocity Transect at MGup.
Red dots are field measurements and thick black lines are FLOW-3D results using coarse grid. The vertical lines indicate locations of three vertical velocity profiles presented in Figure 3-3.

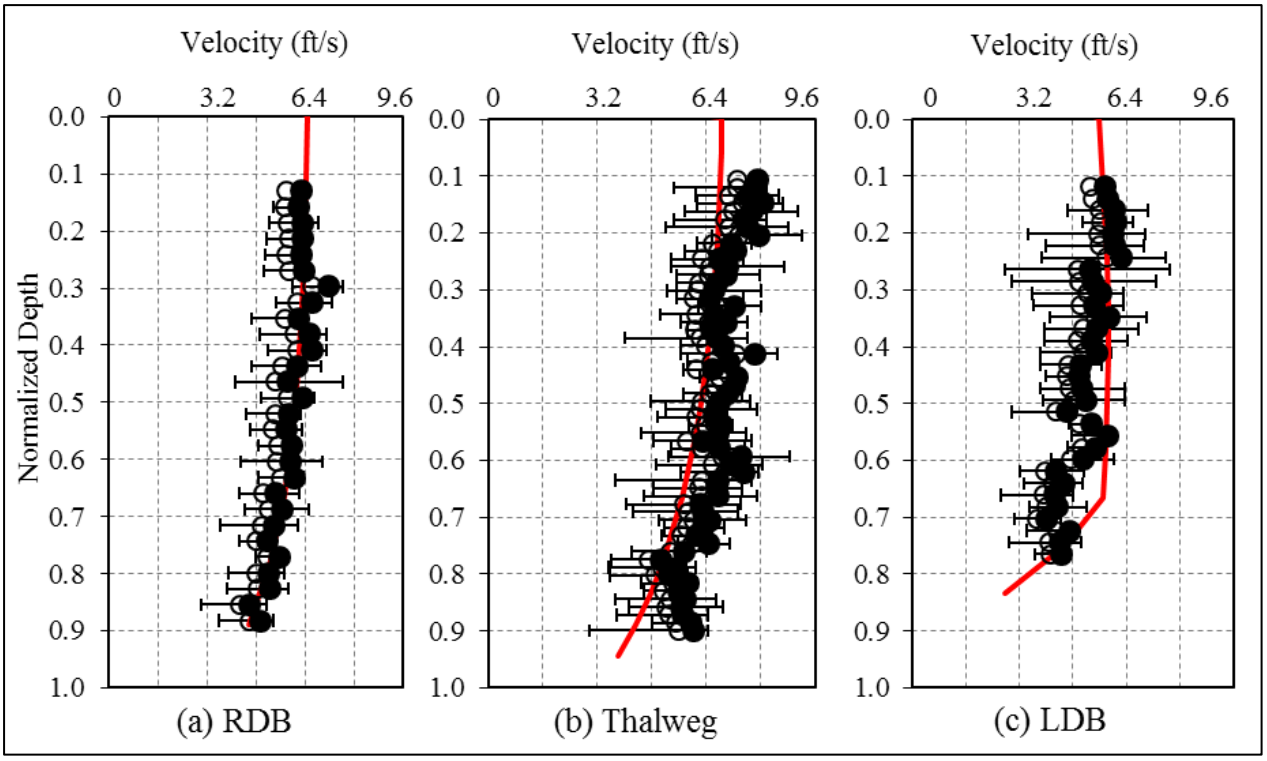

Figure 3-13. Velocity Profile Validation Results for MGup.
In each panel, open and solid circles represent field observation and observation uncertainty, respectively; red line indicates modeled velocity profile.

3.2.5 Extended Domain Sediment Validation

Figure 3-4 shows the locations of field observation used in the model validation, and Figure 3-14 shows the suspended sand concentration predicted by the model compared to field observations. The model's ability to reproduce observed concentrations appears satisfactory, with good agreement throughout the water column at all three sites.

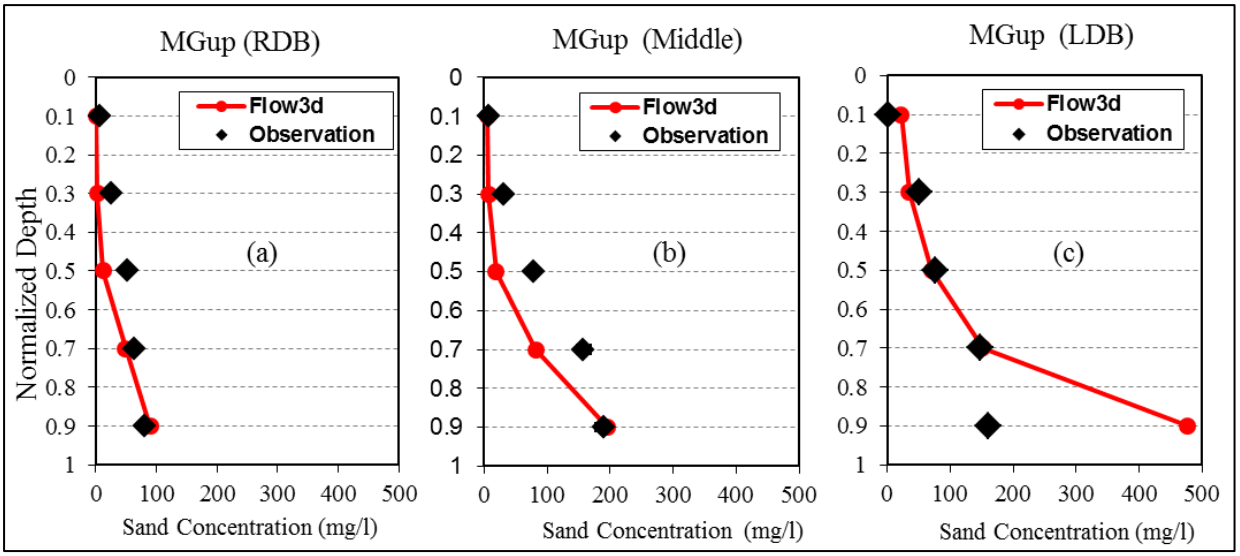

Figure 3-14. **Suspended Sand Calibration Results for MGup; March 2011.**
Flow was used During Model Validation - Red dots and lines indicate FLOW-3D results, and black dots show field observations.

4. ANALYSES

A series of numerical modeling investigations, used to select the most suitable location for the diversion structure and to identify design features to maximize sediment capture, was carried out with the initial domain and extended domain ***FLOW-3D*** models described in Section 2 and Section 3.

The first study under this preliminary engineering design effort, referred to as the Feasibility Study Recommended Design Analysis, was designed to evaluate the performance of the proposed diversion at Location 3 during the feasibility study phase of the White Ditch diversion (USACE and CPRA 2010). This analysis was completed using the initial domain model. The results of this study established a baseline from which the results of other studies were compared.

The second study, called the Initial Domain Design Alternatives Study, required that changes be made to the diversion structure's design and, in one case, to its location. The results of this analysis provided information used to determine alignment angles, to identify structure designs that reduced or eliminated flow separations, and to determine if changes in the structure's location might improve its performance. All simulations, in this portion of the analysis, were completed with the initial model domain and considered Locations 3 and 4 only.

In order to investigate locations beyond those in the domain of the Initial Domain Design Alternatives Study, a third portion of the study was completed using the extended model. This study is referred to as the Extended Domain Design Alternatives Study. However, in this case, the focus of the study was to investigate performance at five locations along the river (Locations 1, 2, 2.5, 3, and 4). The results of this combined work were used to provide recommendations for the most suitable site for the proposed sediment diversion. Based on the model results, Location 1 was recommended. The design was preliminarily optimized prior to this assessment, based on the outcome of the Initial Domain Design Alternatives Study. Further optimization simulations were subsequently completed at Location 1.

The diversion locations and properties that were analyzed are shown in Figure 4-1 and described in Table 4-1 and Table 4-2. Figure 4-1 shows the diversion locations and orientations in plan view. The angles of the lines shown in the figure represent the angle at which the diversion intersects the river in the ***FLOW-3D*** model. Additionally, the line colors (for the outfall channels) in Figure 4-1 correlate to the row colors in Table 4-1, which lists the river mile, latitude, and longitude of the entrance of the outfall channel, as well as the latitude and longitude of the outfall channel boundary in the model.

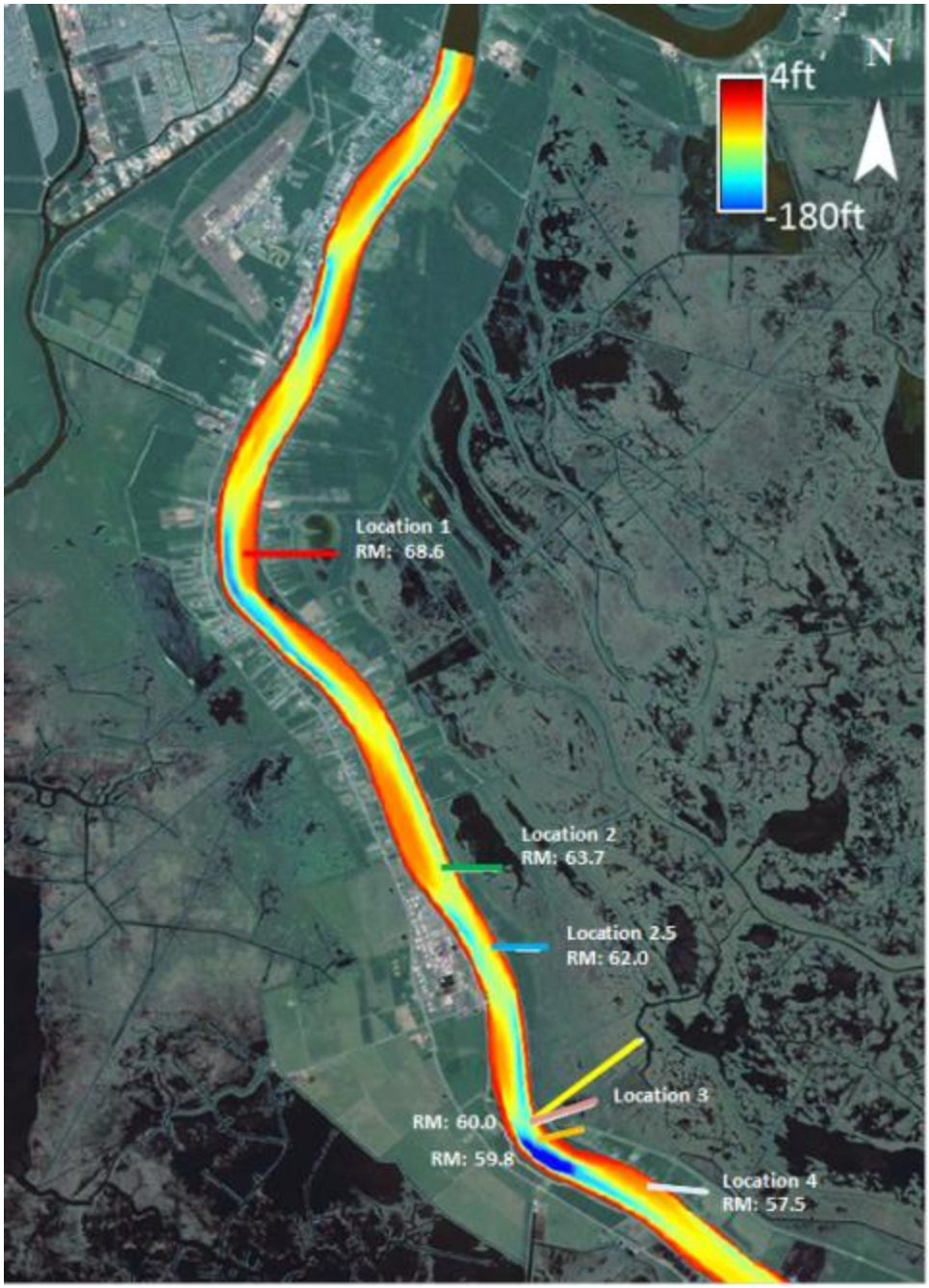

Figure 4-1. Map of Diversion Locations, Angles, and Lengths Analyzed.

The letters in the alternatives column of Table 4-1 are described in Table 4-2, including the type of structure (open channel or box culvert), the effective width of diversion openings, the height of box culverts, the intake structure length, the invert elevation, the angle of intersection with the river, the shape of the approach channel, and the presence of a guide vane. Note that the angle of intersection is

measured between the orientation of the river south of the diversion and the diversion alignment itself. Thus, an angle of 45 degrees aligns closer to the river than an angle of 90 degrees, as shown in Figure 4-1. Details of the various shapes of the approach channel are shown on figures that appear in subsequent sections.

Table 4-1. Locations of Diversions Analyzed

Locations	Alternative	Model Applied	River Mile	Entrance of Approach Channel		Outfall Channel Boundary	
				Latitude	Longitude	Latitude	Longitude
1	G	Extended	68.6	29°45'40.59"N	90°01'08.53"W	29°45'25.73"N	90°00'03.98"W
2	F	Extended	63.7	29°41'57.00"N	89°58'22.15"W	29°41'57.98"N	89°57'46.74"W
2.5	F	Extended	62.0	29°41'03.49"N	89°57'48.31"W	29°41'02.00"N	89°57'09.51"W
3	A	Initial	60.0	29°39'1.91"N	89°57'11.20"W	29°39'59.00"N	89°55'43.85"W
3	B	Initial	60.0	29°39'1.91"N	89°57'11.20"W	29°39'59.00"N	89°55'43.85"W
3	C	Initial	59.8	29°38'59.23"N	89°57'09.98"W	29°39'12.82"N	89°56'22.75"W
3	D	Initial	59.8	29°38'59.23"N	89°57'09.98"W	29°39'12.82"N	89°56'22.75"W
3	F	Extended	60.0	29°39'1.91"N	89°57'11.20"W	29°39'59.00"N	89°55'43.85"W
4	E	Initial	57.5	29°38'14.20"N	89°55'31.08"W	29°38'12.00"N	89°54'46.56"W
4	F	Extended	57.5	29°38'14.20"N	89°55'31.08"W	29°38'12.00"N	89°54'46.56"W

Table 4-2. Diversion Design Properties for Each Alternative (listed in Table 4-1)

Alternatives	Type of Intake Structure	Effective Width (feet)	Height (feet)	Length (feet)	Invert Elevation (feet NAVD88)	Angle of Intersection with the River	Shape of Inflow/ Approach Channel	Guide Vane
A	box culvert	150	15	200	-16	90 degree	straight	No
B	box culvert	150	15	200	-40	90 degree	curve and wide entrance	No
C	open channel	52	n/a	360	-40	45 degree	wide entrance	No
D	open channel	52	n/a	360	-40	45 degree	wide entrance	Yes
E	box culvert	150	15	200	-40	45 degree	curve and wide entrance	No
F	open channel	72	n/a	360	-40	45 degree	wide entrance	No
G	open channel	72	n/a	360	-40	90 degree	wide entrance	No

Note: (1) All intake structures (conduits and channels) were rectangular in cross-section.
(2) Addition simulations, with different angles of intersection with the river, were carried out at Location 4 independently by The Water Institute. The results of these simulations are not presented herein and are not relevant to the findings of this report because no variation of the Location 4 diversion structure was calculated to work better than the Location 1 structure.

4.1 Feasibility Study Recommended Design Analysis

This portion of the study was used to determine the diversion performance at Location 3 as it was described in the feasibility study (USACE and CPRA 2010). The model setup, utilizing the initial domain, includes three major components: the Mississippi River (Figure 4-2a), the diversion intake structure (Figure 4-2b), and the outfall channel (Figure 4-2c). Each component was built separately and combined into a single setup, Figure 4-3. Further details of the feasibility study diversion structure and outfall channel design, as well as model implementation, are provided in Appendix A.1.

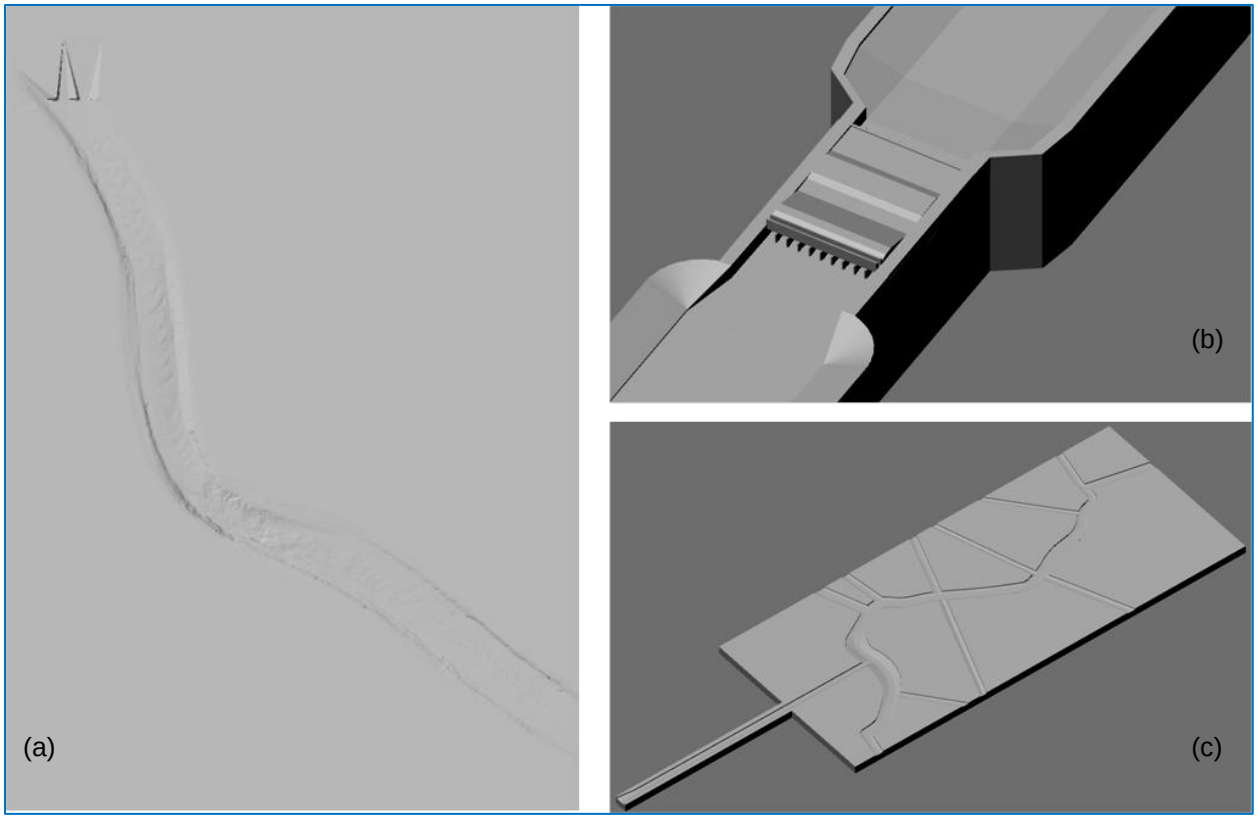

Figure 4-2. Feasibility Study Recommended Design Model Development: (a) Mississippi River, (b) Diversion Intake Structure, and (c) Outfall Channel Model.

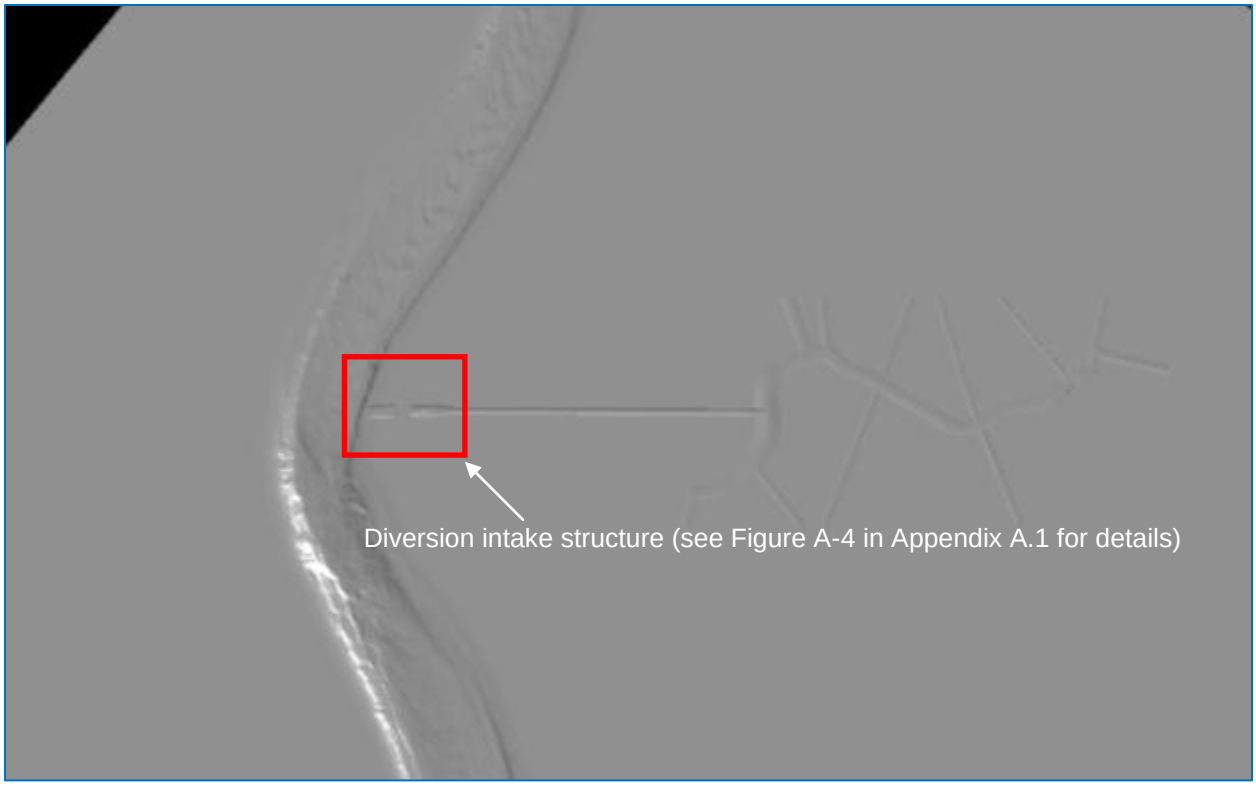

Figure 4-3. Feasibility Study Recommended Design Analysis Model Development. Three sub-models combined into a single, fully coupled, global model.

4.1.1 Model Setup

The three-dimensional Computer Aided Design (CAD) program **Rhino** (McNeel 2012) was used to construct the CFD model of the feasibility study recommended design based on the following information.

1. *Mississippi River* – Model bathymetry was obtained from the 2011 Myrtle Grove diversion study (Meselhe *et al*. 2011). The bathymetry extends from RM 56.0 to RM 62.7 (Figure 4-2).
2. *Diversion intake structure* – CAD drawings of the proposed diversion intake from the previous feasibility study (USACE and CPRA 2010) were provided by the USACE (Appendix A.1) and were used to construct the CFD model of the structure. The proposed structure has ten box culverts (designed for a maximum flow capacity of 35,000 cfs). Each culvert opening is 15 feet by 15 feet and is 200 feet long. The intake structure is attached to an inflow channel at an elevation of -16 feet NAVD88. The inflow channel connects to the riverbank at Location 3 as shown in Figure 4-1. The intake structure is also attached to an outflow channel, which connects to the outfall channel at an elevation of -16 feet NAVD88 (Figure 4-2b).

3. *Outfall channel* – The model of the outfall channel was constructed from cross sections from the previous feasibility study (USACE and CPRA 2010), which were provided by the USACE (Figure 4-2c and Appendix A.1).

The three sub-models were combined into a single, fully coupled, global model as shown in Figure 4-3. Figure 4-4 shows the same information as Figure 4-3 but colored by elevation. **Rhino** was used to convert the CAD data into a stereolithography format so that ***FLOW-3D*** could use the information directly.

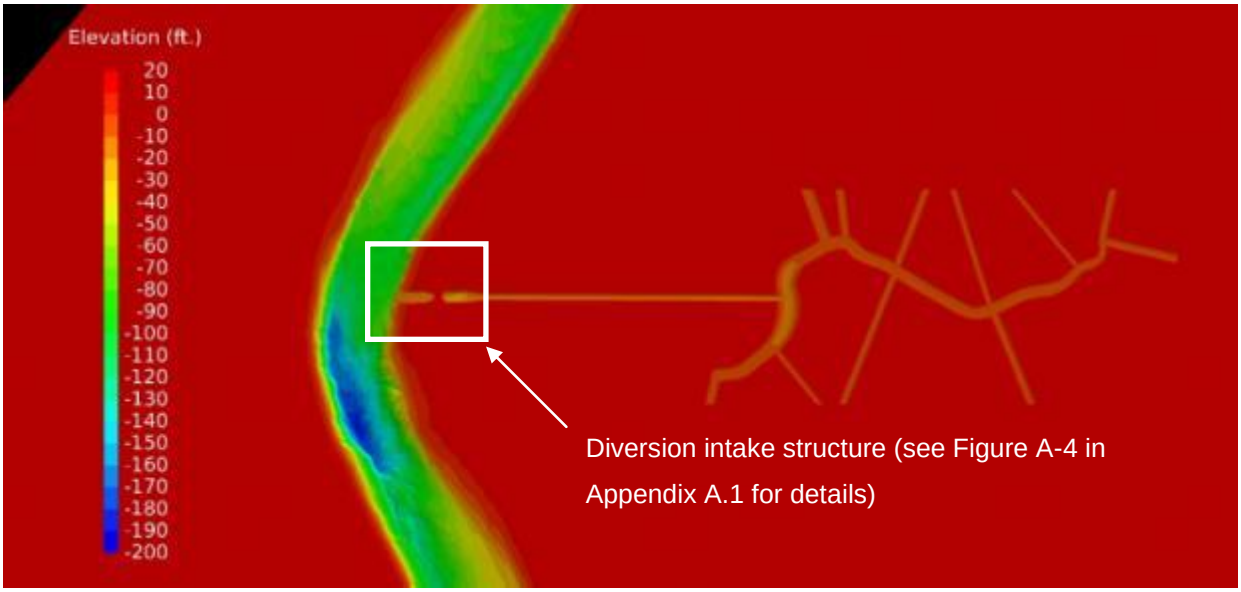

Figure 4-4. Feasibility Study Recommended Design Model Development (bathymetry colored by elevation).

Creating a computational mesh is an important aspect of every numeric modeling study. To do this, the model domain is subdivided into a number of small cells within which the governing equations are solved. The cell size must be small enough to capture flow features of interest, and the total number of cells cannot be too great (based on hardware limitations). In this study, the computational domain was separated into nine mesh blocks (Figure 4-5) and grid spacing within the mesh blocks was similar to that used in the calibration/validation studies. In general, the grid spacing used in all of the calculations matched closely; however, local refinements were made as necessary to properly resolve details of the diversion structure.

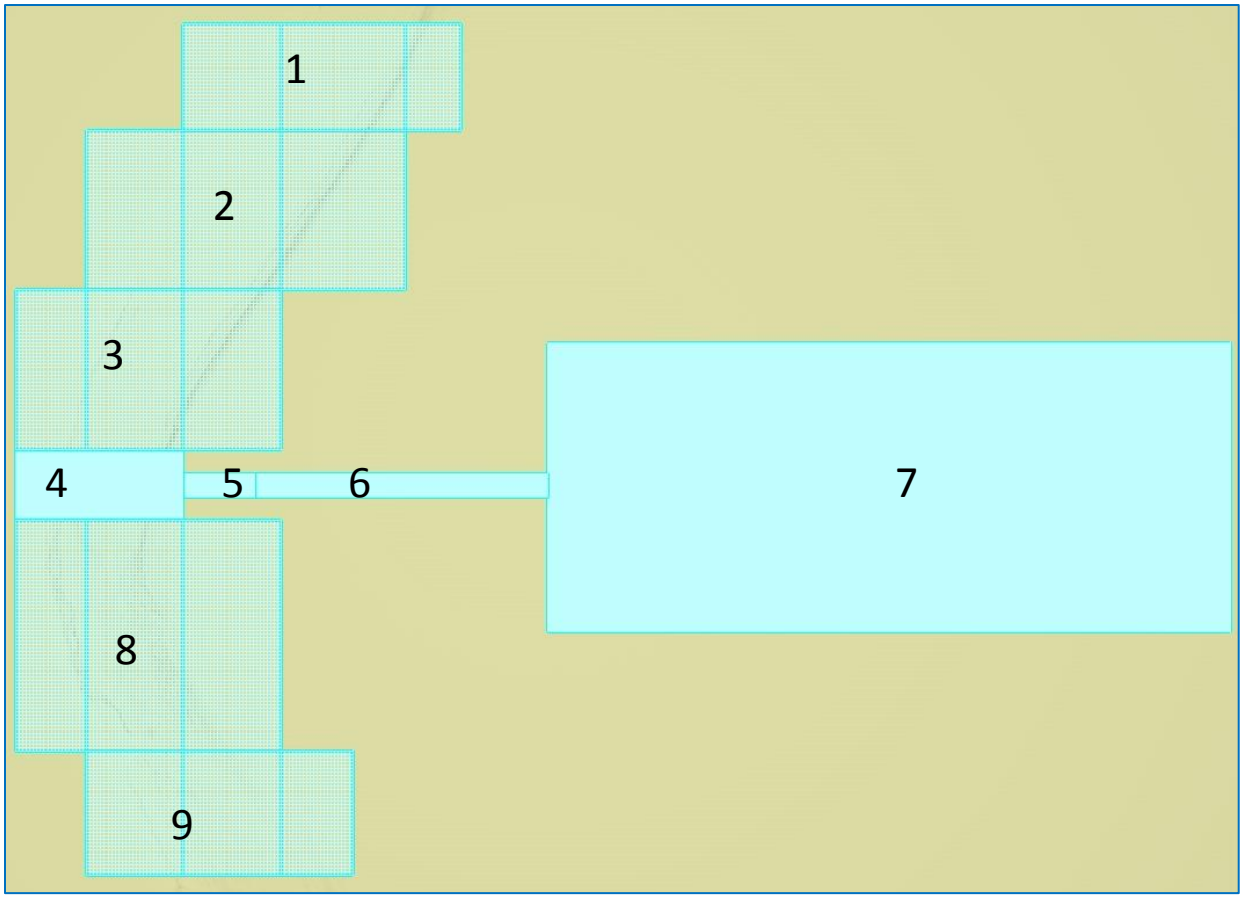

Figure 4-5. Conceptual Design of Feasibility Study Recommended Design Mesh Generation.

4.1.2 Boundary Conditions

The boundary conditions used in this study are as follows:

- No-slip conditions at solid boundaries modified by surface roughness parameters.
- Flow rate in the Mississippi River specified at the upstream boundary (700,000 cfs).
- Water surface elevation specified in the Mississippi River at the downstream river boundary (6.2 feet NAVD88). This boundary condition was established as part of the model calibration using the numerical simulations from HEC-RAS (Davis 2010) to estimate a tail water elevation.
- Water surface elevation specified in the receiving basin at the end of outfall channel (2.0 feet NAVD88). The value of 2.0 feet was obtained from the Location 3 Outfall Channel Tentative Profile provided by the USACE.

Figure 4-6 shows, schematically, where the model boundary conditions were applied.

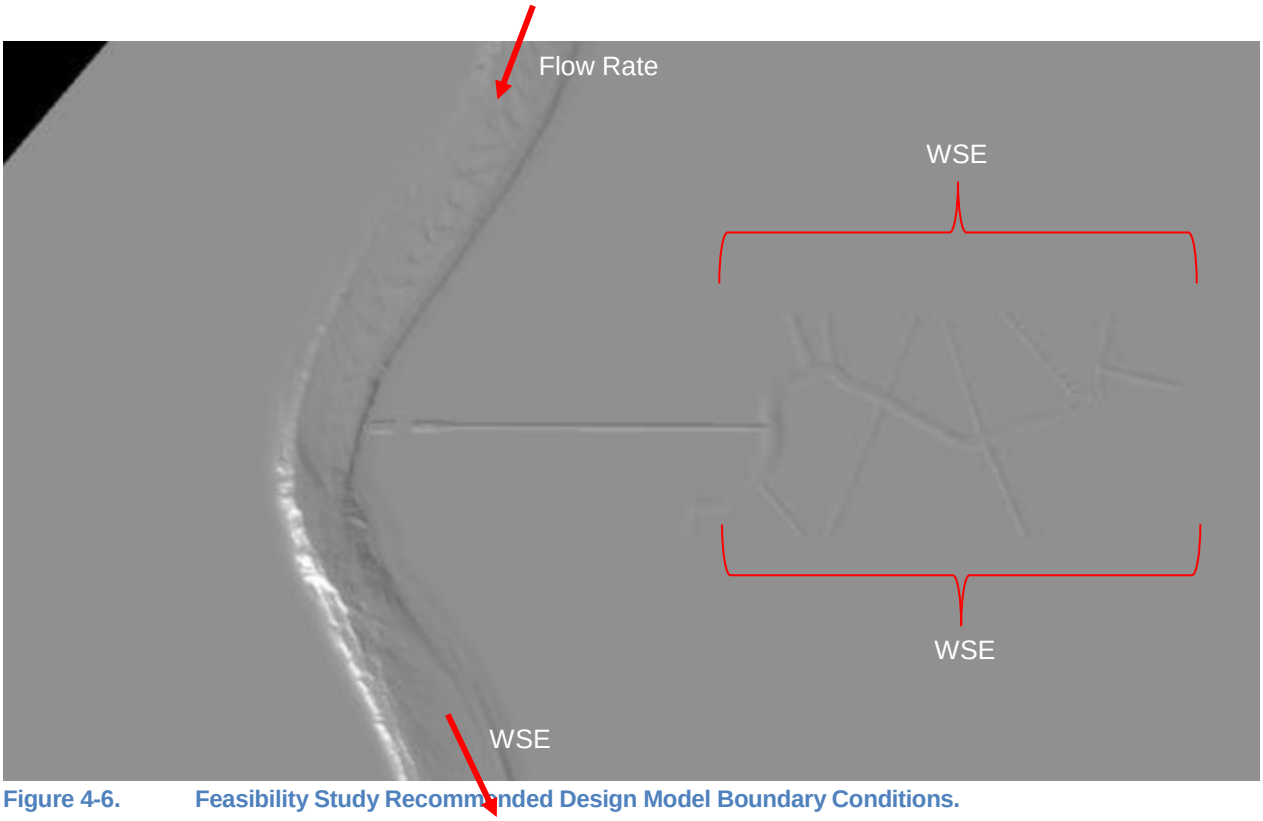

Figure 4-6. Feasibility Study Recommended Design Model Boundary Conditions.

4.1.3 Simulation

The model simulations were carried out in two steps. First, the momentum equations that describe fluid motion were solved numerically to obtain steady flow solutions. Steady flow was established using the coarsest grid first and ultimately using the most locally refined grid. Second, using the most refined hydrodynamic solution, sediment particles ranging in size from 2 to 250 microns were released at the upstream boundary of the model. The movement of the particles was then calculated, and the ability of the proposed structure to divert sediment was determined from these data.

4.1.4 Results

Qualitative and quantitative results were produced from the model data using ***FieldView*** (Intelligent Light 2013) and ***FLOW-3D***. Qualitative results include graphics showing flow patterns in the river and entering the diversion channel (e.g., vector plots, speed contours, and streamlines). Quantitative results include calculations of the amount of water diverted and the amount of sediment captured by the structure.

4.1.4.1 Hydrodynamics

The flow pattern at the diversion structure is shown in Figure 4-7 and Figure 4-8. Note that, with this proposed design, some flow recirculation is observed in the approach channel upstream of the intake structure.[5]

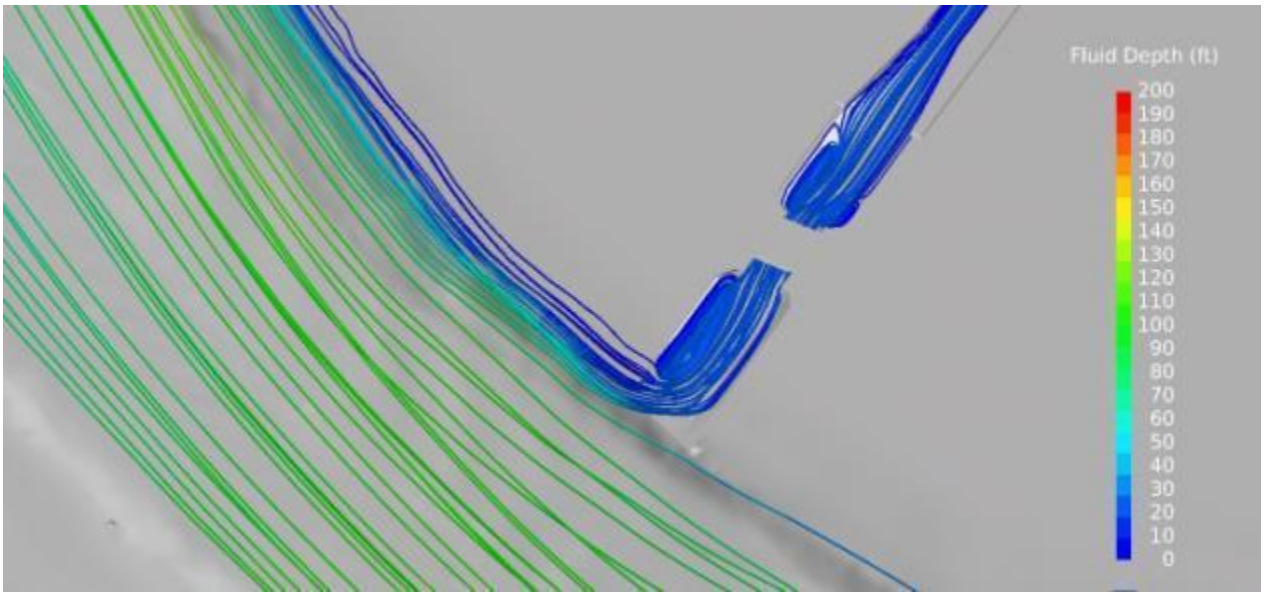

Figure 4-7. Feasibility Study Recommended Design Model Results – Hydrodynamics: Streamlines Colored by Elevation.

[5] See also Appendix A.1 for additional information.

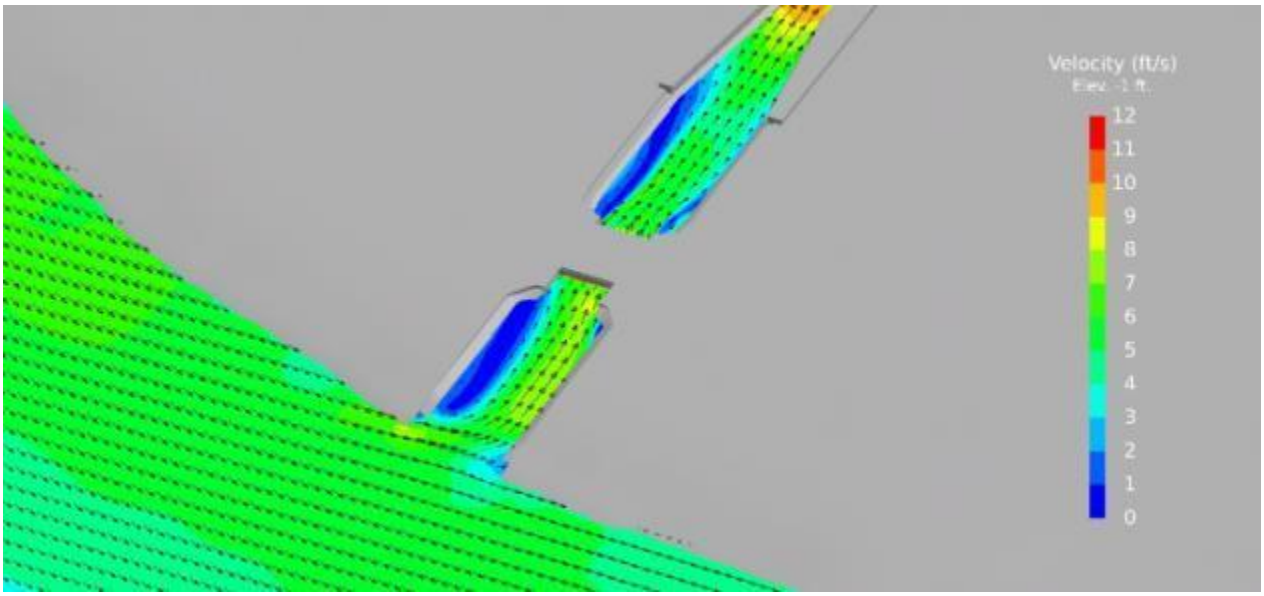

Figure 4-8. Feasibility Study Recommended Design Model Results – Hydrodynamics: Flow Pattern at Diversion Structure (near surface, colored by speed).

4.1.4.2 Sediment Capture

The sediment load in the river was carried by seven different size classes of particles (2, 8, 32, 63, 96, 125, and 250 microns; see Table 2-1. Sediment Size Class and Size Range, for additional information regarding particle size ranges within each of these classifications).[6] These particles were released at the upstream boundary of the river after steady-state flow patterns had been calculated and the particles assigned varying diameters (Note: the density of all particles was equal to 2,650 kilograms per cubic meter). To determine the amount of sediment captured in the diversion intake structure, the number of particles entering the structure was recorded. Table 4-3 shows the amount of flow entering the intake channel and the amount of sediment (in metric tons per day) captured in the diversion intake structure. In this baseline calculation, about 3.4 percent of the total river flow entered the intake channel and about 2 percent of the total sediment load (2 to 250 microns) was captured. As shown in Table 4-3, no sediments in the 250-micron size class were captured. Using Equation 4-1 shown below, the calculated Sediment Water Ratio (SWR) for particles in all size categories was 0.6 (Table 4-4). The sediment load in terms of cubic yards per year is shown in Table 4-5.

[6]Based on supplemental work, material in the 2- and 8-micron size ranges moves with the flow and resulting sediment water capture ratios for these materials are essentially 1.

$$SWR = \frac{\left(\frac{sum\ of\ sediment\ load\ in\ the\ intake\ channel}{sum\ of\ sediment\ load\ in\ the\ river}\right)}{\left(\frac{flow\ diverted\ in\ the\ intake\ channel}{flow\ in\ the\ river}\right)}$$ **Equation 4-1**

Table 4-3. Feasibility Study Recommended Design Calculated Sediment Capture (metric ton per day)

Description		Flow Rate		Sediment Load (metric ton/d)							Total
		(m^3/s)	(cfs)	2 Microns	8 Microns	32 Microns	64 Microns	96 Microns	125 Microns	250 Microns	Load (metric ton/day)
Mississippi River		19,822	700,000	41,898	140,396	77,050	10,839	21,816	34,437	23,460	349,896
Intake Channel	Location 3-A	676	23,873	1,429	4,788	267	47	99	166	0	6,796

Table 4-4. Feasibility Study Recommended Design Calculated Sediment Water Ratios

Description		Flow Rate		Sediment Water Ratios by Size Class							Total
		(m^3/s)	(cfs)	2 Microns	8 Microns	32 Microns	64 Microns	96 Microns	125 Microns	250 Microns	SWR
Intake Channel	Location 3-A	676	23,873	1.0	1.0	0.1	0.1	0.1	0.1	0.0	0.6

Note: The density used in the calculation was 100 pounds per cubic foot.

Table 4-5. Feasibility Study Recommended Design Calculated Sediment Loads

Description		Cubic Yards/Year			Metric Ton/Day		
		Total 2-250 Micron Load	Total 32-250 Micron Load	Total 64-250 Micron Load	Total 2-250 Micron Load	Total 32-250 Micron Load	Total 64-250 Micron Load
Intake Channel	Location 3-A	332,951	28,370	15,285	6,796	579	312

4.1.5 Conclusions and Recommendations

Below is a summary of remarks and conclusions resulting from the analysis of the feasibility study proposed design configuration:

1. The calculated SWR at Location 3 is significantly less than 1.0 and does not meet design requirements for the structure.
2. The calculated SWR for materials of 32 microns or coarser is significantly less than 1.0 making this is a poor location for the capture of larger land-building sediments. NOTE: considering the fact that

SWRs for silts and clays were equal to 1.0 – an aggregate SWR of 0.6 is about the minimum SWR that can be calculated according to this analysis.

3. The entrance to the diversion structure is located at the start of a river bend where secondary flow patterns responsible for bar formation are not present. This makes it difficult for the structure to capture sediment.
4. The sill elevation of the diversion structure is too high to capture material in the 250-micron size class.
5. The alignment of the entrance to the diversion structure is considered poor due to flow separation in the entrance of the structure.

Based on these findings, it was recommended that the design of the intake structure be improved (e.g., its alignment and invert elevation) and/or another location for the diversion structure be considered.

4.2 Initial Domain Design Alternatives Study

Based on results from the analysis of the feasibility study recommended design, four alternative intake configurations were considered in the Initial Domain Design Alternatives Study. See Figure 4-1, Table 4-1, and Table 4-2 for further details on the location or design configuration of the alternatives. The four alternatives are as follows:

- Location 3, Alternative B – The intake channel was moved 1,500 feet south of its original position. The entrance of the diversion channel was streamlined to minimize flow separation and sediment deposition. The sill elevation of the entrance of the diversion channel, as well as the intake structure and discharge channel, was lowered to an elevation of -40 feet NAVD88. The end of the discharge channel was linked to a 6,200-foot outfall channel, which sloped upward and connected to the existing channel of the receiving basin. Figure 4-9 shows the layout of Location 3, Alternative B.

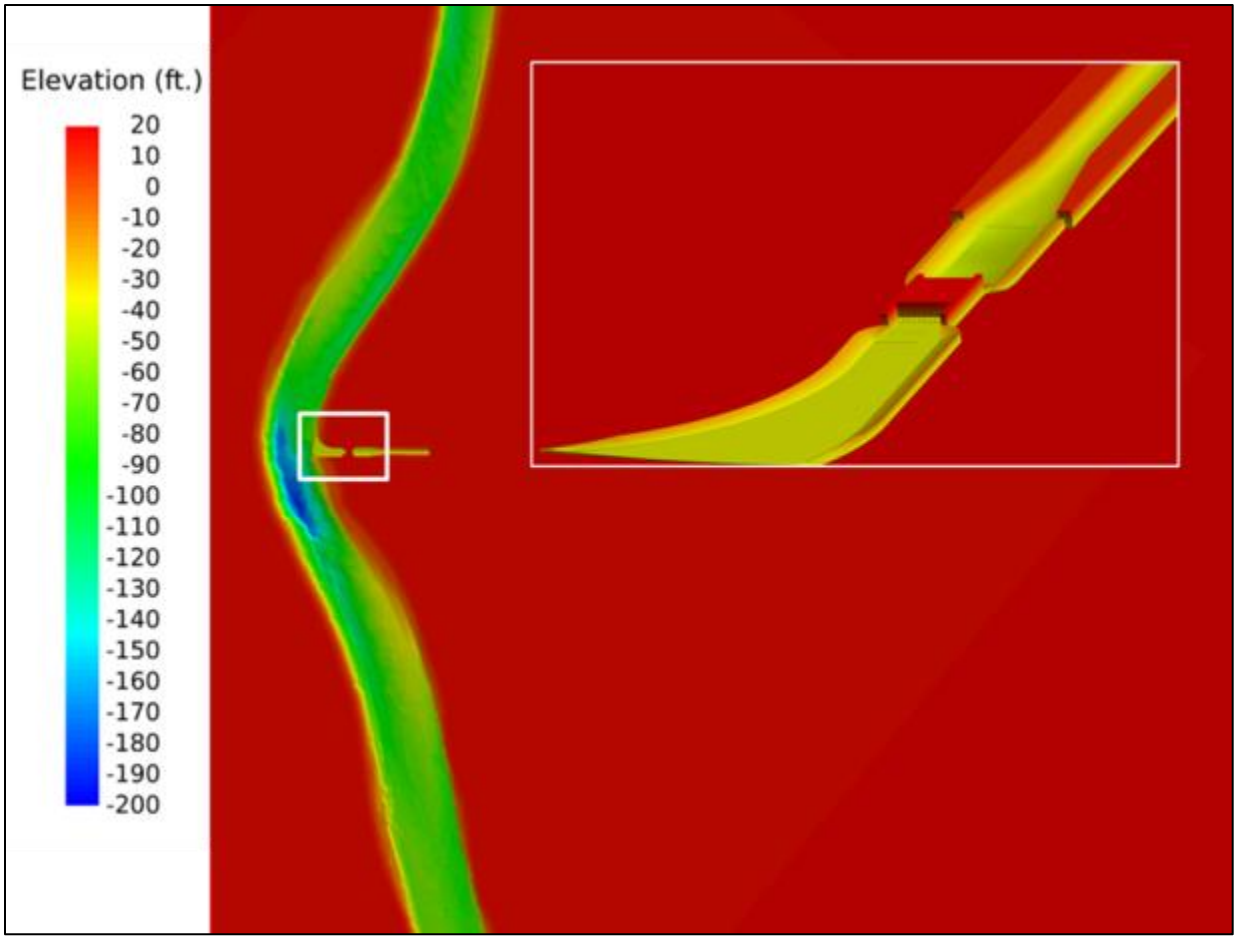

Figure 4-9. Location 3, Alternative B Model Development (bathymetry colored by elevation).

- Location 3, Alternative C – The location of the diversion channel was the same as in the Feasibility Study Recommended Design Analysis; however, the alignment of the diversion channel with the Mississippi River was adjusted from 90 degrees to 45 degrees. The ten box culverts were removed and replaced with one rectangular open channel. The channel was designed to divert 25,000 cfs when the river flow is equal to 700,000 cfs and 35,000 cfs when the river flow is equal to 1,000,000 cfs. Similar to Location 3, Alternative B, the entrance of the diversion channel was streamlined to minimize flow separation and sediment deposition. The sill elevation of the entrance of the diversion channel, as well as the intake and discharge channel, was lowered to an elevation of -40 feet NAVD88. The end of the discharge channel was linked to a 6,200-foot outfall channel, which sloped upward and connected to the existing channel of the receiving basin. Figure 4-10 shows the layout of Location 3, Alternative C.

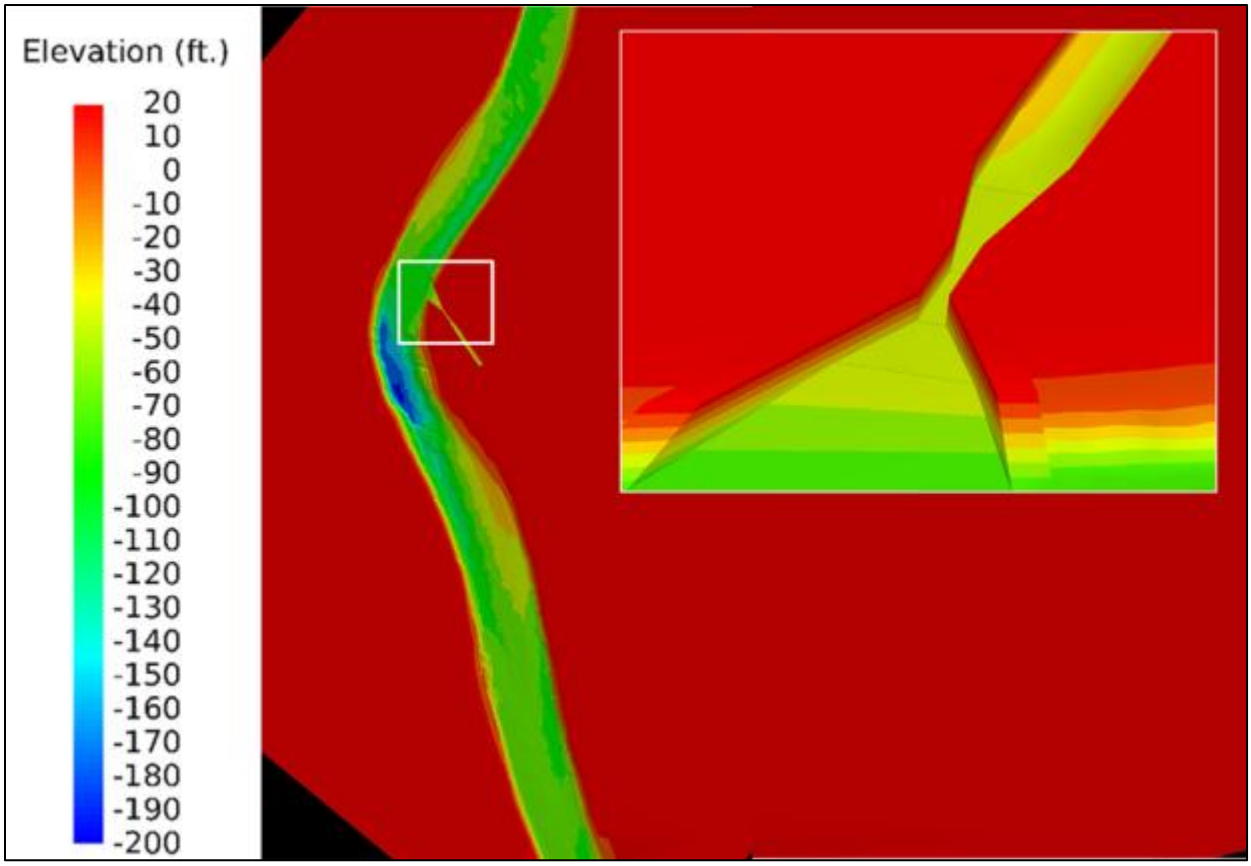

Figure 4-10. Location 3, Alternative C Model Development (bathymetry colored by elevation).

- Location 3, Alternative D – Similar to Alternative B, but with a guide vane extending into the river. The top elevation of the guide vane was set to -30 feet NAVD88. Figure 4-11 shows the layout of Location 3, Alternative 3.

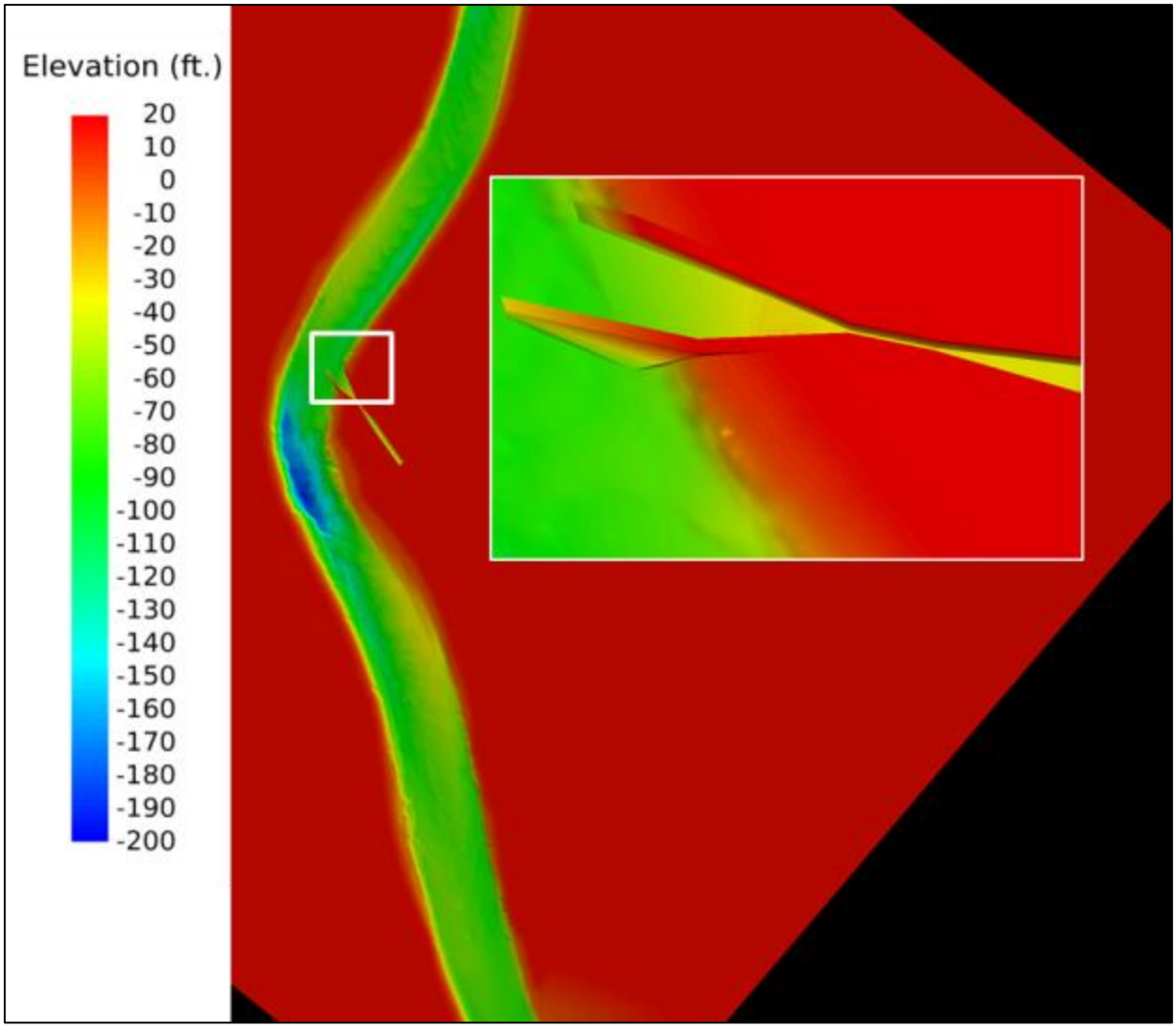

Figure 4-11. Location 3, Alternative D Model Development (bathymetry colored by elevation).

- Location 4, Alternative E – The intake channel was moved 1.9 mile south of the original location to Location 4 as it is defined in the feasibility study. The diversion channel was aligned at 45 degrees with the Mississippi River flow. The entrance of the diversion channel was streamlined to minimize flow separation and sediment deposition. The sill elevation of the entrance of the diversion channel, as well as the intake structure and discharge channel, was lowered to an elevation of -40 feet NAVD88. The end of the discharge channel was linked to a 6,000-foot outfall channel, which sloped upward and connected to the existing channel of the receiving basin. Figure 4-12 shows the layout of Location 4, Alternative E.

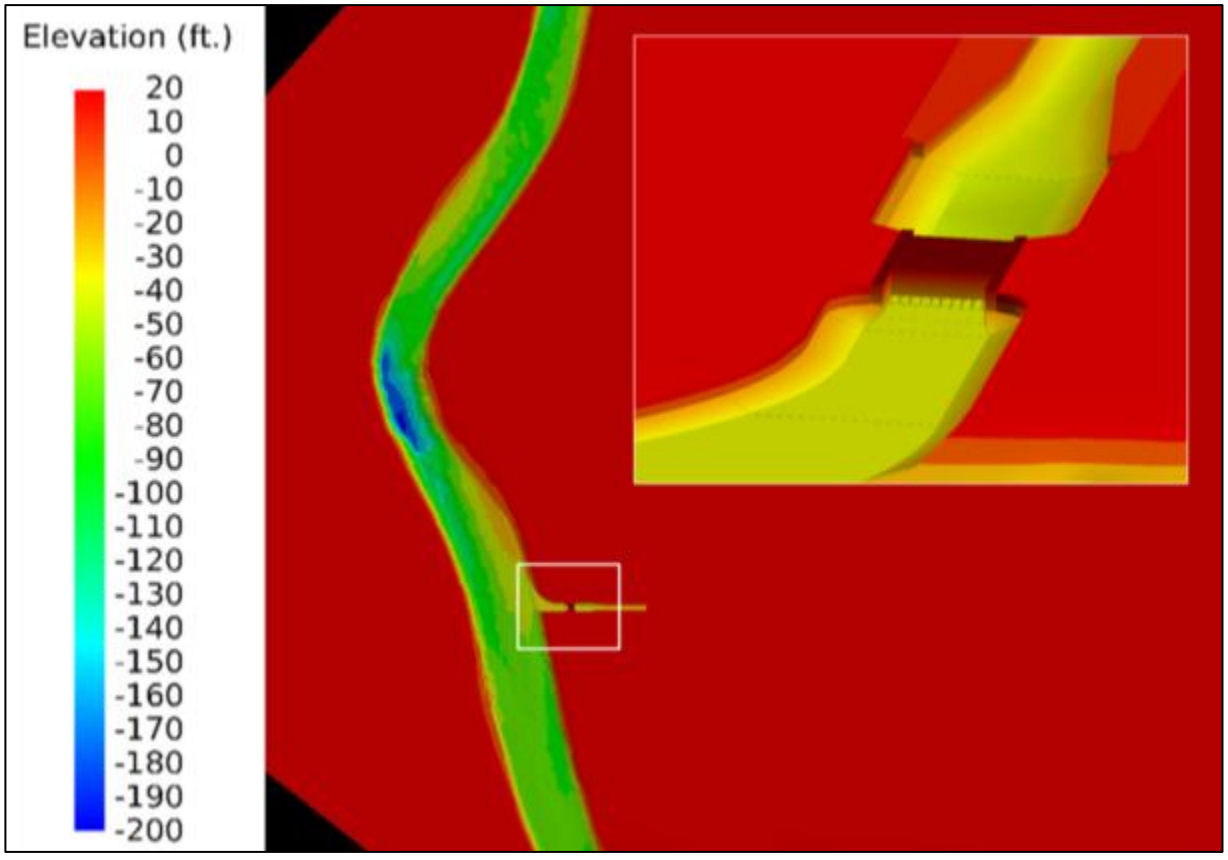

Figure 4-12. Location 4, Alternative E Model Development (bathymetry colored by elevation).

4.2.1 Model Setup

For consistency, model setups were similar to those used in the Feasibility Study Recommended Design Analysis. As before, **Rhino** was used to construct the three-dimensional CFD model of the river, the diversion intake structure, and the outfall channel; the bathymetry of the river was obtained from the base model. Unlike the Feasibility Study Recommended Design Analysis, in the model runs, the outfall channel and receiving basin were removed and the outfall channel was shortened to reduce the computational demands of the simulations.

4.2.2 Boundary Conditions

The boundary conditions were the same as those used for the base model analysis, except at the end of the outfall channel. In this set of calculations, a boundary condition approximately 6,000 feet downstream of the diversion structure along the outfall channel was added in place of the full outfall channel and receiving basin. The boundary condition was a tail water elevation of 4.1 feet, which was determined by extracting the elevation calculated during the Feasibility Study Recommended Design Analysis simulation.

4.2.3 Simulation

Flow conditions were the same as those used in the Feasibility Study Recommended Design Analysis, except that the tail water at the end of the outfall channel was raised to an elevation of 4.1 feet NAVD88. This was the water surface elevation calculated at the end of the outfall channel from the Feasibility Study Recommended Design Analysis.

4.2.3.1 Hydrodynamics

Figure 4-13, Figure 4-14, Figure 4-15, and Figure 4-16 show streamlines entering the diversion channel from different heights in the water column for Location 3 - Alternative B, Location 3 - Alternative C, Location 3 - Alternative D, and Location 4 - Alternative E. Additional results, appearing in Appendix A.2, show water surface elevations and flow speeds in the river for the different alternatives.

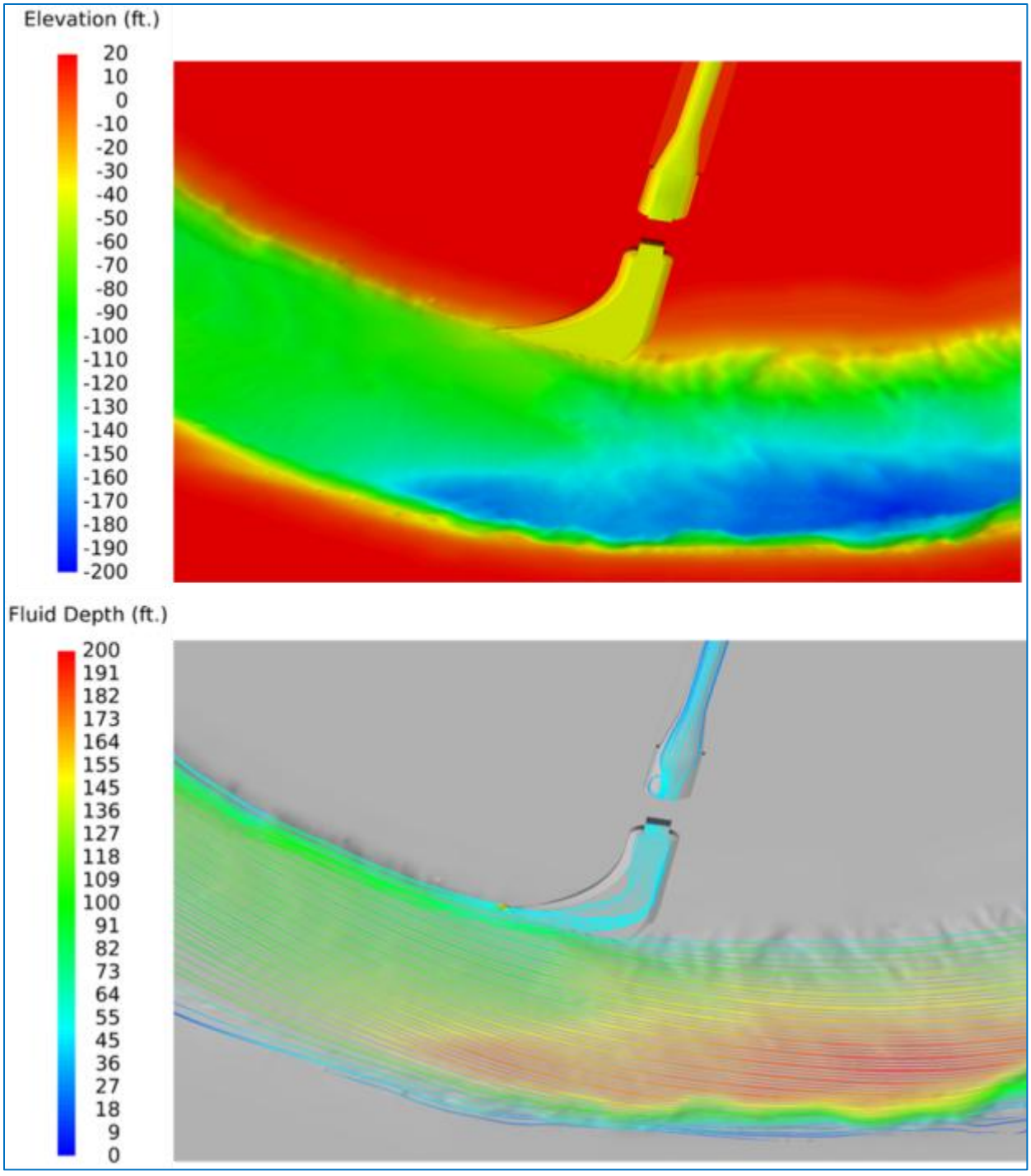

Figure 4-13. **Initial Domain Model Results, Location 3, Alternative B (Top) Bathymetry Colored by Elevation, (Bottom) Streamlines Colored by Fluid Depth.**

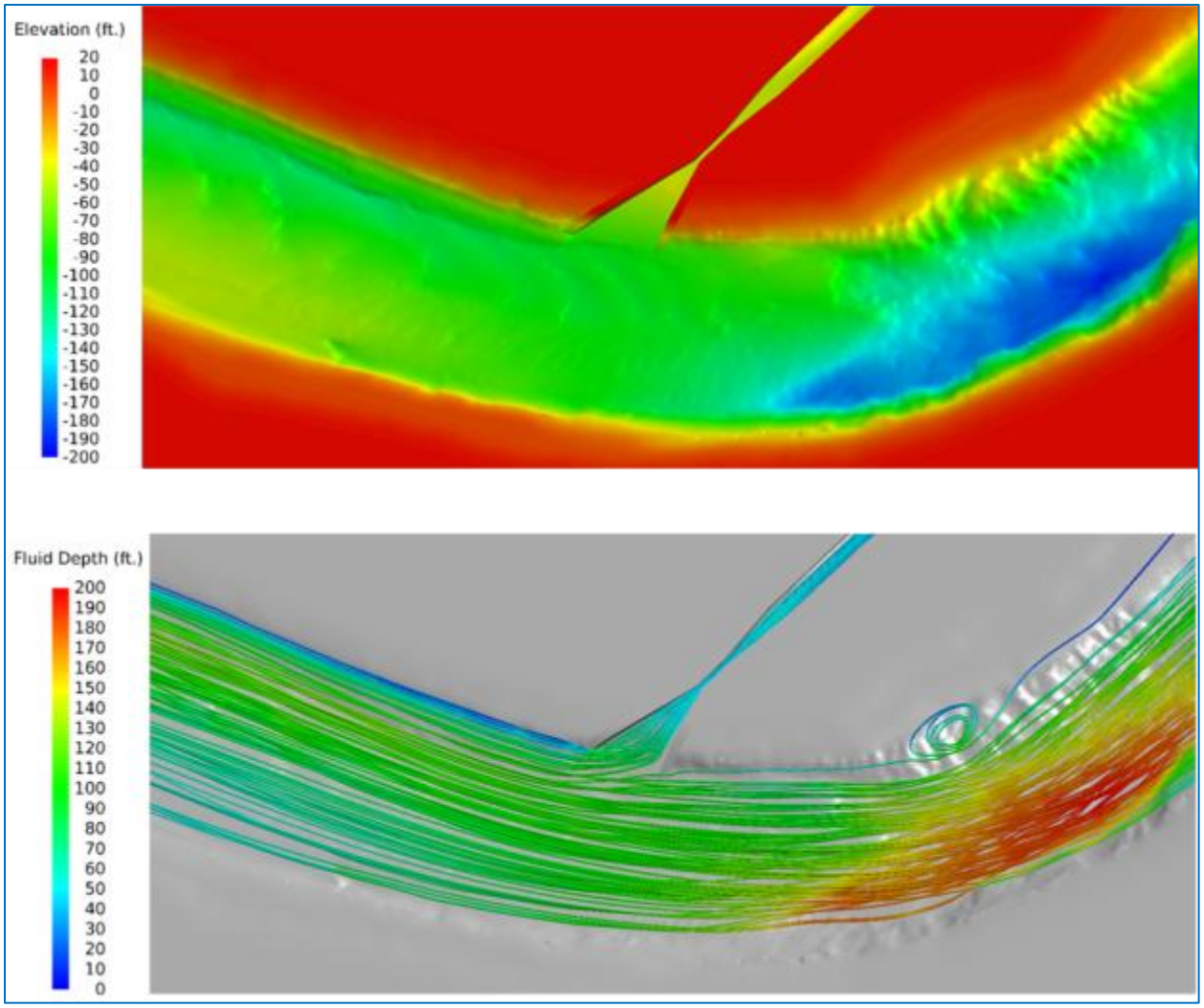

Figure 4-14. **Initial Domain Model Results, Location 3, Alternative C (Top) Bathymetry Colored by Elevation, (Bottom) Streamlines Colored by Fluid Depth.**

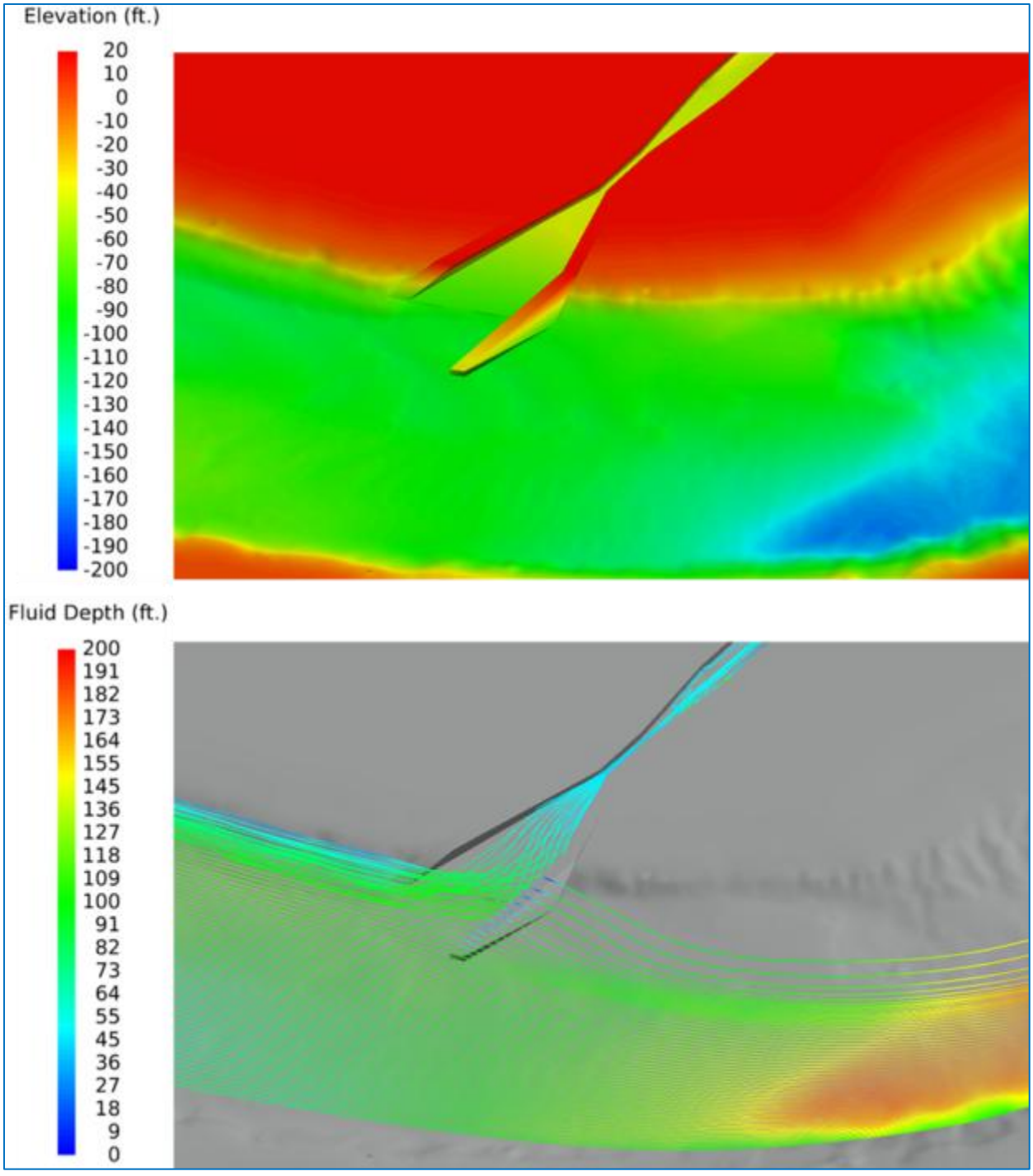

Figure 4-15. Initial Domain Model Results, Location 3, Alternative D (Top) Bathymetry Colored by Elevation, (Bottom) Streamlines Colored by Fluid Depth.

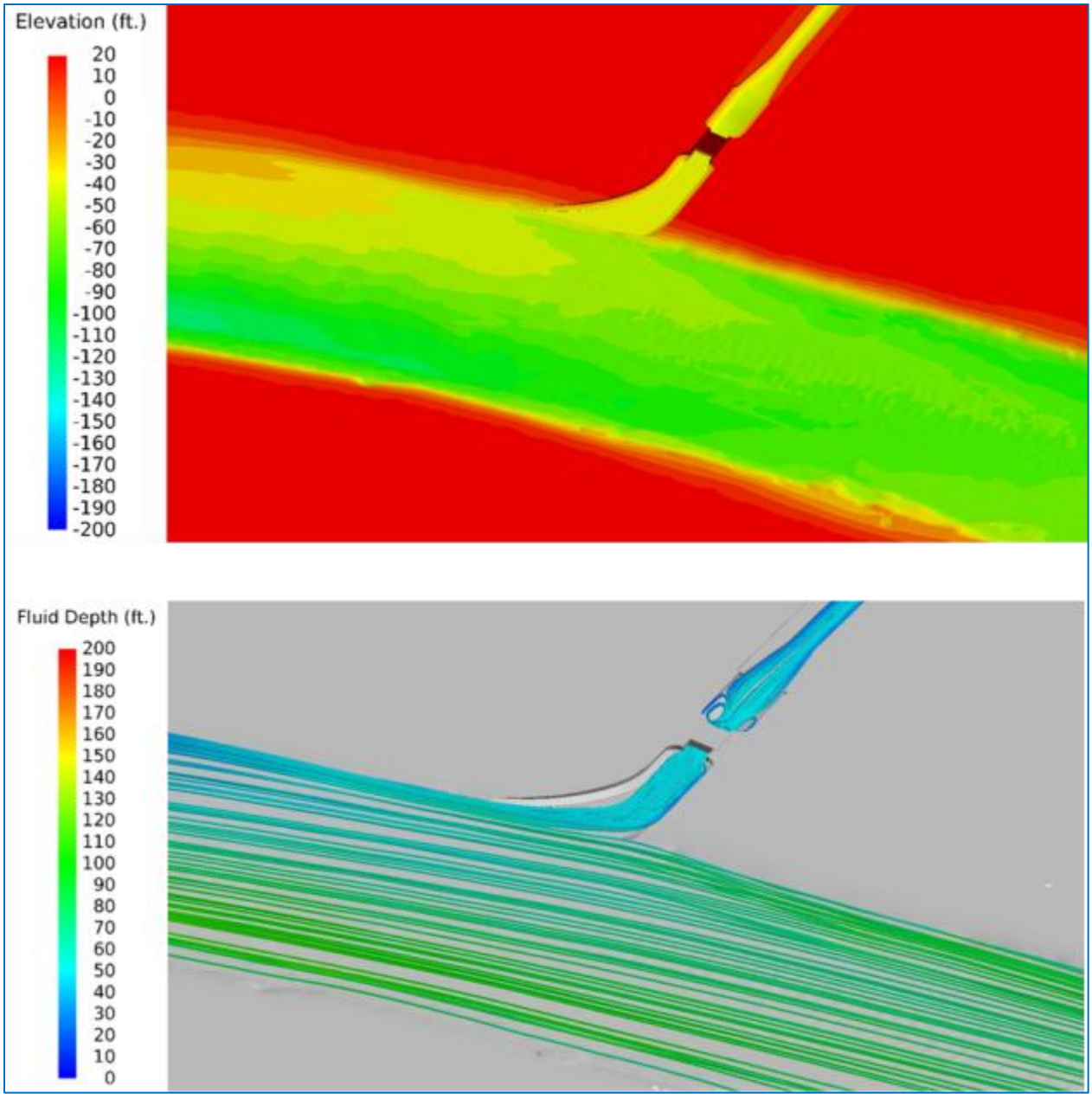

Figure 4-16. Initial Domain Model Results, Location 4, Alternative E (Top) Bathymetry Colored by Elevation, (Bottom) Streamlines Colored by Fluid Depth.

4.2.3.2 Sediment Capture

Similar to the Feasibility Study Recommended Design Analysis, sediments were grouped into seven separate size classes (2, 8, 32, 63, 96, 125, and 250 microns), and particles were released at the upstream boundary of the river after steady flow patterns in the river were calculated. To determine the

amount of sediment captured in the diversion intake structure, the number of particles passing through it was recorded. Results of the sediment analysis are summarized in Table 4-6 and Table 4-7. Table 4-6 shows the amount of flow entering the intake channel and the amount of sediment captured (in metric tons per day) by the diversion intake structure. Table 4-7 presents calculated SWRs. The computed SWR for all alternatives is less than 1.0 (ref. Equation 4-1). The sediment load captured in the intake structure in terms of cubic yards per year is shown in Table 4-8. Note that Table 4-6, Table 4-7, and Table 4-8 include Location 3, Alternative A from the Feasibility Study Recommended Design Analysis, for easy comparison of all simulations completed using the initial model domain.

Table 4-6. Initial Model Calculated Sediment Capture (metric ton per day)

Description		Flow Rate		Sediment Load (metric ton/d)							Total
		(m^3/s)	(cfs)	2 Microns	8 Microns	32 Microns	64 Microns	96 Microns	125 Microns	250 Microns	Load (metric ton/day)
Mississippi River		19,822	700,000	41,898	140,396	77,050	10,839	21,816	34,437	23,460	349,896
Intake Channel	Location 3-A	676	23,873	1,429	4,788	267	47	99	166	0	6,796
	Location 3-B	623	22,001	1,317	4,413	1,690	212	213	277	0	8,122
	Location 3-C	1,156	40,824	2,443	8,188	3,378	431	587	203	6	15,236
	Location 3-D	1,180	41,671	2,494	8,358	2,620	300	394	307	1	14,474
	Location 4-E	612	21,613	1,294	4,335	1,013	135	182	326	0	7,284

Table 4-7. Initial Model Calculated Sediment Water Ratios

Description		Flow Rate		Sediment Water Ratios by Size Class							Total
		(m^3/s)	(cfs)	2 Microns	8 Microns	32 Microns	64 Microns	96 Microns	125 Microns	250 Microns	SWR
Intake Channel	Location 3-A	676	23,873	1.0	1.0	0.1	0.1	0.1	0.1	0.0	0.6
	Location 3-B	623	22,001	1.0	1.0	0.7	0.6	0.3	0.3	0.0	0.7
	Location 3-C	1,156	40,824	1.0	1.0	0.8	0.7	0.5	0.1	0.0	0.7
	Location 3-D	1,180	41,671	1.0	1.0	0.6	0.5	0.3	0.1	0.0	0.7
	Location 4-E	612	21,613	1.0	1.0	0.4	0.4	0.3	0.3	0.0	0.7

Note: The density used in the calculation was 100 pounds per cubic foot.

Table 4-8. Initial Model Calculated Sediment Loading

Description		Cubic Yards/Year			Metric Ton/Day		
		Total 2-250 Micron Load	Total 32-250 Micron Load	Total 64-250 Micron Load	Total 2-250 Micron Load	Total 32-250 Micron Load	Total 64-250 Micron Load
Intake Channel	Location 3-A	332,951	28,370	15,285	6,796	579	312
	Location 3-B	397,908	117,211	34,392	8,122	2,392	702
	Location 3-C	746,453	225,605	60,113	15,236	4,605	1,227
	Location 3-D	709,121	177,466	49,090	14,474	3,622	1,002
	Location 4-E	356,867	81,120	31,502	7,284	1,656	643

4.2.4 Conclusions and Recommendations

The following conclusions and recommendations were reached as a result of this analysis:

1. Design modifications, such as those considered at Location 3, appear to improve the operation of the diversion structure. These improvements were considered in future analyses.
2. The SWRs calculated at Location 3 (all alternatives) and at Location 4 do not meet design requirements for the structure. Although improved from Location 3, Alternative A, the calculated SWR for materials of 96 microns or coarser is significantly less than 1.0 for all alternatives, implying a poor overall diversion location.
3. The sill elevation of -40 feet notably improved the sediment capture at 32 and 64 microns, as well as some minor improvement of 96-micron material.
4. Although Location 3 total SWRs were not substantially improved for higher flow rates (e.g., 40,000 cfs compared to 20,000 cfs), the SWRs for some individual size classes showed some general improvement.
5. The alignment of the entrance to the diversion structure is improved (e.g., flow separation in the entrance of the structure is significantly improved).
6. Open channel diversion designs appear to render similar SWRs as box culvert designs.

Based on these findings, it was recommended that other locations for the diversion structure upstream of Location 3 be considered, particularly to improve the sediment capture of coarse material. A target

diversion flow rate of 35,000 cfs is recommended for river flow rates of 600,000 cfs and greater in order to maximize the sediment output from the diversion. This included a recommendation of further consideration of Location 4 because it was located in area where sediments naturally collect and is close to the discharge basin. Additionally, in coordination with USACE cost estimations, the team determined that all designs moving forward would incorporate an open channel layout rather than box culverts due to cost and constructability considerations.

4.3 Extended Domain Design Alternatives Study

Based on findings from the Initial Domain Design Alternatives Study (Section 4.2), the model domain was extended from RM 56 above the Head of Passes to RM 76 at Belle Chasse. This change was made so that other locations, such as Location 1 (Figure 4-1), could be considered. The extended model also allows flow in the river to develop fully before reaching the proposed diversion locations. The extended model setup, calibration, and validation are further described in Section 3.

The model setups, used in this alternatives analysis, included improvements identified previously in the Initial Domain Design Alternative Study where applicable (e.g., lowering the sill elevation, changing the alignment of the intake channel, enlarging the size of the intake structure, and streamlining the entrance of the diversion channel). Five alternate locations were considered in this part of the study (Locations 1, 2, 2.5, 3, and 4), and each alternative was selected based on recommendations from the feasibility study (USACE and CPRA 2010). See Figure 4-1, Table 4-1, and Table 4-2 for further details on the location or design configuration of the alternatives.

The five alternatives studied in this analysis are identified as follows:

- Location 1, Alternative G – A 72-foot wide intake structure with a rectangular open channel designed for a capacity of 35,000 cfs (the width of the intake structure was calculated using the energy equation, Appendix A.4), and a sill elevation lowered to an elevation of -40 feet NAVD88. The approach angle was 90 degrees at this location to align with the proposed outfall channel. The diversion layout is shown in Figure 4-17.

- Location 2, Alternative F – Similar to Location 1, Alternative G, but with an approach angle of 45 degrees. The layout is shown in Figure 4-18.

- Location 2.5, Alternative F – Similar to Location 2, Alternative F. The layout is shown in Figure 4-19.

- Location 3, Alternative F – Similar to Location 2, Alternative F. The layout is shown in Figure 4-20.
- Location 4, Alternative F – Similar to Location 2, Alternative F. The layout is shown in Figure 4-21.

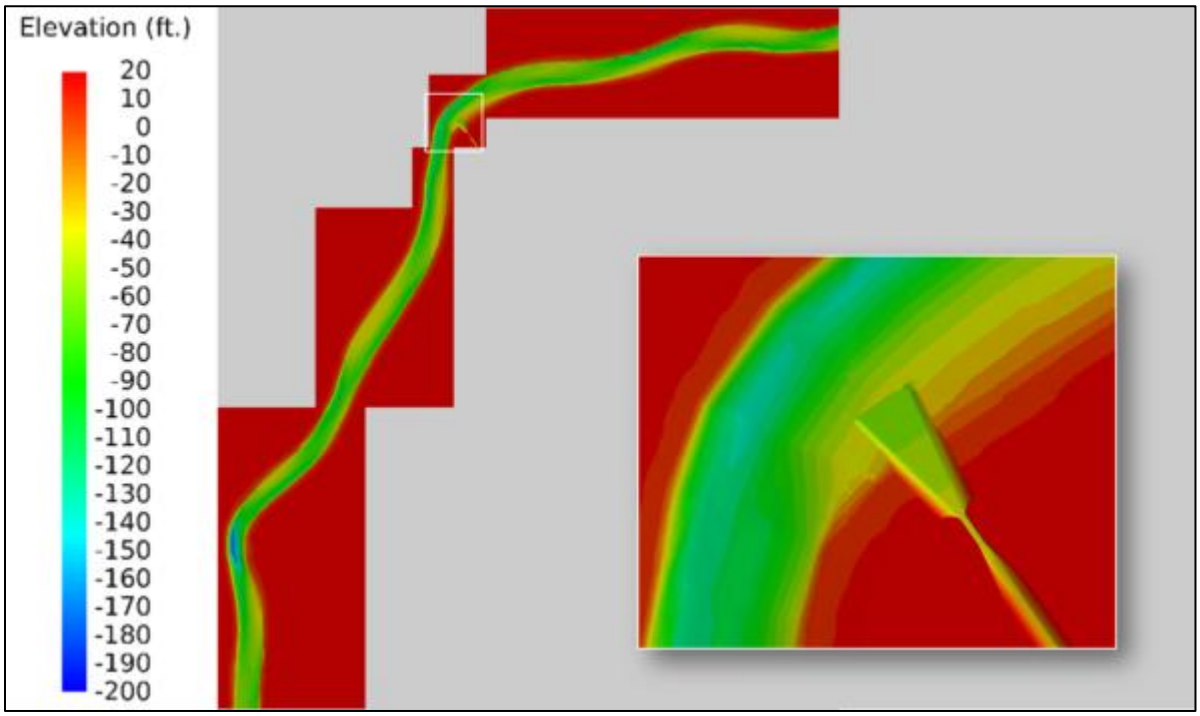

Figure 4-17. Model Development for Location 1, Alternative G (bathymetry colored by elevation).

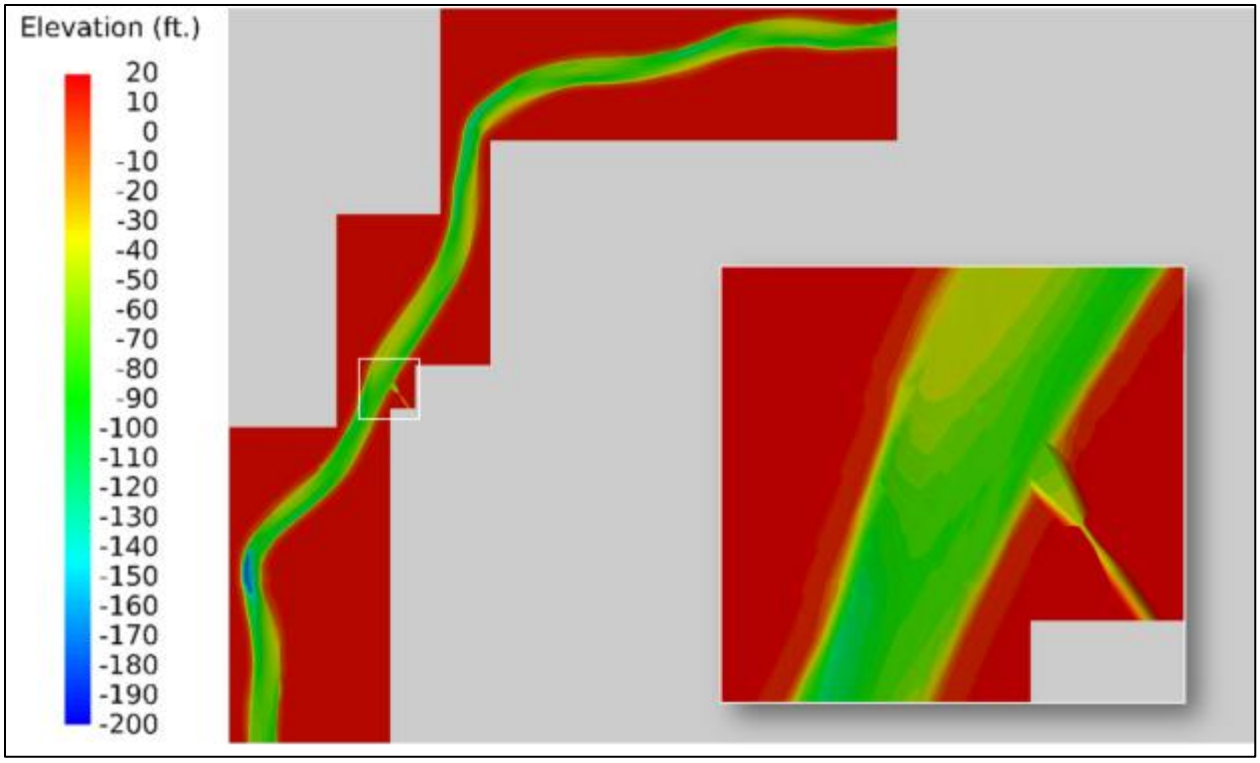

Figure 4-18. Model Development for Location 2, Alternative F (bathymetry colored by elevation).

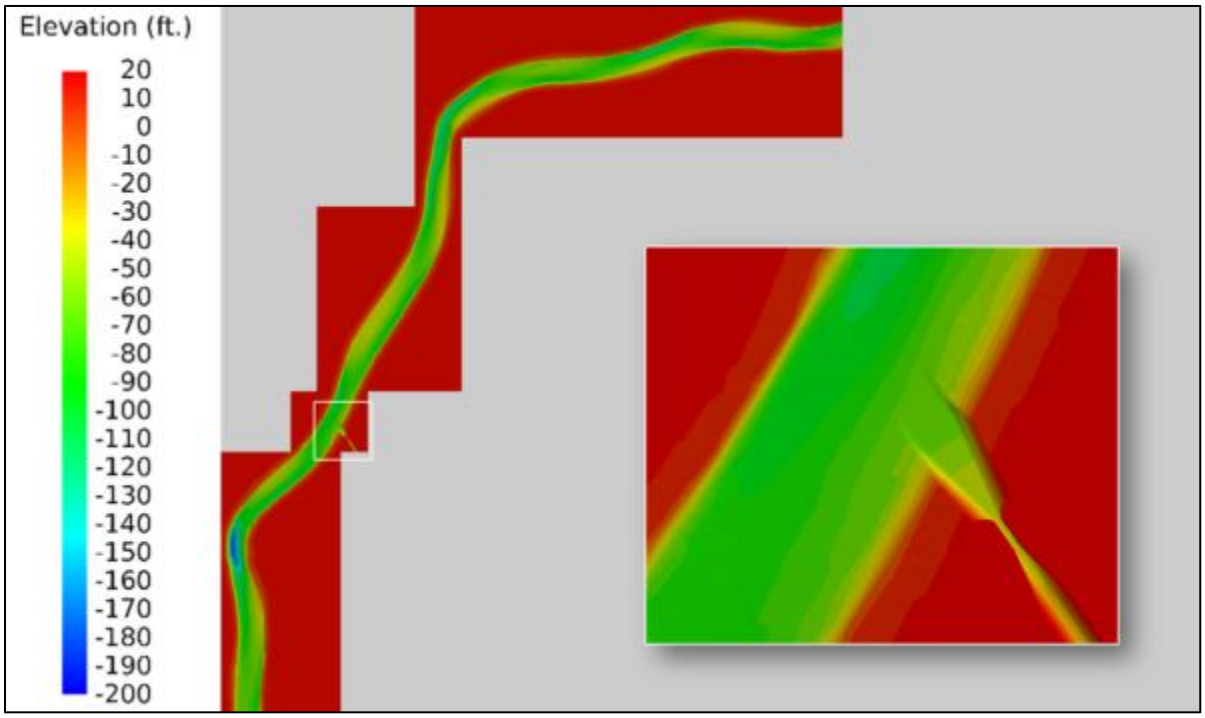

Figure 4-19. Model Development for Location 2.5, Alignment F (bathymetry colored by elevation).

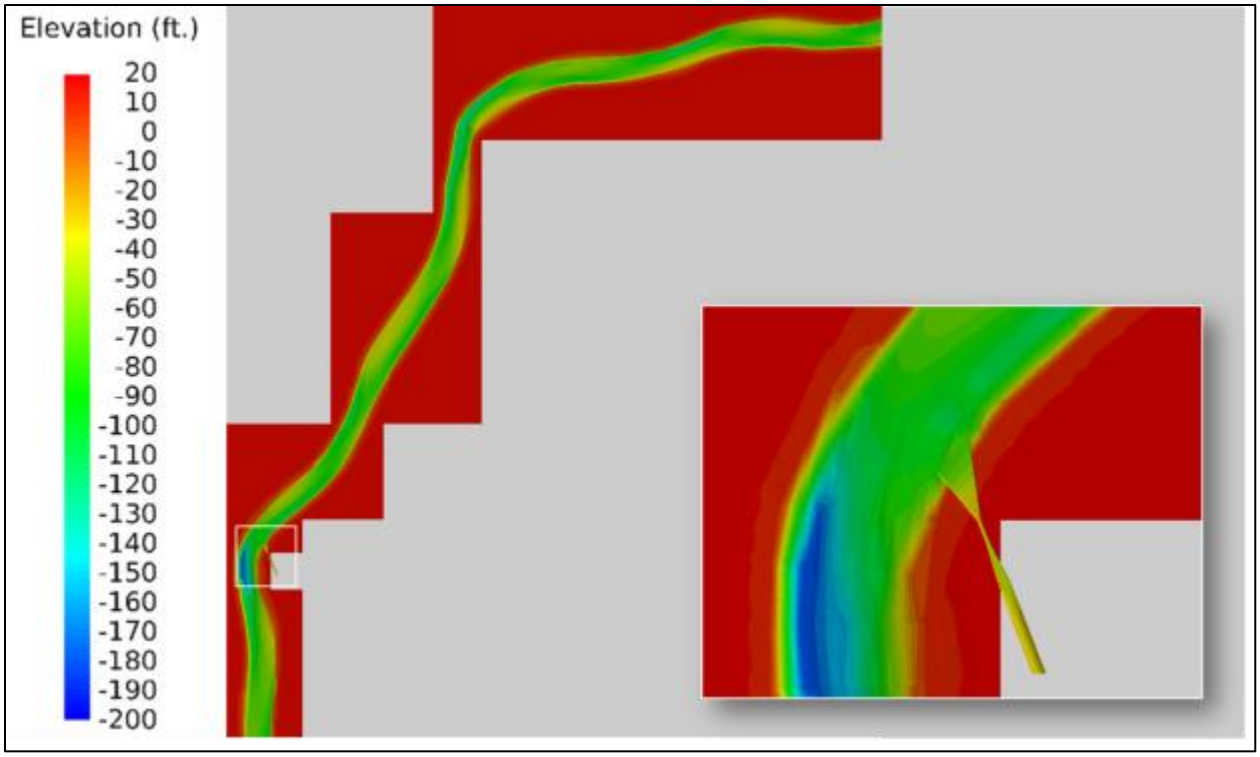

Figure 4-20. Model Development for Location 3, Alignment F (bathymetry colored by elevation).

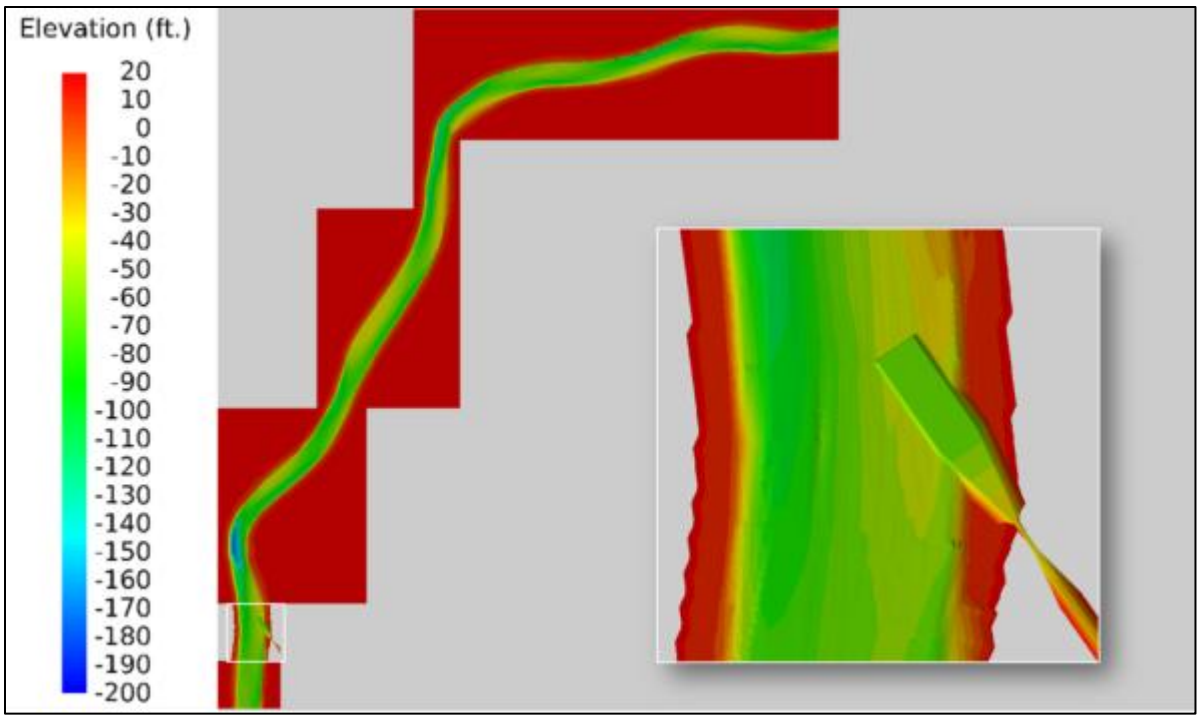

Figure 4-21. Model Development for Location 4, Alignment F (bathymetry colored by elevation).

4.3.1 Model Setup

The extended model domain was set up similar to the initial model domain and the setup described for model calibration and validation in Section 3. The additional bathymetry was obtained from surveyed single-beam data collected by the USACE in 2003. This bathymetric dataset extends from RM 56 above the Head of Passes to RM 76 at Belle Chasse.

4.3.2 Boundary Conditions

The boundary conditions were the same as those used for the Initial Domain Design Alternatives Analysis, including the tail water condition in the outfall channel. Note that the tail water condition used at the end of the outfall channel was updated in an optimization analysis for Location 1, which was completed following the work effort described in this section.

4.3.3 Simulation

4.3.3.1 Hydrodynamics

Results appearing in Figure 4-22, Figure 4-23, Figure 4-24, Figure 4-25, and Figure 4-26 show the variation of flow speed in the river and the approach velocity at the entrance of the diversion channel for Locations 1, 2, 2.5, 3, and 4, respectively. The inserts on the lower right of the figures show the velocity vectors approaching the diversion channel at elevation 0 foot NAVD88. Additional results can be found in Appendix A.4.

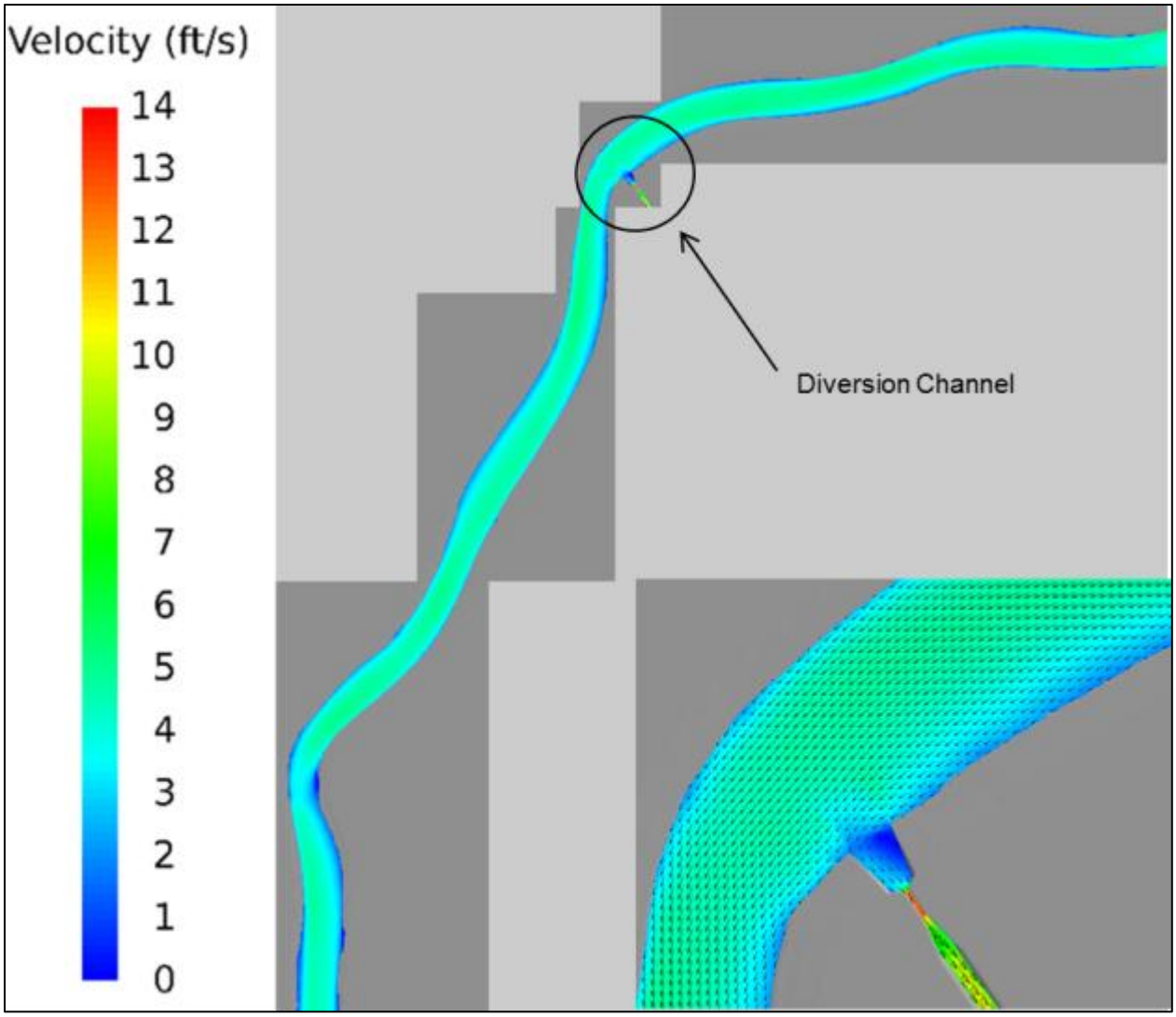

Figure 4-22. **Extended Domain Model Results, Location 1, Alternative G. Flow Speed Variation (near surface, colored by speed).**

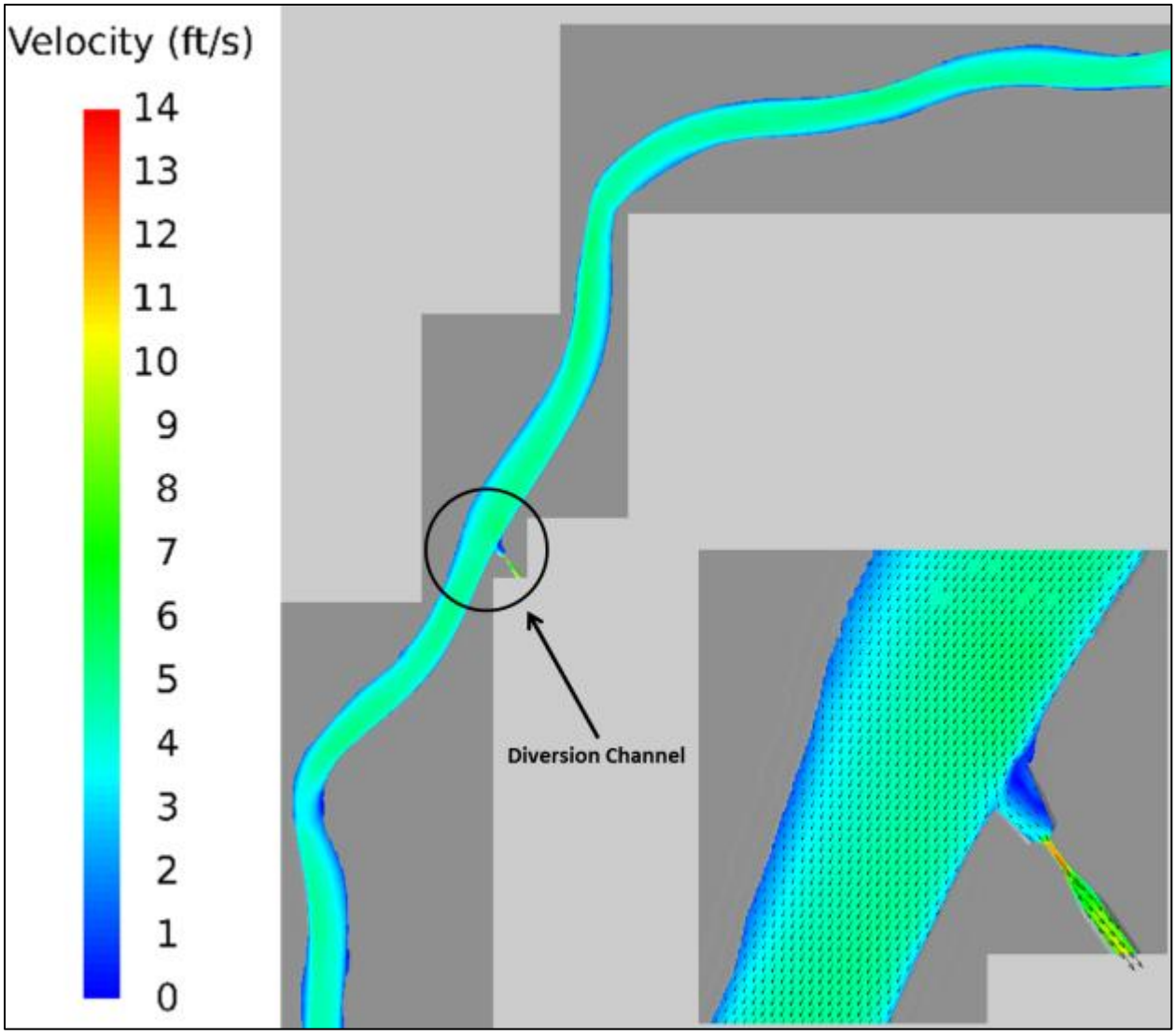

Figure 4-23. Extended Domain Model Results, Location 2, Alternative F. Flow Speed Variation (near surface, colored by speed).

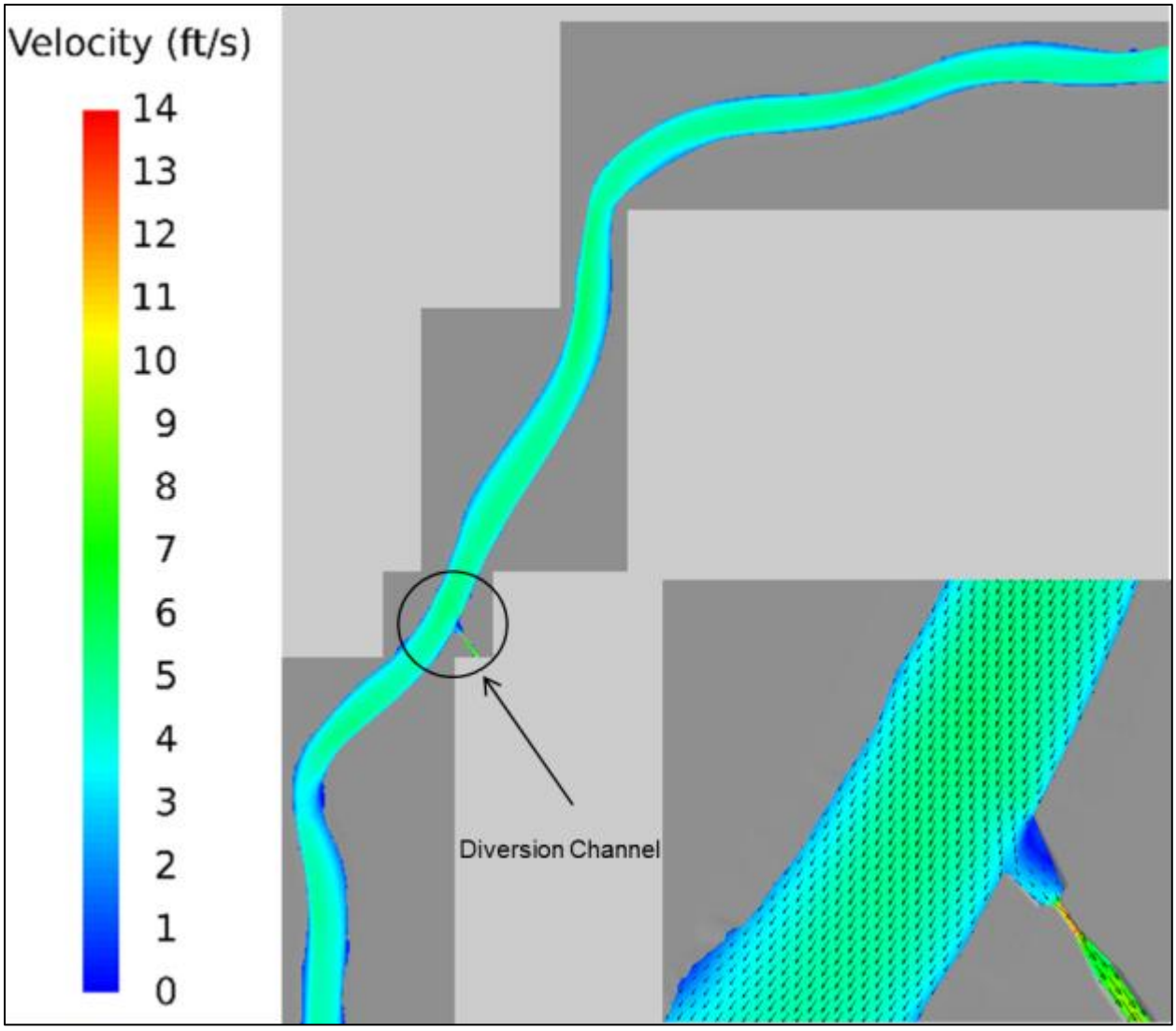

Figure 4-24. **Extended Domain Model Results, Location 2.5, Alternative F. Flow Speed Variation (near surface, colored by speed).**

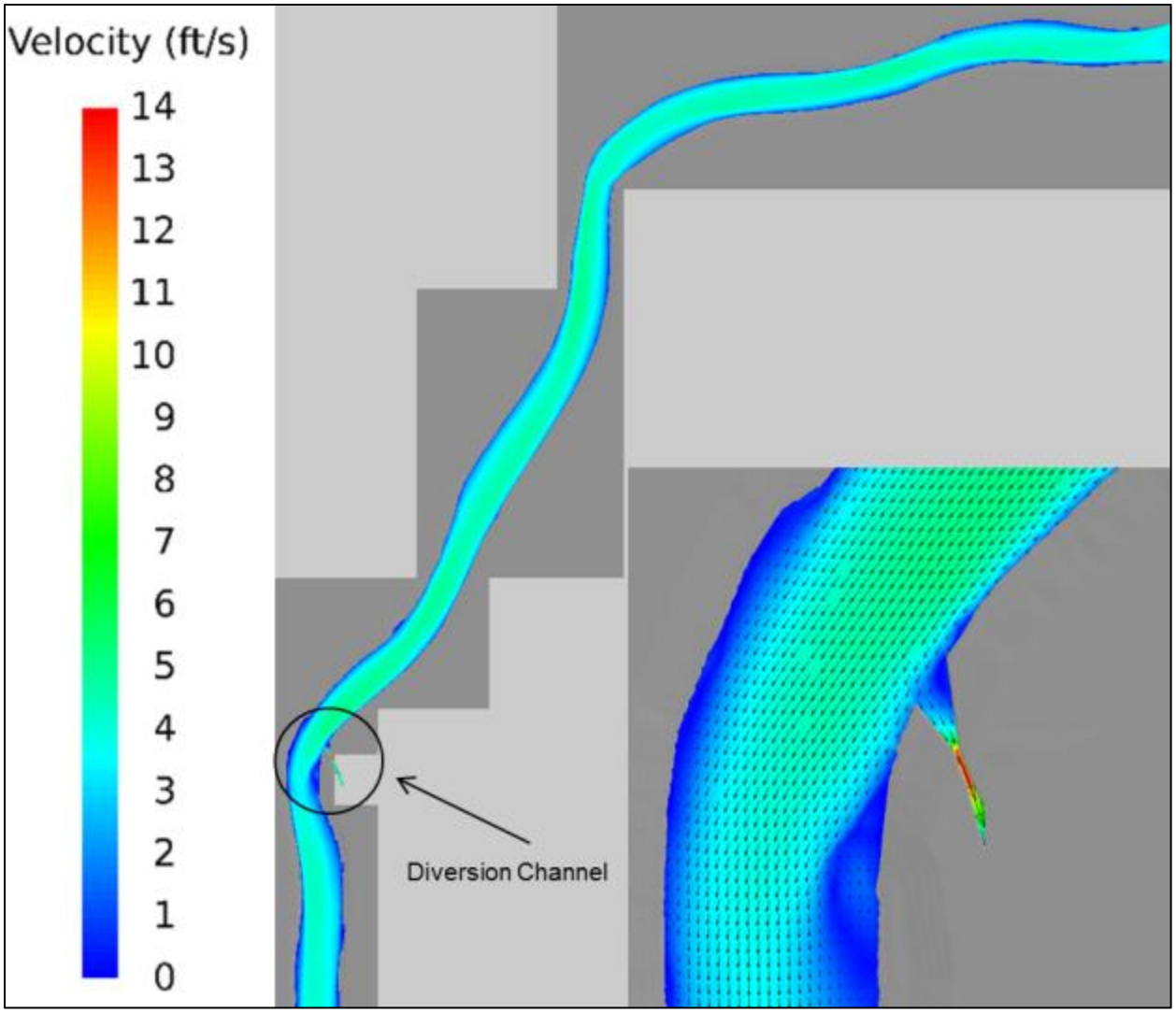

Figure 4-25. Extended Domain Model Results, Location 3, Alternative F. Flow Speed Variation (near surface, colored by speed).

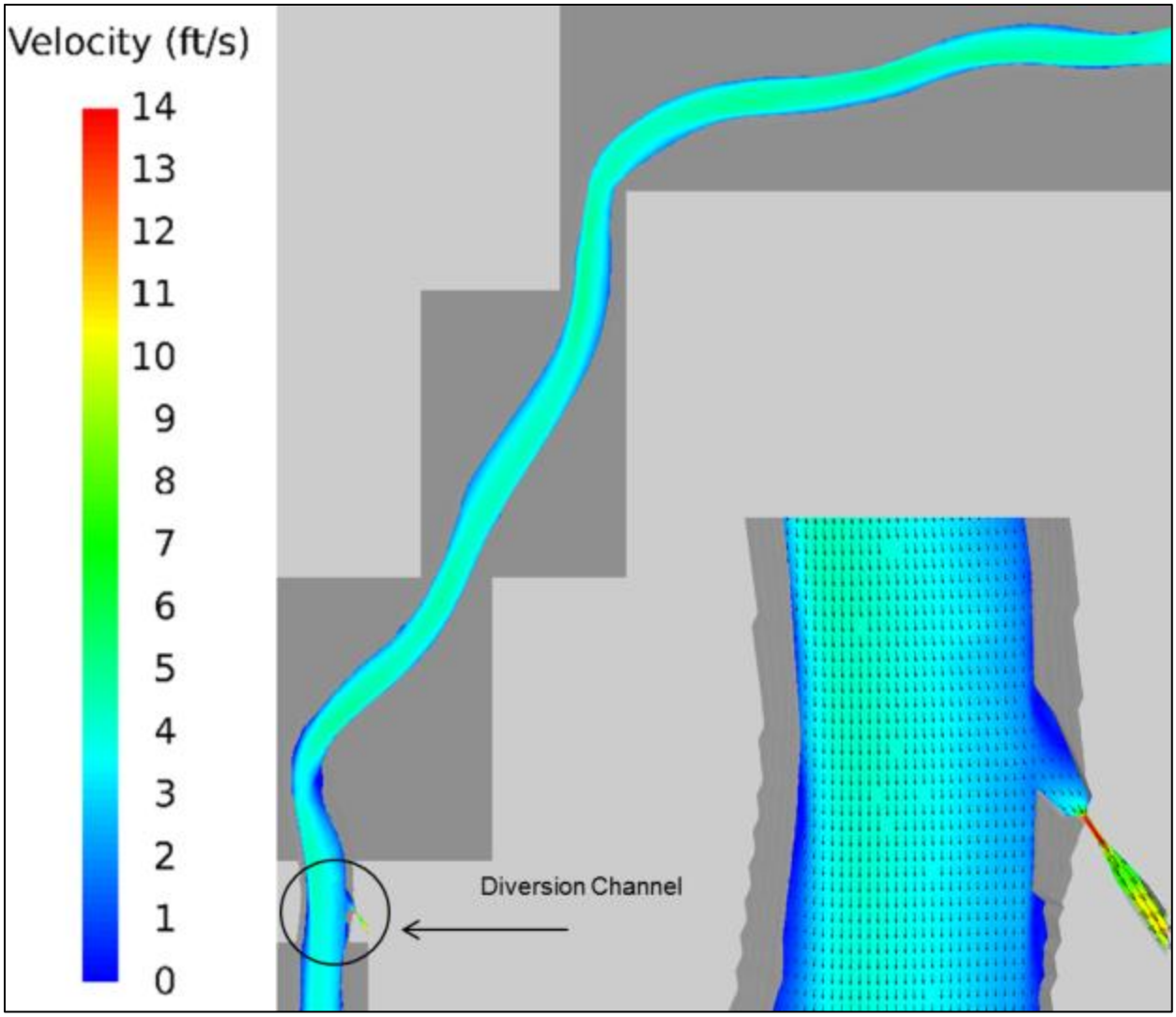

Figure 4-26. Extended Model Results, Location 4, Alternative F. Flow Speed Variation (near surface, colored by speed).

4.3.3.2 Sediment Capture

Table 4-9 identifies the seven sediment size classes used in this analysis, Table 4-10 provides calculated SWRs for each size class and in aggregate, and Table 4-11 provides loadings in metric tons per day. According to these results, sediment capture is the greatest at Location 1 and Location 4, with Location 1 being slightly more favorable for the coarsest materials.

Table 4-9. Extended Model Calculated Sediment Capture (metric tons per day)

Description		Flow Rate		Sediment Load (metric ton/d)							Total
		(m^3/s)	(cfs)	2 Microns	8 Microns	32 Microns	64 Microns	96 Microns	125 Microns	250 Microns	Load (metric ton/day)
Mississippi River		19,822	700,000	41,898	140,396	77,050	10,839	21,816	34,437	23,460	349,896
Intake Channel	Location 1-G	1,104	38,950	2,400	8,000	2,800	900	1,900	5,800	6,300	28,100
	Location 2-F	984	34,720	2,078	6,964	1,135	185	213	258	197	11,030
	Location 2.5-F	1,028	36,275	2,235	7,451	1,600	175	175	0	0	11,636
	Location 3-F	957	33,770	2,000	7,000	1,400	150	175	0	0	10,725
	Location 4-F	1,195	42,160	2,400	8,500	3,500	1,000	2,500	5,600	2,100	25,600

Table 4-10. Extended Model Calculated Sediment Water Ratios

Description		Flow Rate		Sediment Water Ratios by Size Class							Total
		(m^3/s)	(cfs)	2 Microns	8 Microns	32 Microns	64 Microns	96 Microns	125 Microns	250 Microns	SWR
Intake Channel	Location 1-G	1,104	38,950	1.0	1.0	0.7	1.5	1.6	3.0	4.8	1.4
	Location 2-F	984	34,720	1.0	1.0	0.3	0.3	0.2	0.2	0.2	0.6
	Location 2.5-F	813	28,600	1.0	1.0	0.4	0.3	0.2	0.0	0.0	0.6
	Location 3-F	957	33,770	1.0	1.0	0.4	0.3	0.2	0.0	0.0	0.6
	Location 4-F	1,195	42,160	1.0	1.0	0.8	1.5	1.9	2.7	1.5	1.2

Table 4-11. Extended Model Calculated Sediment Load

Description		Cubic Yards/Year			Metric Ton/Day		
		Total 2-250 Micron Load	Total 32-250 Micron Load	Total 64-250 Micron Load	Total 2-250 Micron Load	Total 32-250 Micron Load	Total 64-250 Micron Load
Intake Channel	Location 1-G	1,376,663	867,150	729,974	28,100	17,700	14,900
	Location 2-F	1,110,418	97,371	41,760	22,666	1,988	852
	Location 2.5-F	570,066	95,534	17,147	11,636	1,950	350
	Location 3-F	525,434	84,510	15,922	10,725	1,725	325
	Location 4-F	1,254,184	720,176	548,705	25,600	14,700	11,200

4.3.4 Conclusions and Recommendations

According to these results, a diversion at Location 1 and Location 4 would capture the greatest amount of sediment, with Location 1 rendering an overall sediment load and coarse sediment load approximately 10 percent and 33 percent larger than Location 4, respectively. Location 1 is in a river bend where secondary flow patterns carry sediment into the entrance of the diversion structure. At this location, particularly for larger material, SWRs are calculated to be greater than 1.0.

Additionally, an important trend to note is that both the flow rate and SWR for Location 4, Alternative F (Table 4-10) are nearly twice as high as those parameters for Location 4, Alternative E (Table 4-7). This trend highlights the importance of diverting a sufficient flow rate to mobilize coarse silts and sands, regardless of the diversion location or design. These results support the recommendation in Section 4.2 to operate the diversion at a flow rate of 35,000 cfs for river flow rates of 600,000 cfs and greater in order to maximize the sediment output from the diversion.

Figure 4-27 shows the distribution of silt (8 microns) and sand (96, 125, and 250 microns) near the diversion channel at Location 1. Sediment particles of unique classes are represented by various colors in the figure. As shown, heavier particles move closer to the LDB of the river near Location 1. The movement of particles toward the riverbank near Location 1 is influenced by both the curvature and shape of the river channel upstream and downstream of the intake channel. As a result of flow patterns that develop and the particles' own momentum, a larger proportion of the total sediment load is calculated to

enter the diversion structure at Location 1 compared to the other locations that were studied (and this behavior becomes more pronounced as the diameter of the particles gets larger as shown in Table 4-10).

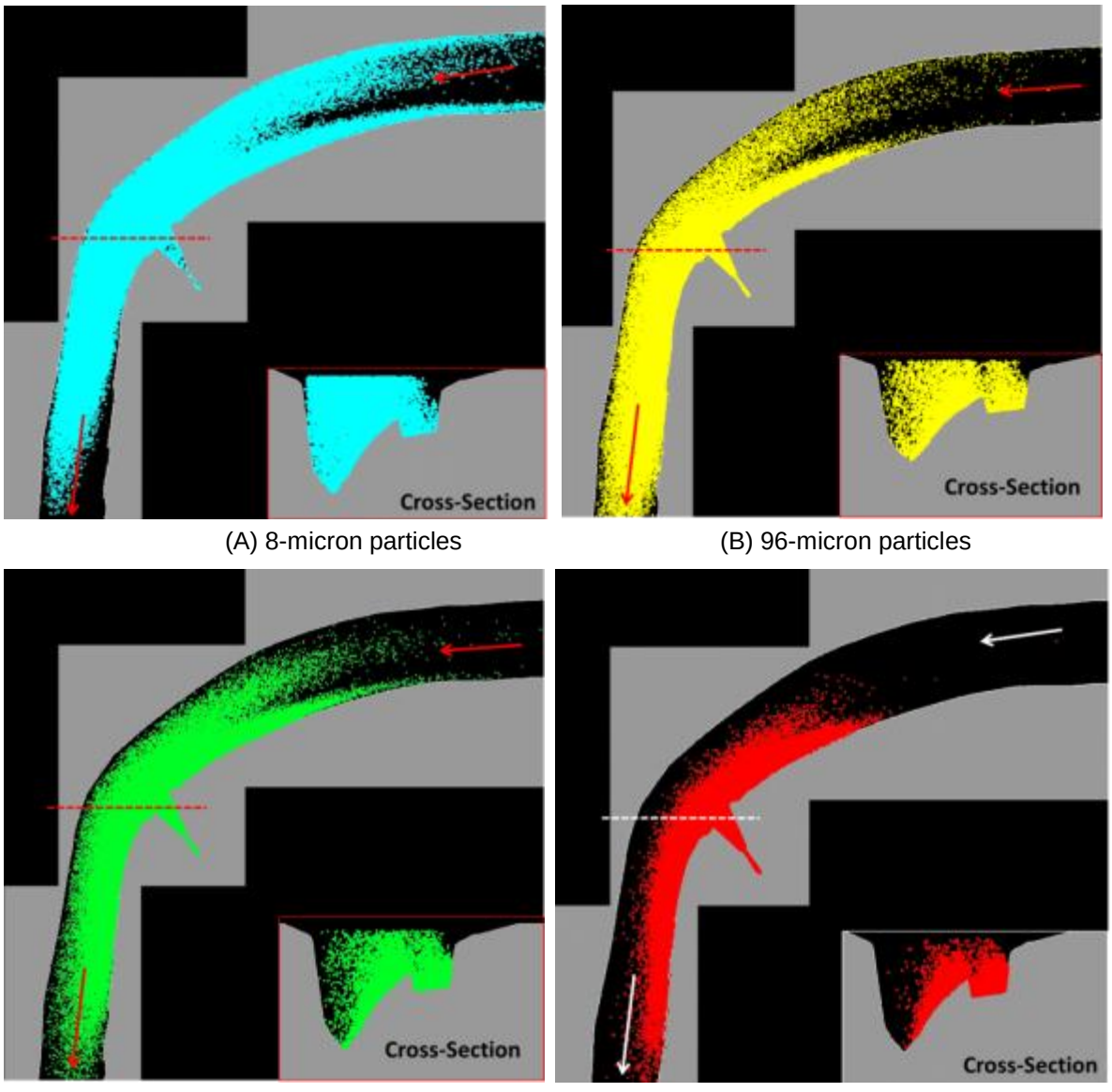

(A) 8-micron particles (B) 96-micron particles

(C) 125-micron particles (D) 250-micron particles

Figure 4-27. Particle Distributions at Location 1. (A) 8 microns, (B) 96 microns, (C) 125 microns, and (D) 250 microns.

Figure 4-28 shows the distribution of 250-micron particles near the entrance to diversions at Locations 1, 2, 2.5, 3, and 4. Similar to results shown for Location 1, 250-micron particles at Location 4 are carried

into the diversion in large numbers. Referring again to Table 4-10, SWRs at Location 4 are similar, but somewhat less than those calculated at Location 1; SWRs at Locations 2, 2.5, and 3 are rather low.

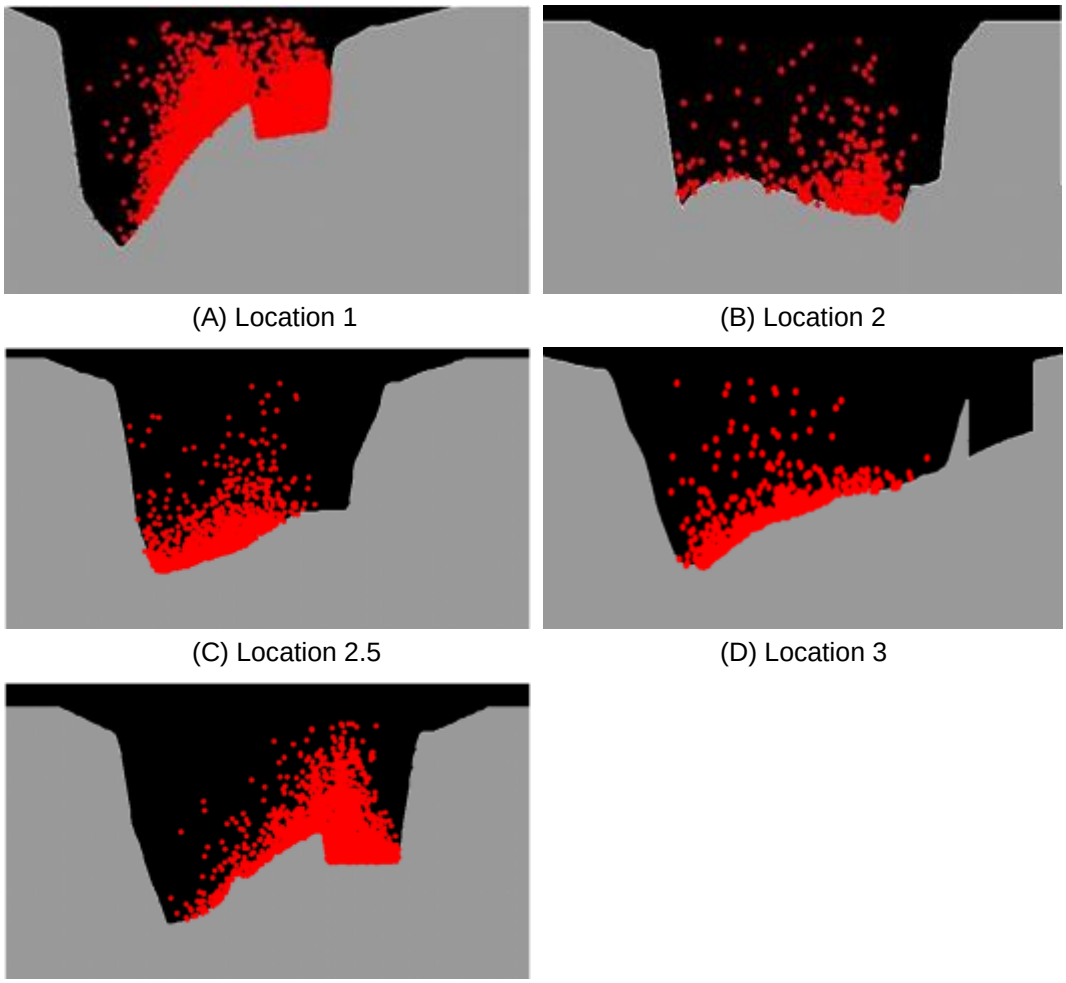

(A) Location 1 (B) Location 2

(C) Location 2.5 (D) Location 3

(E) Location 4

Figure 4-28. Particle Distributions at Different Diversion Locations. (A) Location 1, (B) Location 2, (C) Location 2.5, (D) Location 3, and (E) Location 4.

Based on these findings and discussions with the USACE, CPRA, and others, it is recommended that the diversion structure be positioned at Location 1 and that further design improvements be considered in the final design of the structure. Location 1 was selected rather than Location 4 primarily due to considerations beyond those examined in this study, including cost considerations and potentially improved ecosystem benefits due to the positioning of the outfall in the upper reaches of the receiving basin.

4.4 Diversion Structure Design Variations

A final group of simulations was carried out to investigate design variations intended to improve the design of the diversion structure at Location 1. Similar to the designs evaluated in Section 4.3, the diversion structures in this section are intended to divert 35,000 cfs when the flow rate in the Mississippi River is equal to 600,000 cfs or greater. Design parameters considered in the analyses were: (a) sill elevation of the diversion structure; (b) size of the intake structure; (c) alignment of the diversion structure with respect to the riverbank; and (d) the shape of the diversion channel entrance, particularly consideration of an approached slope into the river. In all, six different design variations were modeled as shown in Table 4-12 (these are referred to as Base and Optimizations 1, 2, 3, 4, and 5 in the table).

Table 4-12. Location 1 Diversion Structure Design Variations.

Design Variations	Type of Intake Structure	Invert Elev. (ft. NAVD88)	Effective Width (feet)	Length (feet)	Approach Channel Bottom	Angle of Intersection with the River	Shape of Inflow/ Approach Channel	Shape of Outfall Channel (Trapezoid)
Base	open channel	-40	72	360	sloped to the -50 foot contour	90 degree	wide entrance	Base: 72’ Side Slope: 1:3
Optimization 1	open channel	-30	89	360	flat	90 degree	wide entrance	Base: 380’ Side Slope: 1:3
Optimization 2	open channel	-25	89	360	flat	90 degree	wide entrance	Base: 380’ Side Slope: 1:3
Optimization 3	open channel	-40	72	360	flat	90 degree	wide entrance	Base: 380’ Side Slope: 1:3
Optimization 4	open channel	-40	60	360	flat	45 degree (curve)	wide entrance	Base: 380’ Side Slope: 1:3
Optimization 5	open channel	-40	72	360	flat	90 degree (rounded leading edge)	wide entrance	Base: 380’ Side Slope: 1:3
	with gate	-40	72	360	flat	90 degree (rounded leading edge)	wide entrance	Base: 380’ Side Slope: 1:3

The goal of these analyses was to identify a diversion design that maximized capture efficiency (SWRs) and minimized flow separation in the entrance of the structure to avoid sediment deposition and reduce headloss.

All of the simulations in this phase were completed assuming a tail water elevation of 5 feet NAVD88 in the outfall channel. The tail water elevation was provided by the USACE Engineering Research and Development Center (ERDC) and determined as part of the Adaptive Hydraulics (ADH) model analysis in the receiving basin.

The simulations in this phase of the project were completed serially such that the results of each simulation could inform the next. The project scope was adjusted during this phase of the study to accommodate these additional design optimization simulations. The revised scope resulted from the additional analyses necessary to determine an optimal diversion location. Because of project schedule and budget constraints, the number of optimization simulations was limited to six for this phase. The six simulations were strategically designed to analyze critical design features, but were not an exhaustive design analysis suitable for final project design.

The six design variations studied in this analysis are described as follows:

- Base – The setup for the baseline analysis was based on the one used at Location 1 for site selection. In this study, the diversion structure was moved along the river to an exact river mile location dictated by the USACE, and the entrance of the diversion channel was aligned 90 degrees with respect to the riverbank. The invert elevation of the diversion structure was set at an elevation of -40 feet NAVD88 with a sloping channel bottom to an elevation of -50 feet in the river. The intake structure was modeled as a rectangular open channel with an effective width of 72 feet and length of 360 feet, and the outfall channel was modeled as a trapezoidal channel with base of 72 feet and side slope of 1:3. Following completion of the simulations for this geometry, USACE engineers reviewed the design cost estimation and maintenance considerations. Ultimately, this design was identified as an unfeasible configuration because of maintenance and constructability concerns raised by USACE engineers due to the sloped approach channel bottom; an invert elevation of -50 feet NAVD88 and sloped channel bottom into the river were identified as potentially too costly to construct and maintain. However, this setup was included in the analysis as a basis of comparison, as well as to document a potential adaptive management strategy (e.g., sloping the channel bottom) for future consideration.

- Optimization 1 – The sill of the Base model was raised to an elevation of -30 feet NAVD88, and the width of the intake structure was increased to 89 feet so that the effective flow area of the diversion was maintained. The entrance alignment angle to the structure with respect to the riverbank was maintained at 90 degrees, but with a flat approach channel bottom. The length of the outfall channel was increased to 380 feet and side slope was equal to 1:3 (Note: these changes were made to be

consistent with USACE ERDC ADH modeling). Results of the simulation were used to indicate whether or not the calculated performance of the structure could be maintained or improved if the entrance to the structure was raised in coordination with a flat approach channel bottom. The diversion layout is shown in Figure 4-29 (top frame).

- Optimization 2 – The setup was similar to Optimization 1, except the sill elevation was raised to an elevation of -25 feet NAVD88. The diversion layout is shown in Figure 4-29 (lower frame). Again, the results were used to indicate whether or not the calculated performance of the structure could be maintained or improved if the entrance to the structure was raised in coordination with a flat approach channel bottom.

- Optimization 3 – Based on modeling results from the first two optimization runs, the sill elevation was set to an elevation of -40 feet NAVD88, the effective width of the intake structure was changed to 72 feet, and the length was set to 360 feet. The entrance alignment angle to the structure with respect to the riverbank was maintained at 90 degrees, but with a flat approach channel bottom. The length of the outfall channel was set to 380 feet with a side slope of 1:3. This optimization run is similar to the base run without the sloped approach channel bottom and with a revised outfall channel. The diversion layout is shown in Figure 4-30 (top frame).

- Optimization 4 – The setup was similar to Optimization 3, except the effective width of the intake structure was reduced to 60 feet and the entrance alignment angle to the structure was changed from 90 degrees to about 45 degrees with respect to the riverbank. The approach channel was also curved to better approximate the trajectory of flow patterns. The diversion layout is shown in Figure 4-30 (bottom frame).

- Optimization 5 – The setup was similar to Optimization 3 with the addition of a rounded leading edge which was less rounded than Optimization 4. In this setup, two series of simulations were carried out – one for an open channel and several orifice-flow conditions for a gated intake structure. Simulation flow rates for Optimization 5 were equal to 975,000 cfs (reference Figures 4-31 and 4-32). Because of the limited number of simulations, this setup was applied to assess the benefit of a rounded leading edge for the Optimization 3 design, the potential SWRs at a high river stage, and the impact of a gate structure on diversion SWRs. Although the setup is different than Optimization 3 at the leading edge, the SWRs from the two setups are assumed to be similar for the two flow rates that were analyzed (e.g., Optimization 3 would render a similar SWR as Optimization 5 for a Mississippi River flow rate of 975,000 cfs). The primary difference between the two setups is believed to be in the flow patterns at the entrance, with the superior geometry being the one resulting in less flow separation.

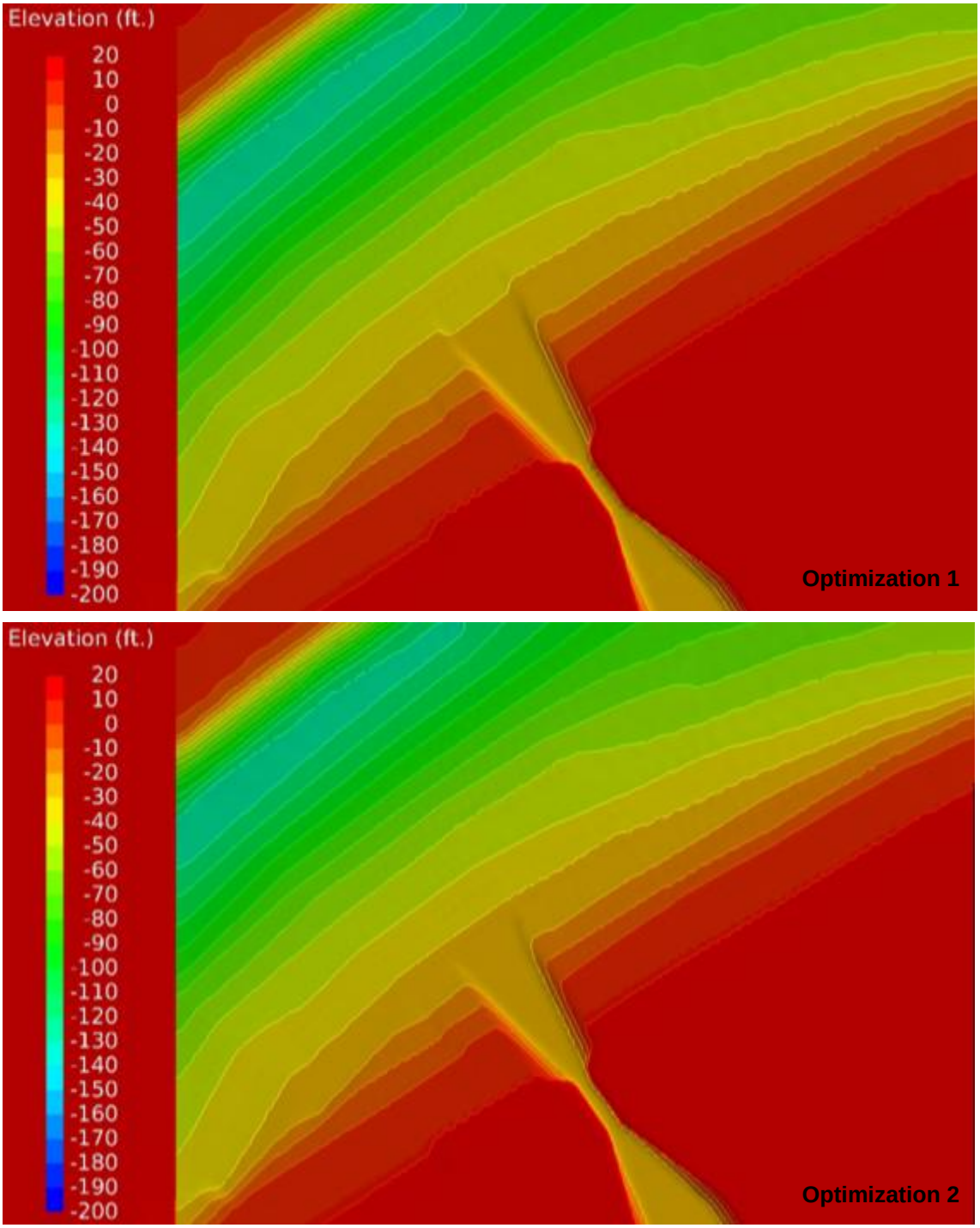

Figure 4-29 Model Development for Optimization 1 (Top) and Optimization 2 (Bottom) (bathymetry colored by elevation). Model Development for Optimization 1 (Top) and Optimization 2 (Bottom) (bathymetry colored by elevation).

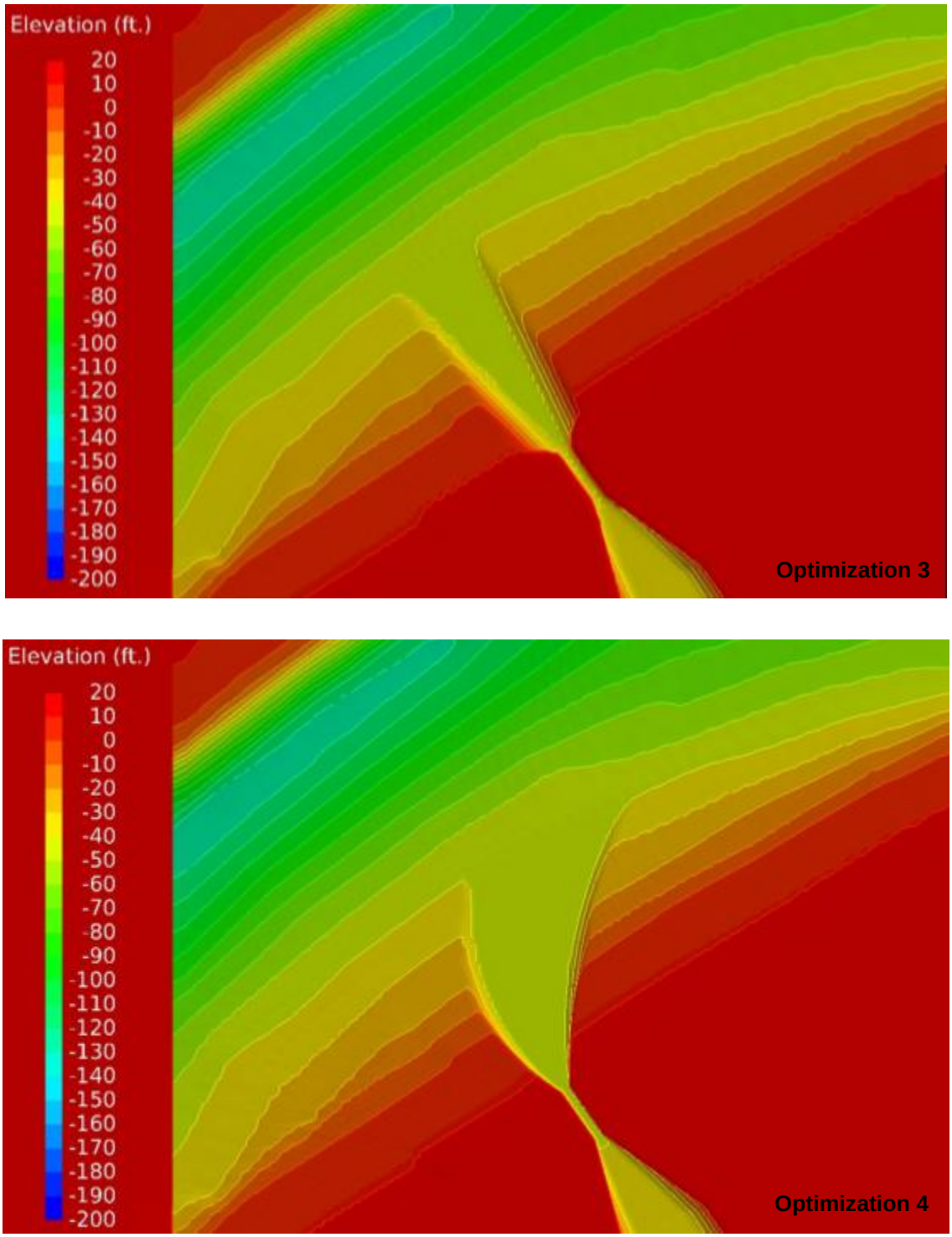

Figure 4-30. Model Development for Optimization 3 (Top) and Optimization 4 (Bottom) (bathymetry colored by elevation).

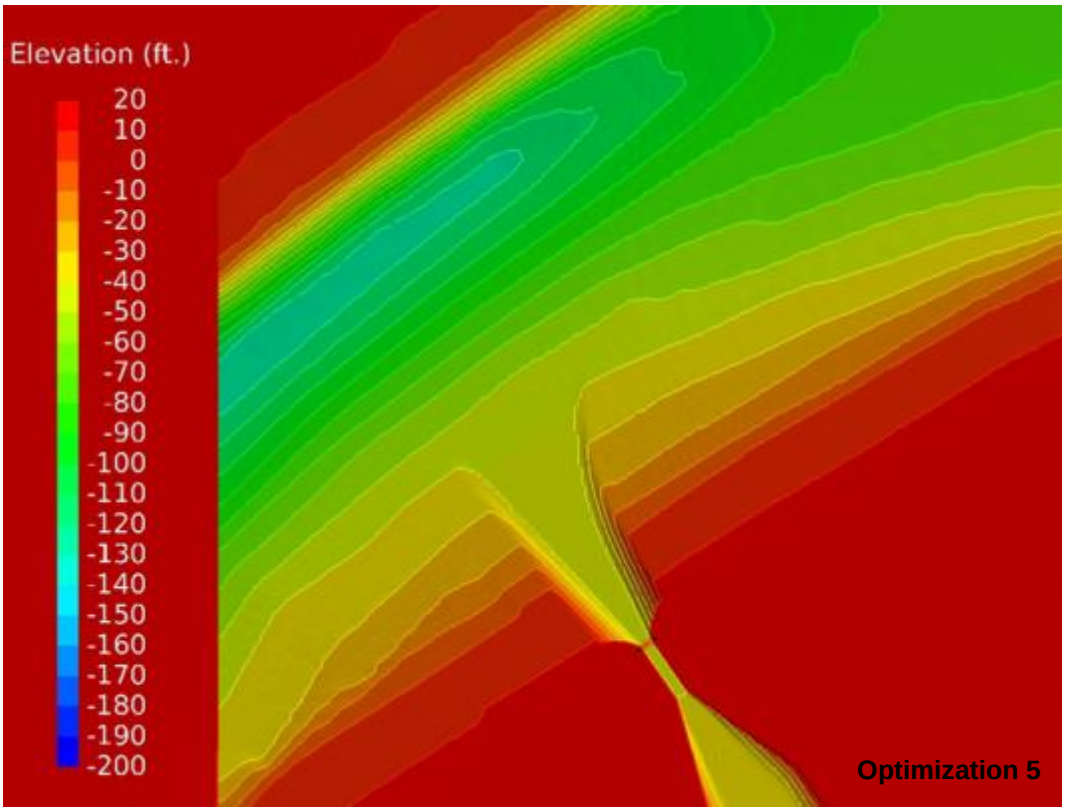

Figure 4-31. Model Development for Optimization 5 (Plan View) (bathymetry colored by elevation).

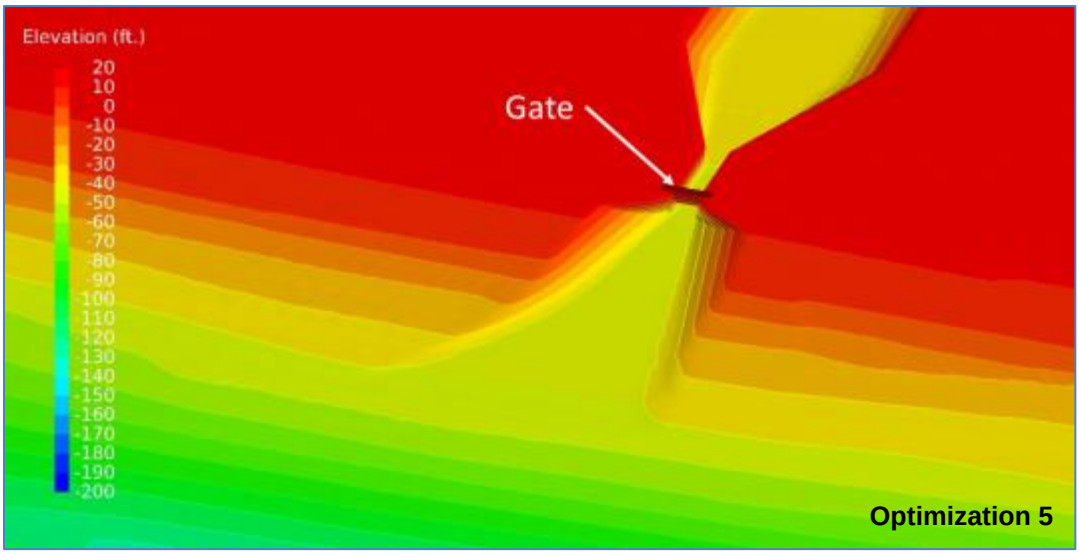

Figure 4-32. Model Development for Optimization 5 with a Gate Structure (Isometric View) (bathymetry colored by elevation).

4.4.1 Model Setup

The setup from the Extended Domain Design Alternatives Analysis at Location1 was used in this part of the study; changes to the design of the diversion structure, considered in the optimization studies, are noted in Table 4-12.

4.4.2 Boundary Conditions

Boundary conditions were the same as those used in the Extended Domain Design Alternatives Analysis, except that the tail water at the end of the outfall channel was set to an elevation of 5.0 feet NAVD88. This was the recommended water surface elevation at the end of the outfall channel by USACE ERDC staff as part of the ADH modeling analysis.

4.4.3 Simulation

The river flow rate in the Base model and the first four optimization runs (Optimizations 1 through 4) was equal to 700,000 cfs; in the final optimization run (Optimization 5), the river flow rate was equal to 975,000 cfs. In all of the simulations, except in Optimization 5, the intake structure was modeled without a gate (e.g., as an open channel).

In Optimization 5, the intake structure was modeled both without a gate and with a gate to control the discharge through the structure. To determine a relationship between discharge and flow rate, simulations with a number of different gate openings were carried out. First, the intake structure was modeled with a fully opened gate to determine its maximum capacity; then, the position of the gate was varied and the analysis was repeated. The resulting information was then used to determine the relationship between gate opening and discharge. Figure 4-33 shows calculated flow rates as a function of gate opening.

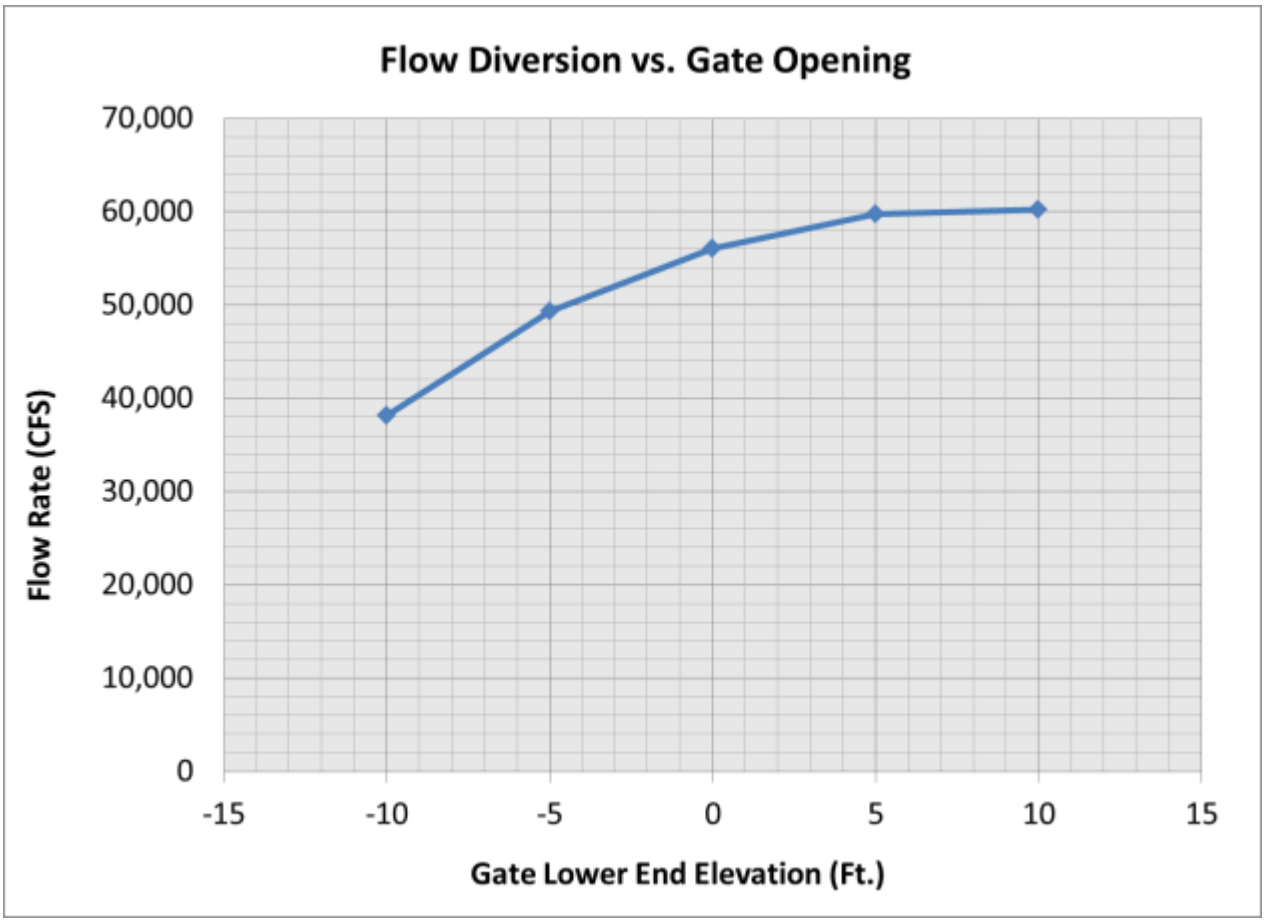

Figure 4-33. Flow Rate in the Intake Structure as a Function of Gate Opening.

4.4.3.1 Hydrodynamics

Results appearing in Figure 4-34 through Figure 4-49 show the flow patterns in the river and in the entrance of the diversion channel near the bottom of the intake channel and 10 feet above the channel floor for the Base model and Optimizations 1, 2, 3, 4, and 5.

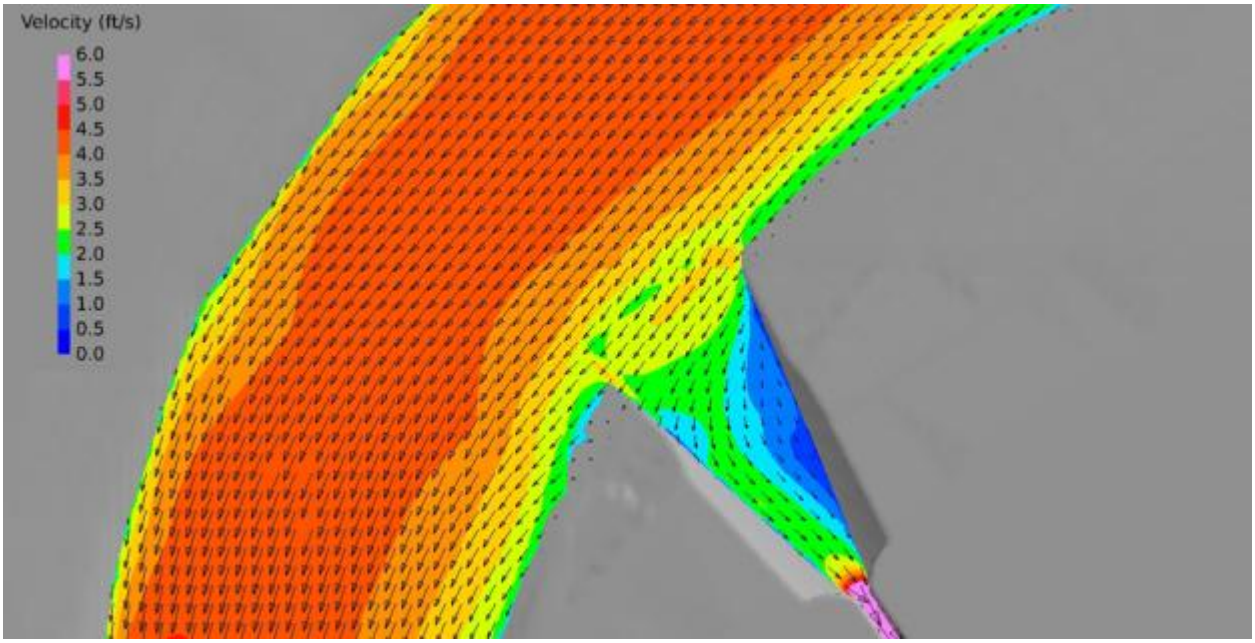

Figure 4-34. Water Velocity with Vectors at 1 foot above Intake Channel Floor for Base.

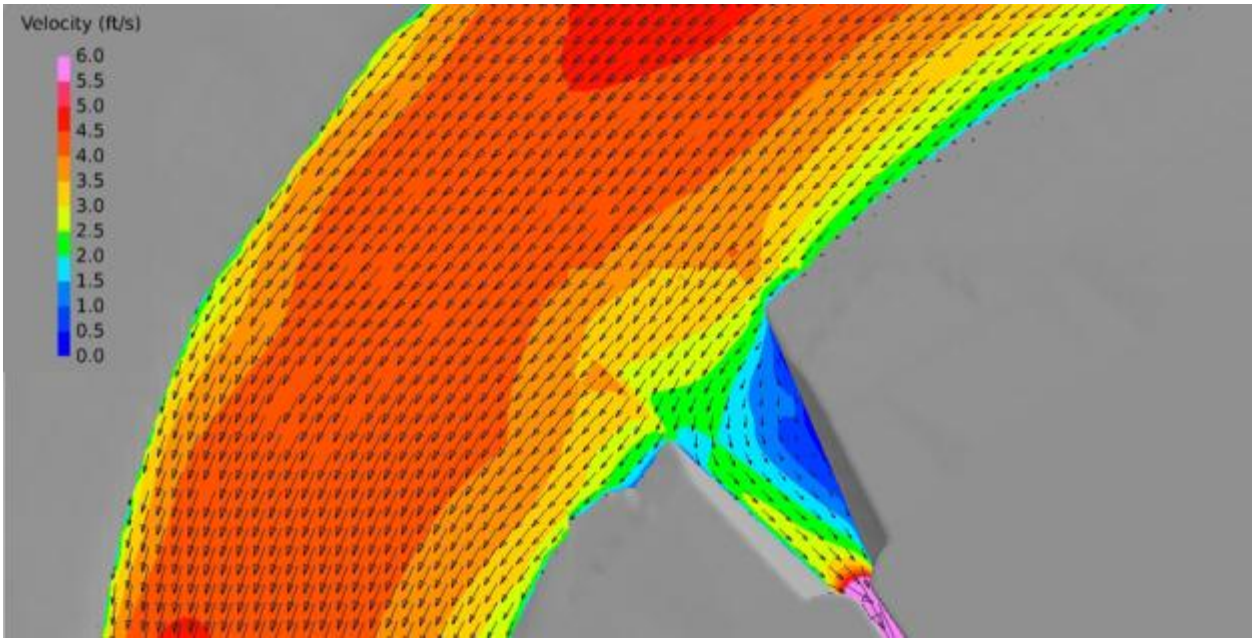

Figure 4-35. Water Velocity with Vectors at 10 feet above Intake Channel Floor for Base.

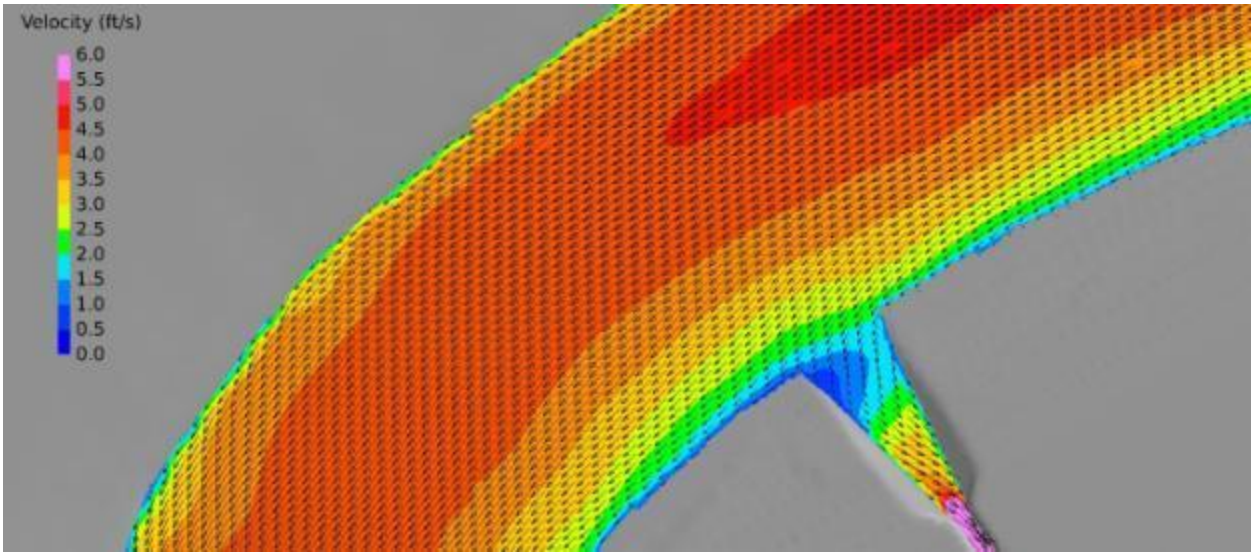

Figure 4-36. Water Velocity with Vectors at 1 foot above Intake Channel Floor for Optimization 1.

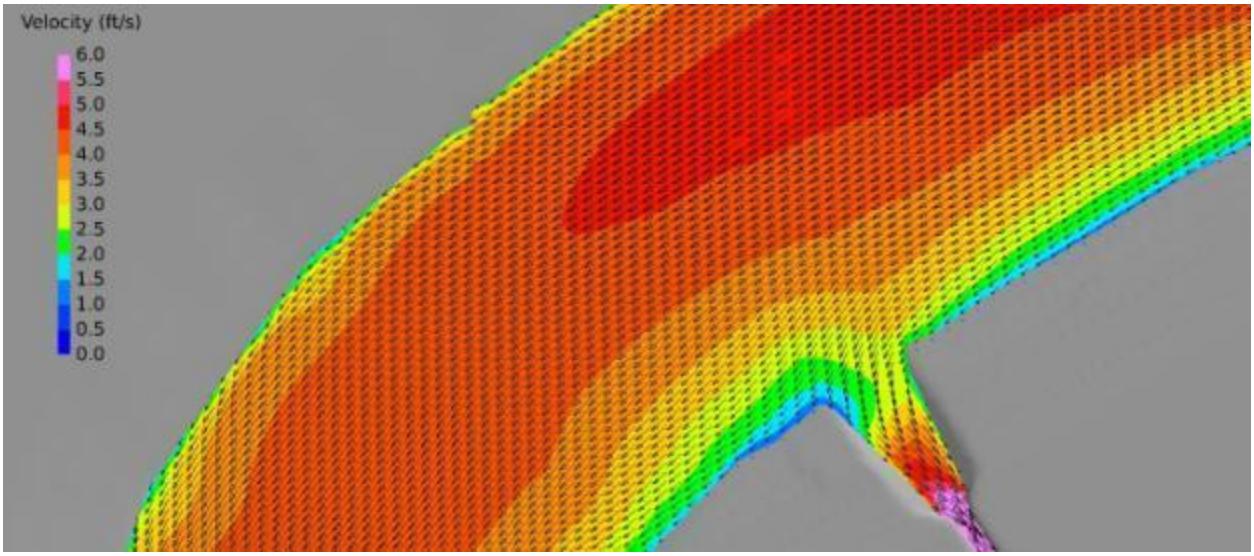

Figure 4-37. Water Velocity with Vectors at 10 feet above Intake Channel Floor for Optimization 1.

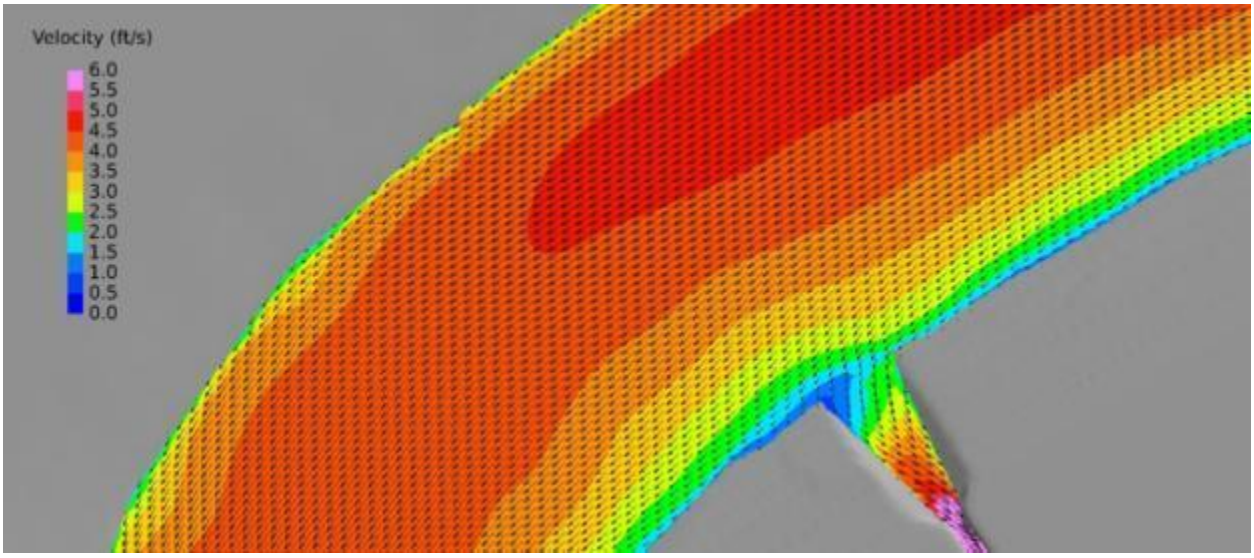

Figure 4-38. Water Velocity with Vectors at 1 foot above Intake Channel Floor for Optimization 2.

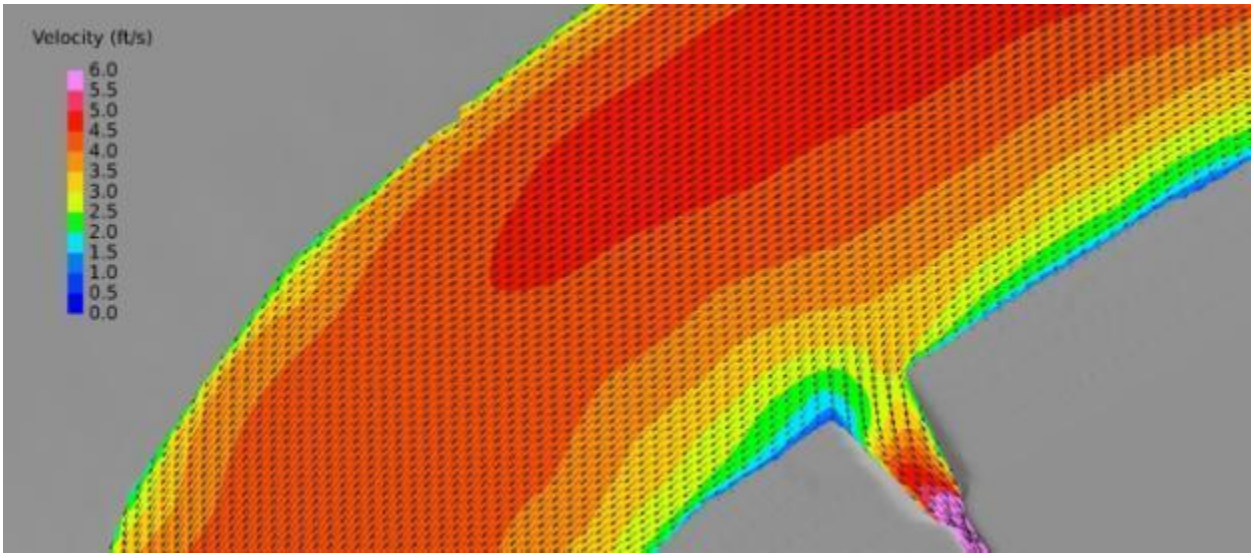

Figure 4-39. Water Velocity with Vectors at 10 feet above Intake Channel Floor for Optimization 2.

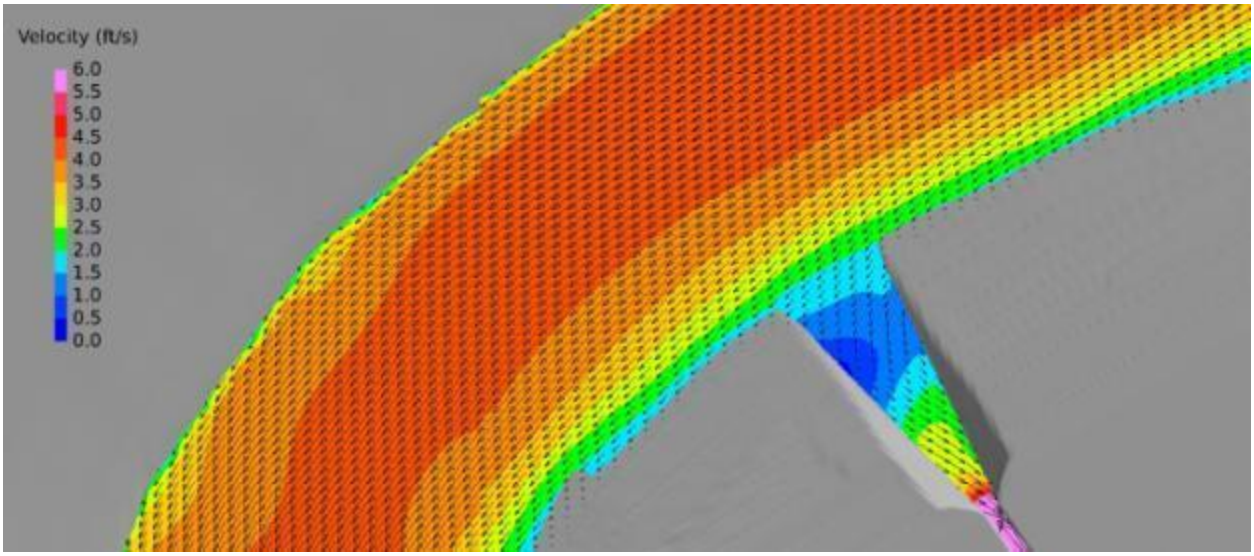

Figure 4-40. Water Velocity with Vectors at 1 foot above Intake Channel Floor for Optimization 3.

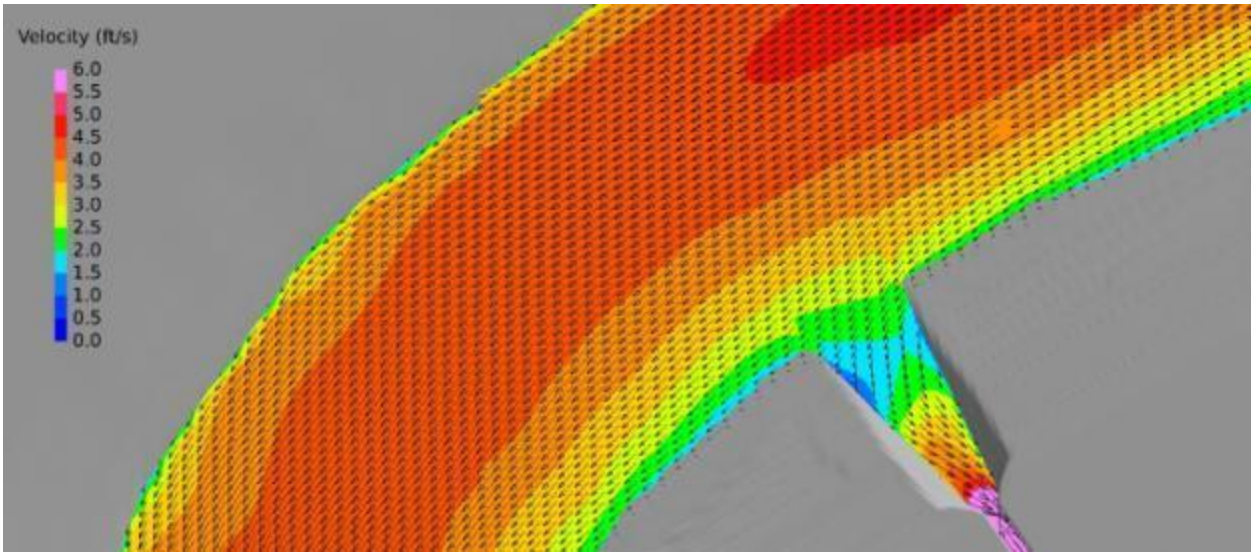

Figure 4-41. Water Velocity with Vectors at 10 feet above Intake Channel Floor for Optimization 3.

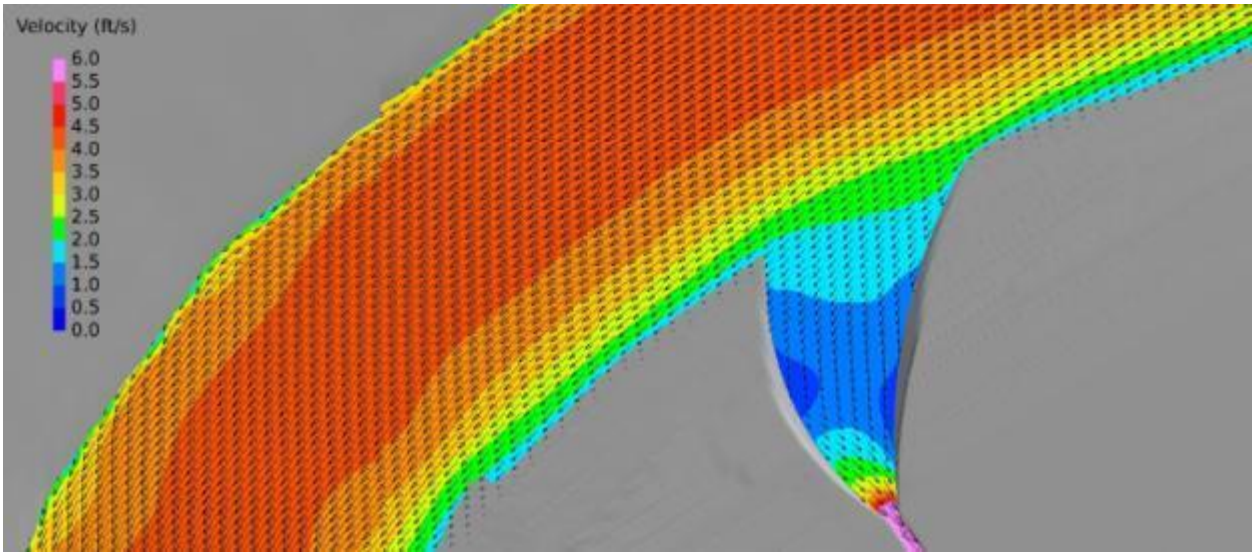

Figure 4-42. Water Velocity with Vectors at 1 foot above Intake Channel Floor for Optimization 4.

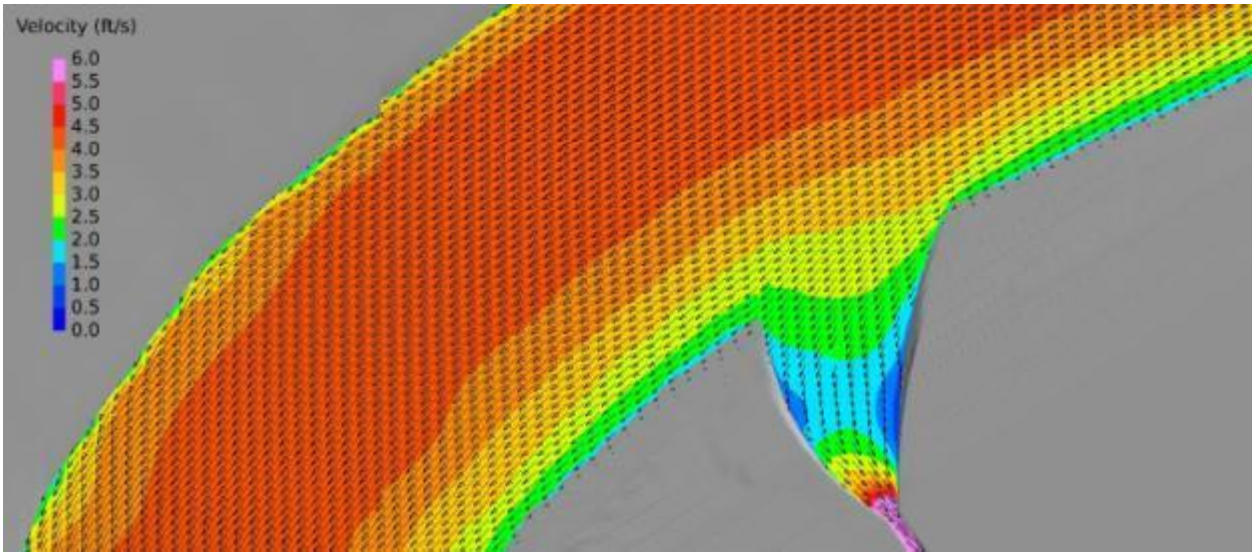

Figure 4-43. Water Velocity with Vectors at 10 feet above Intake Channel Floor for Optimization 4.

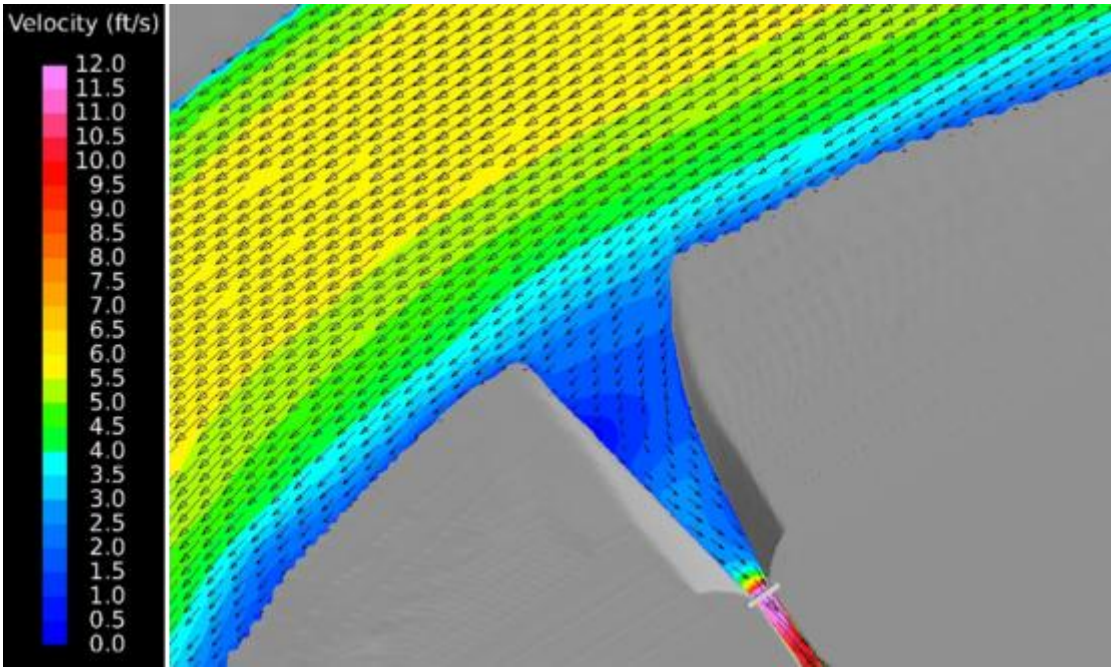

Figure 4-44. Water Velocity with Vectors at 1 foot above Intake Channel Floor for Optimization 5, River Flow equals 975,000 cfs.

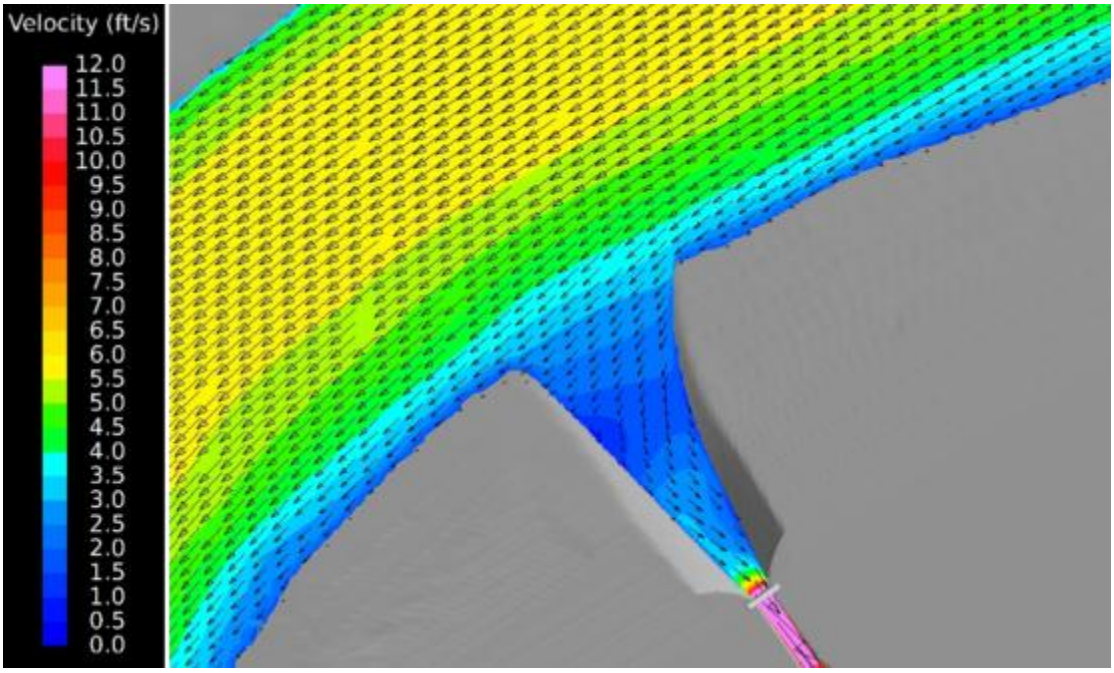

Figure 4-45. Water Velocity with Vectors at 3 feet above Intake Channel Floor for Optimization 5, River Flow equals 975,000 cfs.

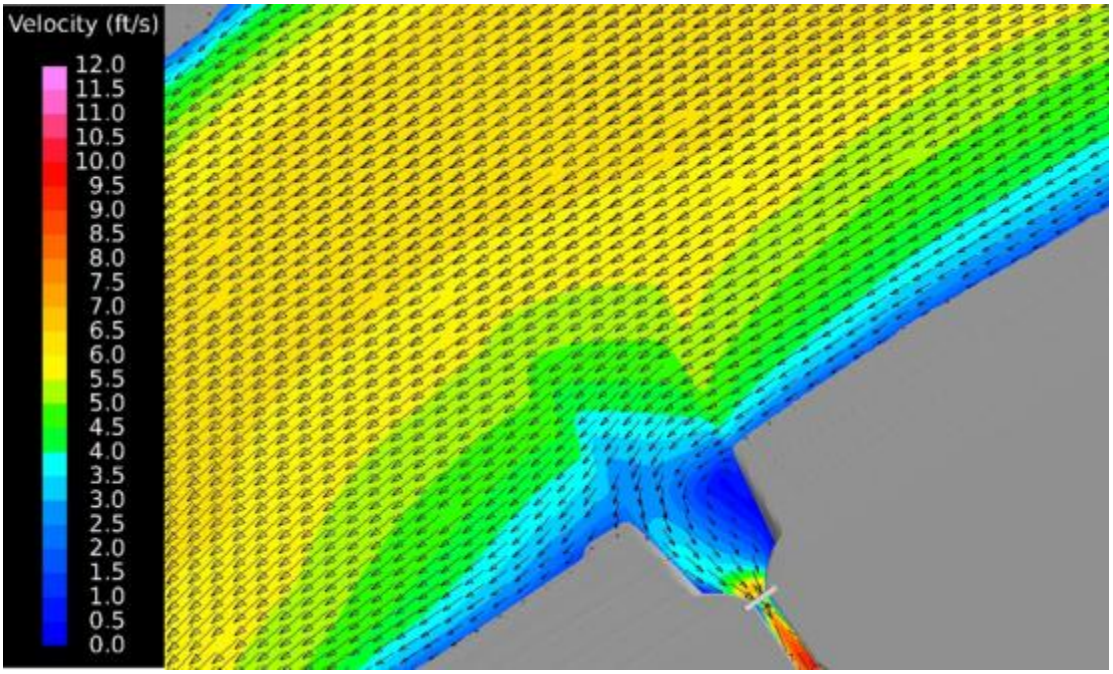

Figure 4-46. **Water Velocity with Vectors at the Intake Channel Floor for Optimization 5, River Flow equals 975,000 cfs.**

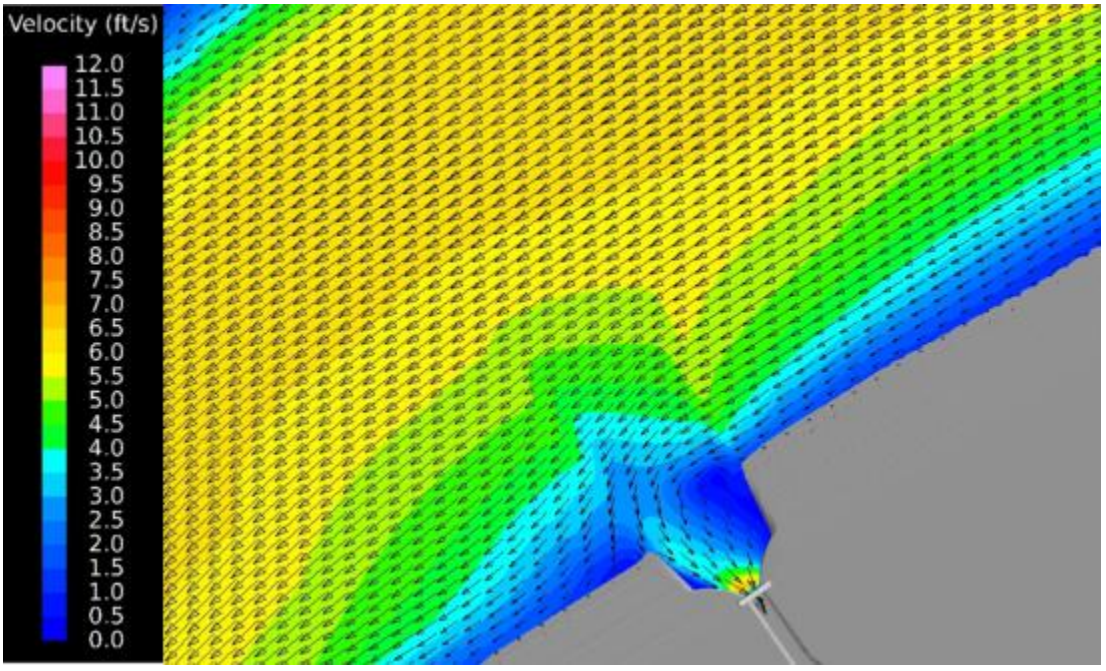

Figure 4-47. **Water Velocity with Vectors at 5 feet above Intake Channel Floor for Optimization 5, River Flow equals 975,000 cfs.**

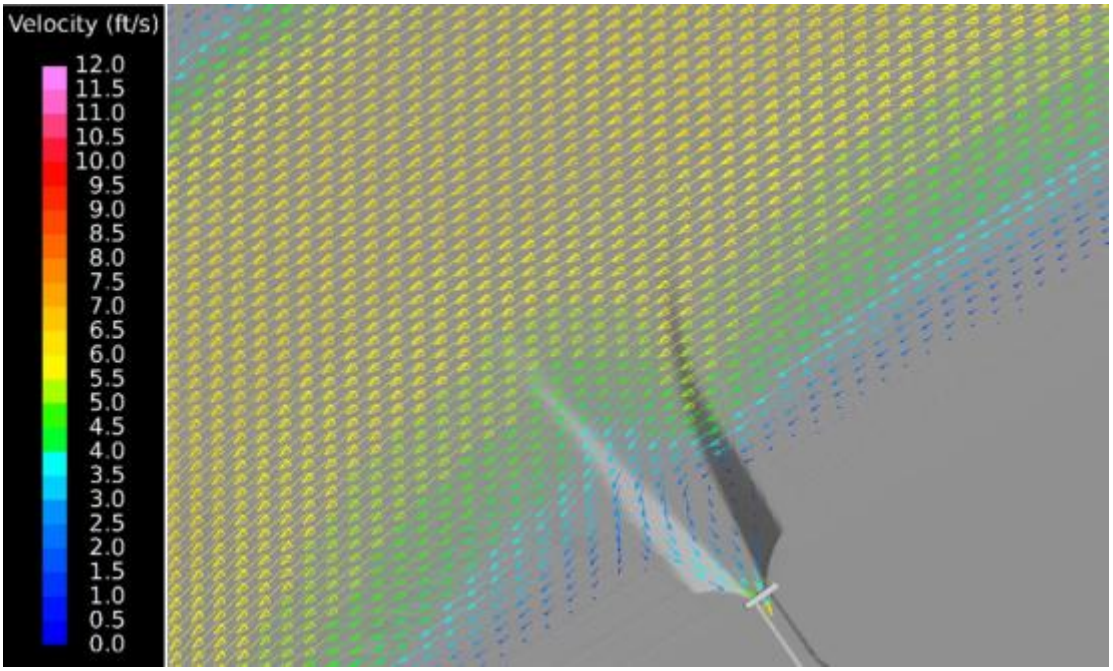

Figure 4-48. Velocity Vectors at 5 feet above Intake Channel Floor for Optimization 5, River Flow equals 975,000 cfs.

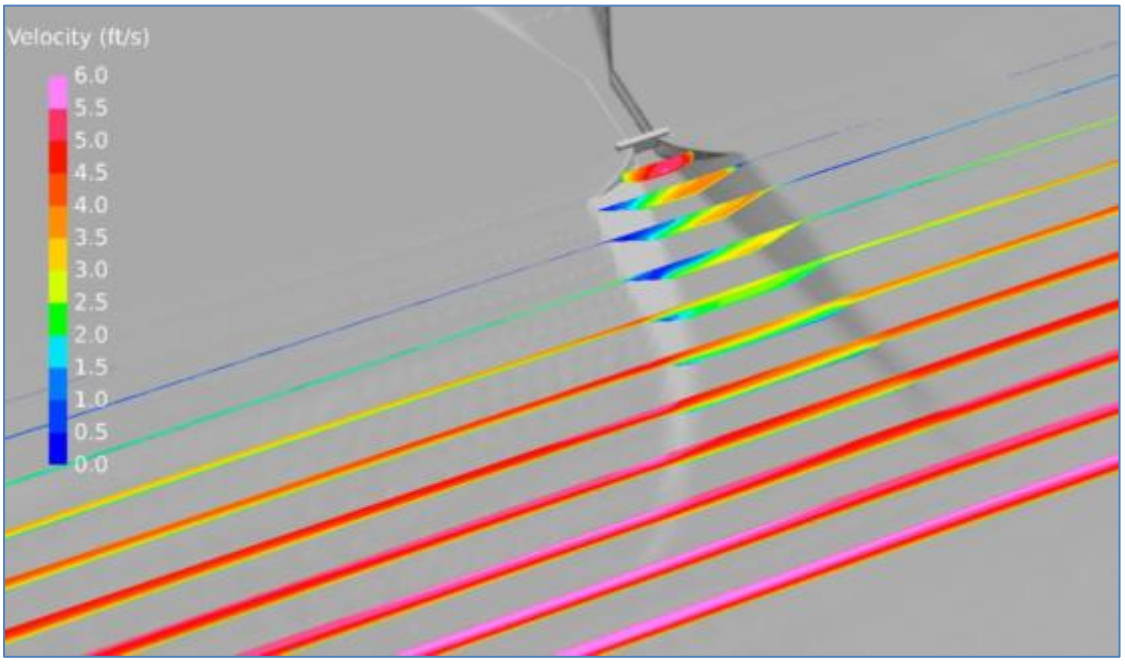

Figure 4-49. Water Velocity at Different Cross-Sections in the Approach Channel for Optimization 5, River Flow equals 975,000 cfs.

4.4.3.2 Sediment Capture

Results of the sediment transport analyses, summarized in Table 4-13 and 4-16, show the amount of flow entering the intake channel and the amount of sediment captured by the diversion intake structure in metric tons per day. Table 4-14 and Table 4-17 provide calculated SWRs for each size class and in aggregate. The sediment load captured in the intake structure in terms of cubic yards per year is shown in Table 4-15 and Table 4-18. According to these results, Optimizations 3 and 5 capture more sediment than do the configurations studied in Optimizations 1, 2, and 4. Note that results shown in Table 4-13, Table 4-14, and Table 4-15 are for Base and Optimizations 1, 2, 3, and 4 based on 700,000 cfs river flow. Results shown in Table 4-16, Table 4-17, and Table 4-18 are for Optimization 5 based on 975,000 cfs river flow.

Table 4-13. Diversion Structure Optimization Calculated Sediment Capture (metric ton per day), River Flow equals 700,000 cfs.

Description	Flow Rate		Sediment Load (metric ton/d)							Total
	(m3/s)	(cfs)	2 Microns	8 Microns	32 Microns	64 Microns	96 Microns	125 Microns	250 Microns	Load (metric ton/day)
Mississippi River	19,822	700,000	41,898	140,396	77,050	10,839	21,816	34,437	23,460	349,896
Base	1,104	38,950	2,400	8,000	2,800	900	1,900	5,800	6,300	28,100
Optimization 1	1,239	43,700	2,615	8,764	3,463	704	1,662	3,913	3,749	24,869
Optimization 2	1,025	36,152	2,164	7,251	1,592	336	789	1,956	1,817	15,905
Optimization 3	1,241	43,800	2,622	8,785	3,375	678	1,638	3,900	4,374	25,372
Optimization 4	1,081	38,150	2,283	7,652	2,100	473	1,308	3,378	4,091	21,285

Table 4-14. Diversion Structure Optimization Calculated Sediment Water Ratios, River Flow equals 700,000 cfs.

Description	Flow Rate		Sediment Water Ratios by Size Class							Total
	(m3/s)	(cfs)	2 Microns	8 Microns	32 Microns	64 Microns	96 Microns	125 Microns	250 Microns	SWR
Base	1,104	38,950	1.0	1.0	0.7	1.5	1.6	3.0	4.8	1.4
Optimization 1	1,239	43,700	1.0	1.0	0.7	1.0	1.2	1.8	2.6	1.1
Optimization 2	1,025	36,152	1.0	1.0	0.4	0.6	0.7	1.1	1.5	0.9
Optimization 3	1,241	43,800	1.0	1.0	0.7	1.0	1.2	1.8	3.0	1.2
Optimization 4	1,081	38,150	1.0	1.0	0.5	0.8	1.1	1.8	3.2	1.1

Table 4-15. Diversion Structure Optimization Calculated Sediment Load, River Flow equals 700,000 cfs.

Description	Flow Rate (cfs)	Cubic Yards/Year			Metric Ton/Day			SWR		
		Total 2-250 Micron Load	Total 32-250 Micron Load	Total 64-250 Micron Load	Total 2-250 Micron Load	Total 32-250 Micron Load	Total 64-250 Micron Load	Total 2-250 Micron Load	Total 32-250 Micron Load	Total 64-250 Micron Load
Base	38,950	1,376,663	867,150	729,974	28,100	17,700	14,900	1.4	1.9	3.0
Optimization 1	43,700	1,218,388	660,913	491,255	24,869	13,490	10,027	1.1	1.3	1.8
Optimization 2	36,152	779,211	317,955	239,961	15,905	6,490	4,898	0.9	0.7	1.0
Optimization 3	43,800	1,243,014	684,167	518,821	25,372	13,965	10,590	1.2	1.3	1.9
Optimization 4	38,150	1,042,785	556,054	453,172	21,285	11,350	9,250	1.1	1.2	1.9

Table 4-16. Diversion Structure Optimization Calculated Sediment Capture (metric ton per day), River Flow equals 975,000 cfs.

Description	Flow Rate		Sediment Load (metric ton/day)							Total
	(m3/s)	(cfs)	2 Microns	8 Microns	32 Microns	64 Microns	96 Microns	125 Microns	250 Microns	Load (metric ton/day)
Mississippi River	27,630	975,000	47,013	158,668	88,149	3,270	19,652	74,327	53,338	444,417
Optimization 5 - No Gate	1,706	60,203	2,903	9,797	4,082	220	1,565	8,949	11,395	38,912
Optimization 5 - With Gate (Lower End at El. 5 ft.)	1,692	59,707	2,879	9,716	3,617	208	1,528	8,876	11,497	38,322
Optimization 5 - With Gate (Lower End at El. -10 ft.)	1,082	38,181	1,841	6,213	1,726	90	693	4,366	6,266	21,195

Table 4-17. Diversion Structure Optimization Calculated Sediment Water Ratios, River Flow equals 975,000 cfs.

Description	Flow Rate		Sediment Load (metric ton/day)							Total
	(m3/s)	(cfs)	2 Microns	8 Microns	32 Microns	64 Microns	96 Microns	125 Microns	250 Microns	Load (metric ton/day)
Optimization 5 - No Gate	1,706	60,203	1.0	1.0	0.8	1.1	1.3	2.0	3.5	1.4
Optimization 5 - With Gate (Lower End at El. 5 ft.)	1,692	59,707	1.0	1.0	0.7	1.0	1.3	2.0	3.5	1.4
Optimization 5 - With Gate (Lower End at El. -10 ft.)	1,082	38,181	1.0	1.0	0.5	0.7	0.9	1.5	3.0	1.2

Table 4-18. Diversion Structure Optimization Calculated Sediment Load, River Flow equals 700,000 cfs.

Description	Flow Rate (cfs)	Cubic Yards/Year			Metric Ton/Day			SWR		
		Total 2-250 Micron Load	Total 32-250 Micron Load	Total 64-250 Micron Load	Total 2-250 Micron Load	Total 32-250 Micron Load	Total 64-250 Micron Load	Total 2-250 Micron Load	Total 32-250 Micron Load	Total 64-250 Micron Load
Optimization 5 - No Gate	60,203	1,906,382	1,284,183	1,084,191	38,912	26,212	22,130	**1.4**	**1.8**	**2.4**
Optimization 5 - With Gate (Lower End at El. 5 ft.)	59,707	1,877,436	1,260,368	1,083,182	38,322	25,726	22,110	**1.4**	**1.8**	**2.4**
Optimization 5 - With Gate (Lower End at El. -10 ft.)	38,181	1,038,369	643,767	559,210	21,195	13,140	11,414	**1.2**	**1.4**	**1.9**

4.4.4 Conclusions and Recommendations

Based on the findings of this analysis, the Optimization 5 design was considered to be the best compared to the Base design and Optimizations 1 through 4. The Base design captures the most sediment. However, the Base scenario was not selected due to cost and maintenance concerns related to the sloped approach channel bottom from an invert of -40 feet NAVD88 to -50 feet NAVD88. Optimization 3 and Optimization 5 result in favorable SWRs and acceptable approach flow patterns at the intake structure. The SWRs for Optimization 3 and Optimization 5 are particularly high for larger sized material (Table 4-15 and Table 4-18). Optimization 5 is recommended rather than Optimization 3 due to the improved flow patterns from the rounded leading edge.

The Optimization 5 structure is similar to the one studied in Optimization 3, but it is designed with a rounded leading edge to improve approach flow patterns. The Optimization 5 design should be easier to construct than the Optimization 4 design; velocities are slightly higher near the bottom of the channel, which will help move material that settles onto the bottom when the structure is not operating. Although there are some eddies near the water surface, there is no flow separation at depth for Optimization 5.

Multiple potential adaptive management techniques were also identified during this phase. First, if necessary, a diversion setup like Optimization 5 could be adaptively managed to include a sloped approach channel bottom, which could render higher SWRs as demonstrated by the Base model

simulations. Second, with the inclusion of the gate structure, diversion flow rates can be controlled. A design like Optimization 5 allows for the flexibility to manage flow rates through the structure with limited future construction costs. The tainter gates also allow for an easier adjustment to the diversion operation for future basin conditions, including sea level rise, subsidence, and land building, while maintaining a desired flow rate including the authorized maximum of 35,000 cfs (Note: it is expected that SWRs for Optimization 5, diverting 35,000 cfs, would be similar to those reported in Table 4-18, row 3).

5. RECOMMENDATIONS

The simulations carried out as part of this study fall into two general categories: those used to determine the best location for the LCA Medium Diversion at White Ditch; and those used to identify design features that increase the amount of sediment entering the diversion.

In the first group of analyses, five different locations for the diversion and seven different configurations for the diversion were studied (see Tables 4-1 and 4-2 for details). Based on the simulation results, it is recommended that the diversion be constructed at Location 1 (see Figure 4-1), rather than Location 3 which was proposed in the previously completed feasibility study (USACE and CPRA 2010) and Location 4 which rendered a similar SWR as Location 1 in this analysis. Location 1 is on a sand bar at the inside of a bend, and calculated SWRs are greatest at this location compared to the others studied. According to the model results, secondary flow patterns in the bend help to deliver material to the diversion structure, and the fact that a bar has formed at this location naturally supports this finding. Based on the results of this study and discussions with the USACE, CPRA, and others, it was recommended that the diversion structure be positioned at Location 1 rather than Location 4 primarily due to considerations beyond those evaluated in this study, including cost considerations and potentially improved ecosystem benefits due to the positioning of the outfall in the upper reaches of the receiving basin, thereby maximizing the land-building potential of the diversion.

Results from the second group of analyses were used to identify design features that could improve the ability of the structure to divert sediment from the Mississippi River. As shown in Table 4-12, a baseline analysis and five alternative analyses were carried out. The preferred design, due to optimal SWRs and flow approach patterns, was referred to as Optimization 5 (see Figures 4-31 and 4-32). The intake channel for this design was oriented at a 90-degree angle to the riverbank, at an invert elevation of -40 feet NAVD88, a flat approach channel bottom, and the leading (upstream) edge of the entrance to the intake channel was rounded to minimize flow separations and to reduce the likelihood of sedimentation in the channel during periods of time when the structure is not in operation. Based on these simulation results, it is recommended the Optimization 5 configuration be incorporated in the next design phase of the LCA Medium Diversion at White Ditch.

These design recommendations represent the most favorable design configuration based on the analyses described within. It is recommended that future analyses be performed to further evaluate design parameters prior to final design considerations including, but not limited to, a more detailed assessment of the approach channel geometry, the leading edge alignment, and gate operations. In addition, evaluation of additional steady state Mississippi River flow rates and consideration of unsteady flows are

recommended to more accurately approximate sediment loading estimates for a given operation cycle (e.g., the 2-month authorized operation period), such that sediment supply and thus land building benefits can be quantified with a higher level of confidence. In support of this evaluation, it is suggested that additional field data be collected in the vicinity of the recommended location for the diversion structure. As before, these data would take the form vertical and horizontal velocity and sediment profiles and would be used to improve the reliability of the ***FLOW-3D*** model.

Lastly, many of the analyses serve as lessons learned for diversion structure design optimization, which can be considered in future design iterations and adaptive management strategies. Evaluation of additional adaptive management strategies could result in a more sustainable and cost-effective design over the life of the structure.

6. REFERENCES

Allison, M.A. 2011. *Interpretative Report on Water and Sediment Surveys of the Mississippi River Channel Conducted at Myrtle Grove and Magnolia in Support of Numerical Modeling (October 2008-May 2010)*. Prepared for the State of Louisiana Office of Coastal Protection and Restoration. February 2011.

Allison, M.A. 2013. Personal communication with Dr. Ehab Meselhe.

Chow, V.T. 1959. *Open Channel Hydraulics*, McGraw-Hill Publishing Company, New York, NY.

Davis, M. 2010. *Numerical simulation of unsteady hydrodynamics in the Lower Mississippi River*. Master's Thesis. University of New Orleans. New Orleans, LA. May 2010.

Flow Science. 2010. ***FLOW-3D*** *– Excellence in flow modeling software. User Manual 9.4 Volumes 1 and 2*. Santa Fe, NM, www.flow3d.com.

Harlow, Francis H., and Paul I. Nakayama. 1967. *Turbulence Transport Equations. Phys. Fluids 10, 2323.*

Hirt, C.W., and B.D. Nichols. 1981. *Volume of Fluid (VOF) Method for the Dynamics of Free Boundaries.* Los Alamos Scientific Laboratory, Los Alamos, New Mexico.

Hirt, C.W., and J.M. Sicilian. 1985. *A Porosity Technique for the Definition of Obstacles in Rectangular Cell Meshes.* Fourth International Conference on Ship Hydrodynamics. Washington, D.C. September.

Intelligent Light. 2013. *FieldView 13.* Rutherford, NJ, www.ilight.com.

Meselhe, E.A., I. Georgiou, and J.A. McCorquodale. 2011. *Myrtle Grove Delta Building Diversion: Numerical Modeling of Hydrodynamics and Sediment Transport in Lower Mississippi near Myrtle Grove River Bend*. Prepared for the State of Louisiana Office of Coastal Protection and Restoration. October 2011.

McNeel, Robert. 2012. *Rhino 5.* Seattle, WA.

USACE and CPRA. 2010. *LCA Ecosystem Restoration Study, Volume VI of VI, Final Integrated Feasibility Study and Supplemental Environmental Impact Statement for the Medium Diversion at White Ditch Plaquemines Parish Louisiana*. September 2010.

Yakhot, Victor, and Steven A. Orszag. 1986. *Renormalized group analysis of turbulence. I. Basic Theory. Journal of Scientific Computing, Volume 1, Issue 1, pp 3-51.*

Yakhot, Victor, and Leslie M. Smith. 1992. *The renormalization group, the epsilon-expansion and derivation of turbulence models. Journal of Scientific Computing. Volume 7, No. 1, pp 35-61*

Appendix A

A.1 Feasibility Study Recommended Design Model Analysis at Location 3

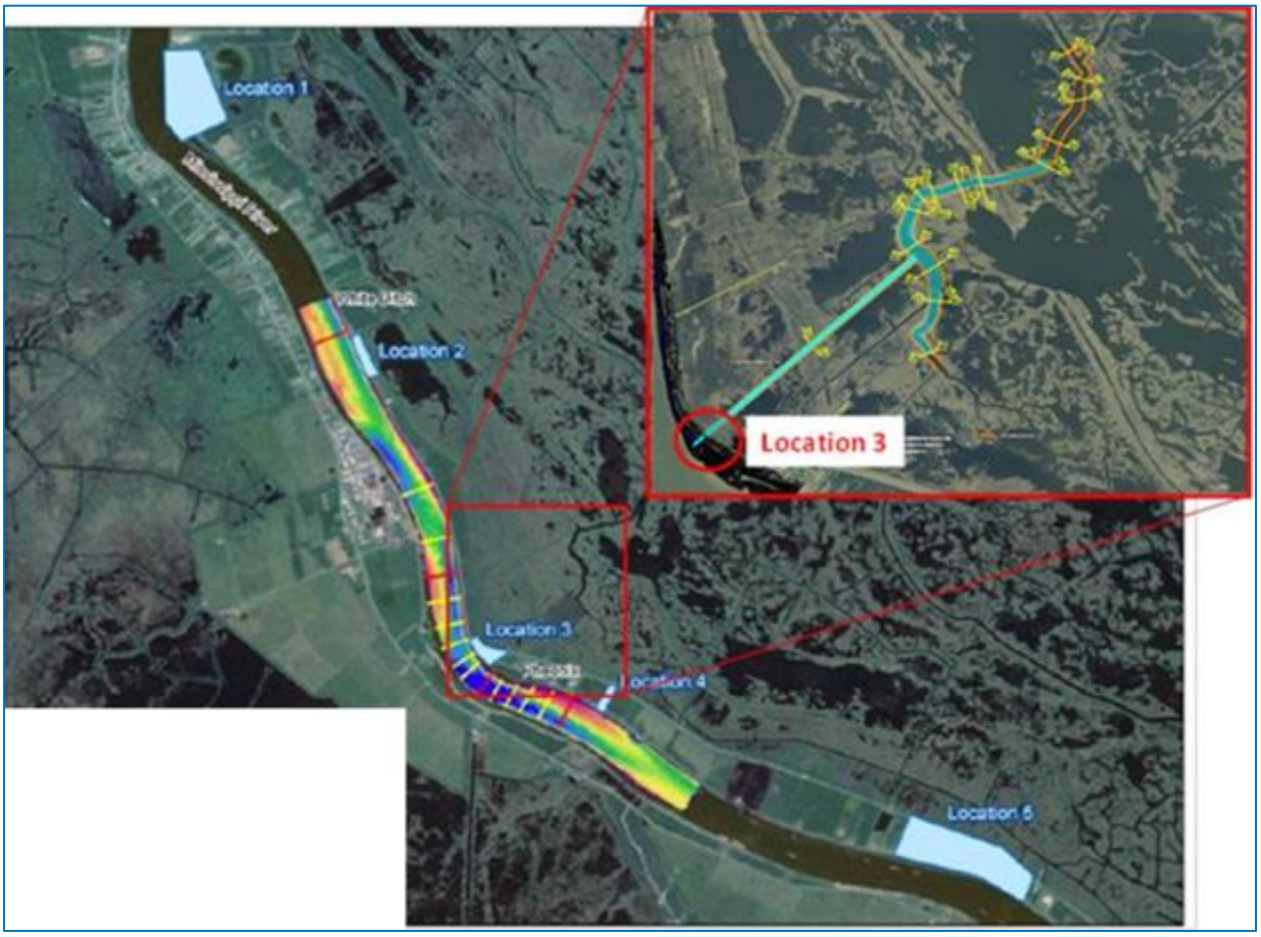

Figure A1–1. Locus Map.

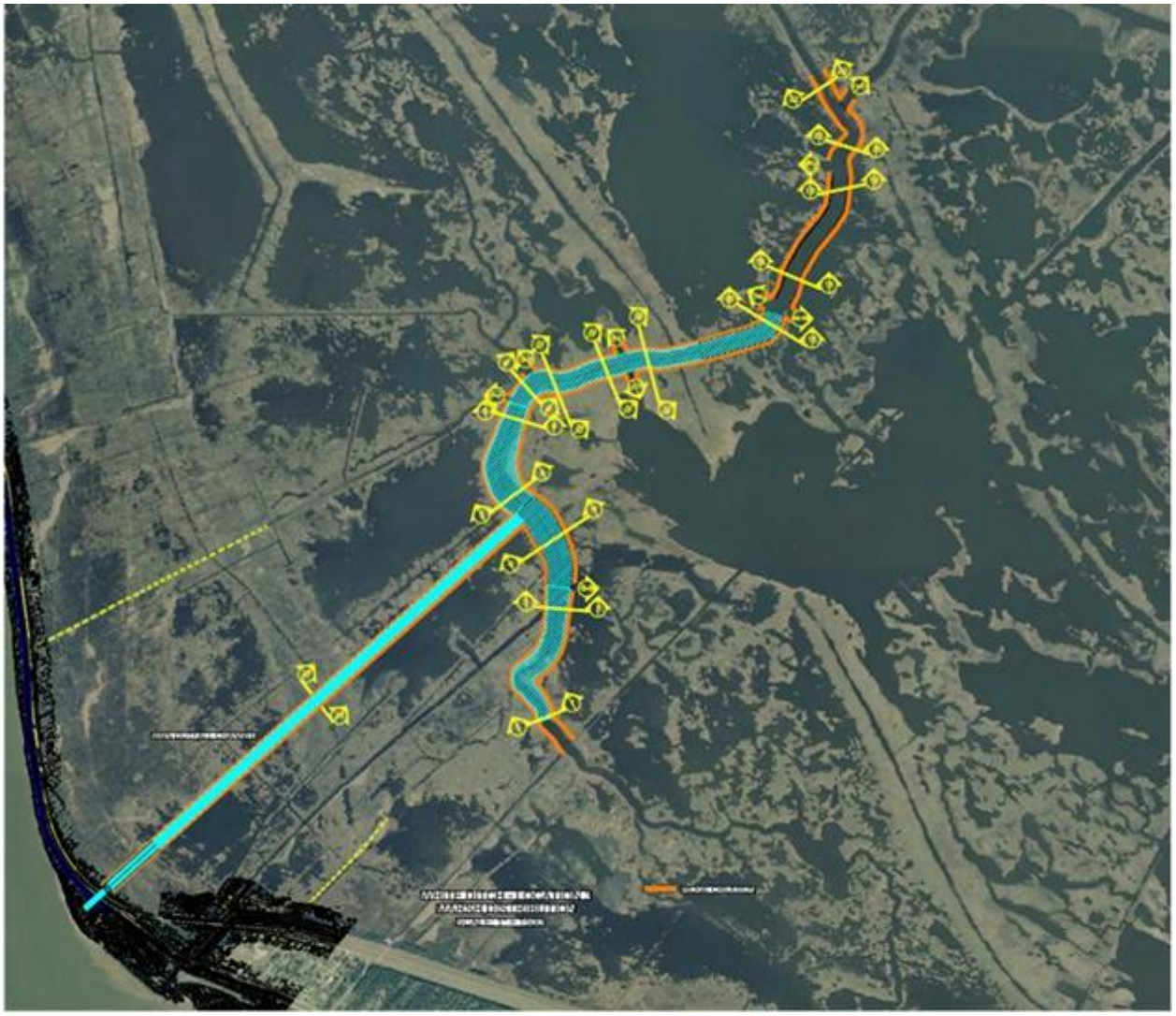

Figure A1–2. Feasibility Study Outfall Channel and Cross-Sections.

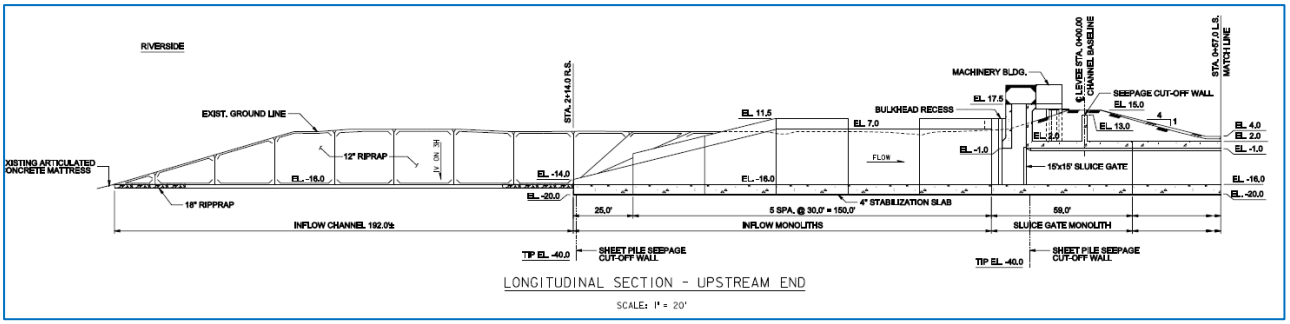

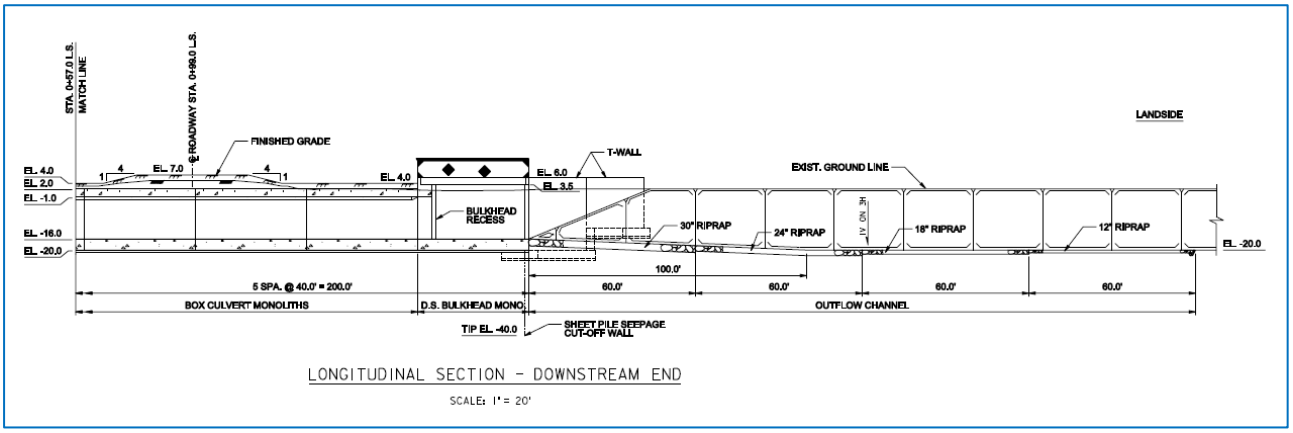

Figure A1–3. Feasibility Study Proposed Diversion Intake Structure CAD Drawing (Elevation View).

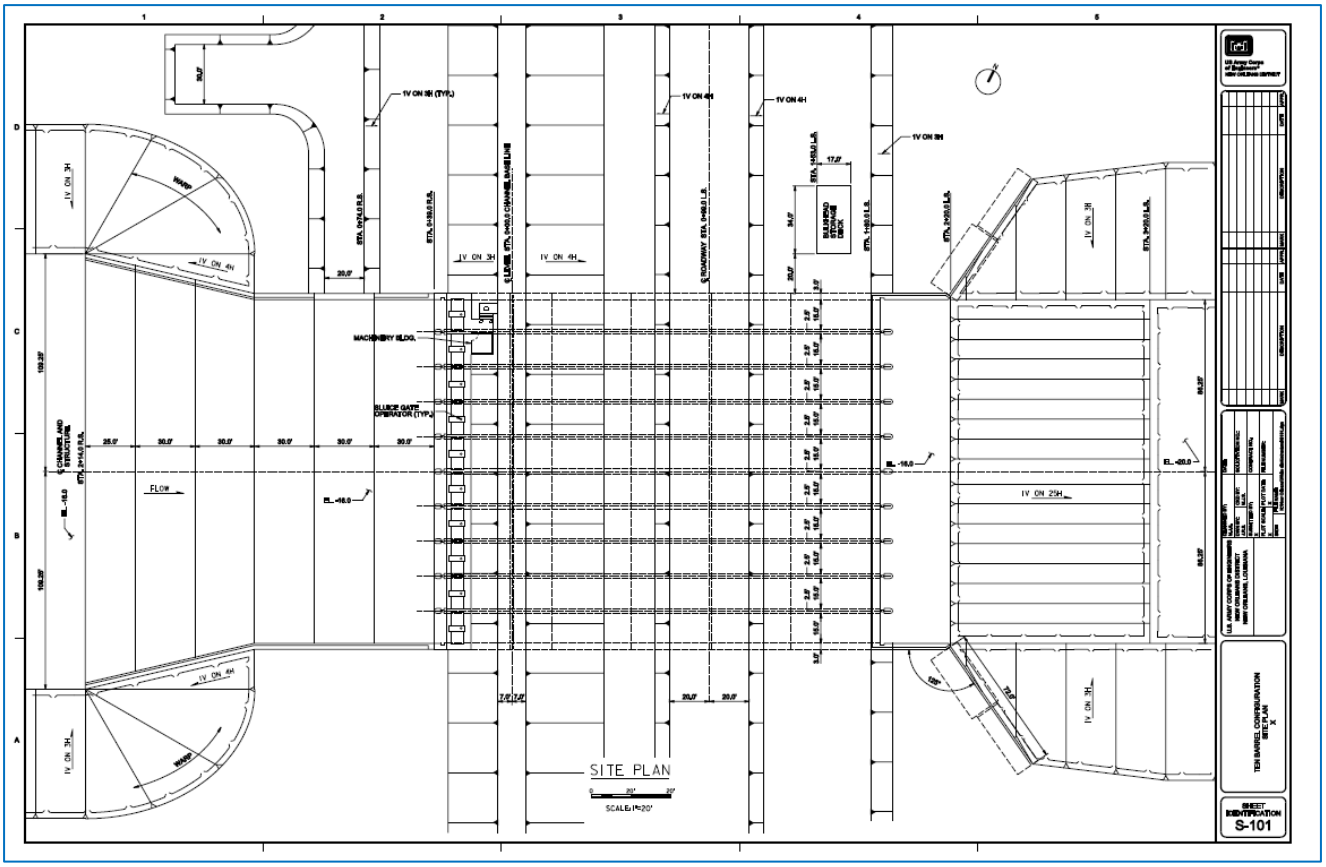

Figure A1–4. Feasibility Study Proposed Diversion Intake Structure CAD Drawing (Plan View).

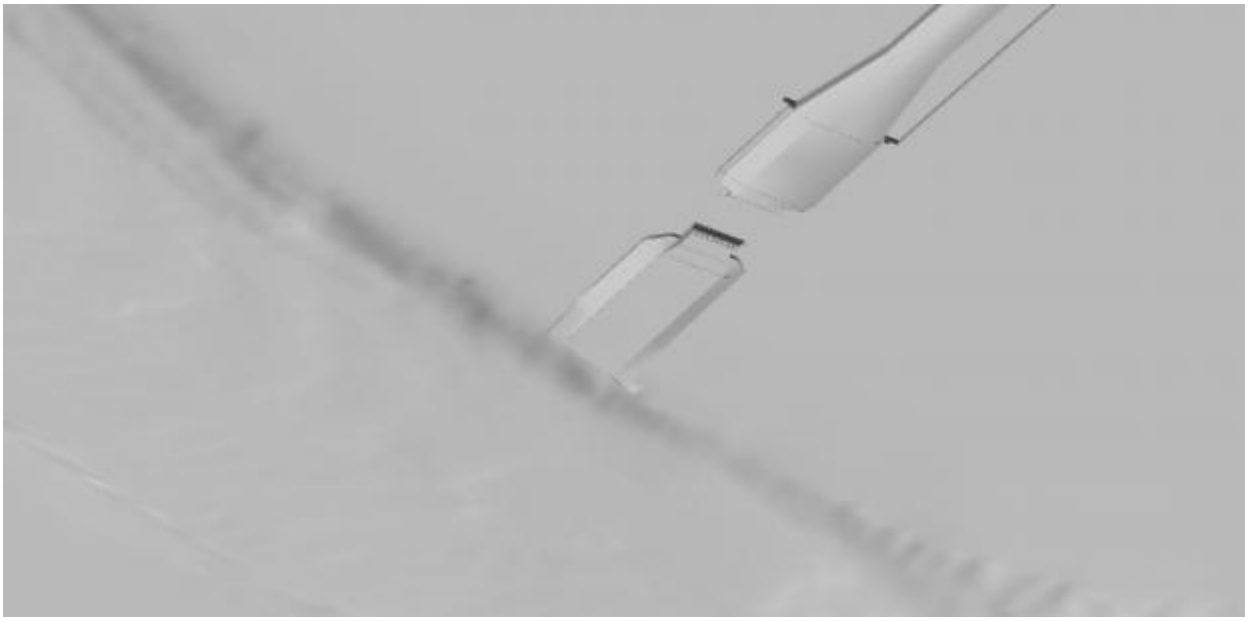

Figure A1–5. **Feasibility Study Recommended Design Model Development: Mississippi River, Diversion Intake, and Outfall Channel Model.**

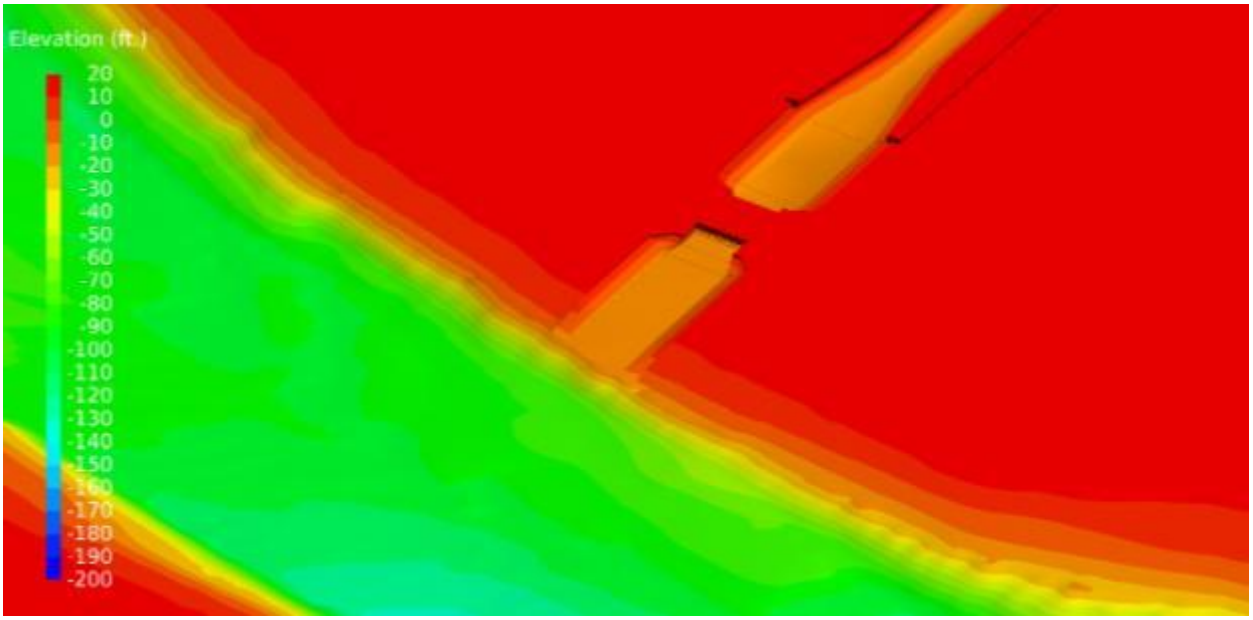

Figure A1–6. **Feasibility Study Recommended Design Model Development (bathymetry colored by elevation).**

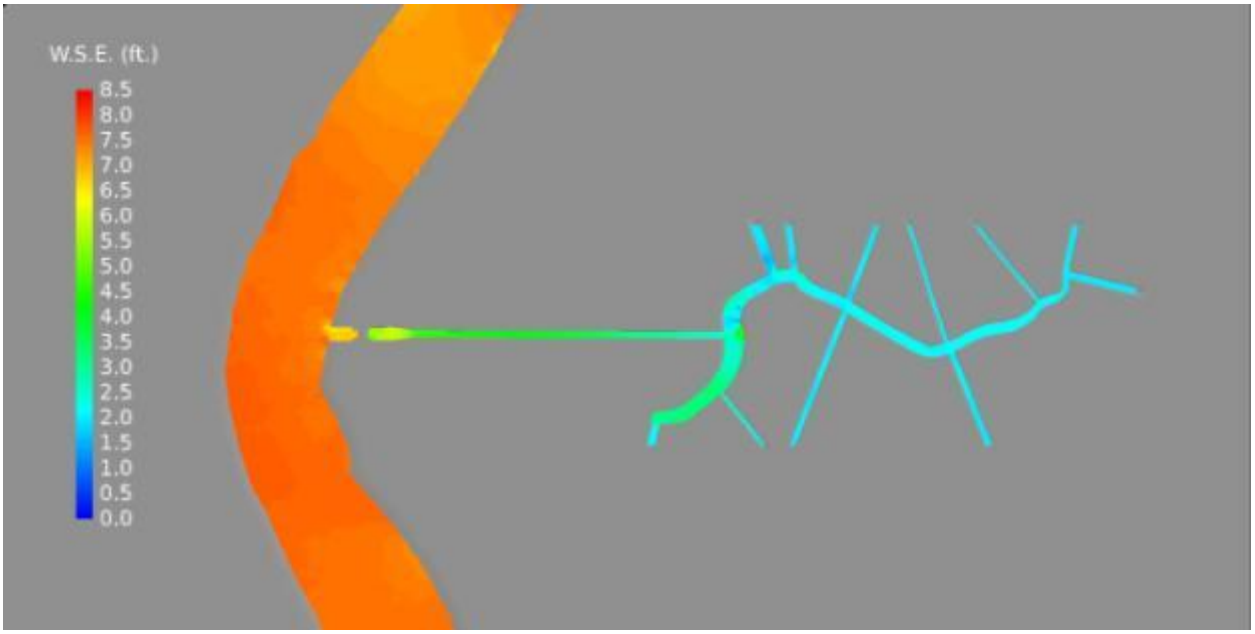

Figure A1–7. **Feasibility Study Recommended Design Model Results – Hydrodynamics: Water Surface (colored by elevation).**

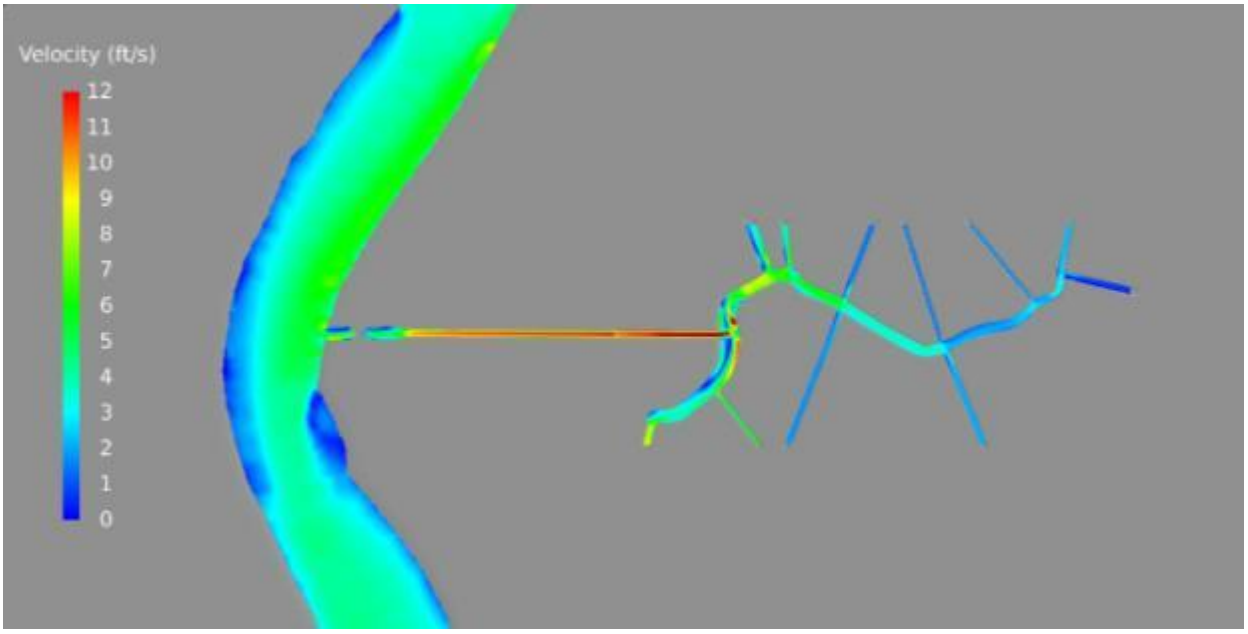

Figure A1–8. **Feasibility Study Recommended Design Model Results – Hydrodynamics: Flow Speed Variation (near surface, colored by speed).**

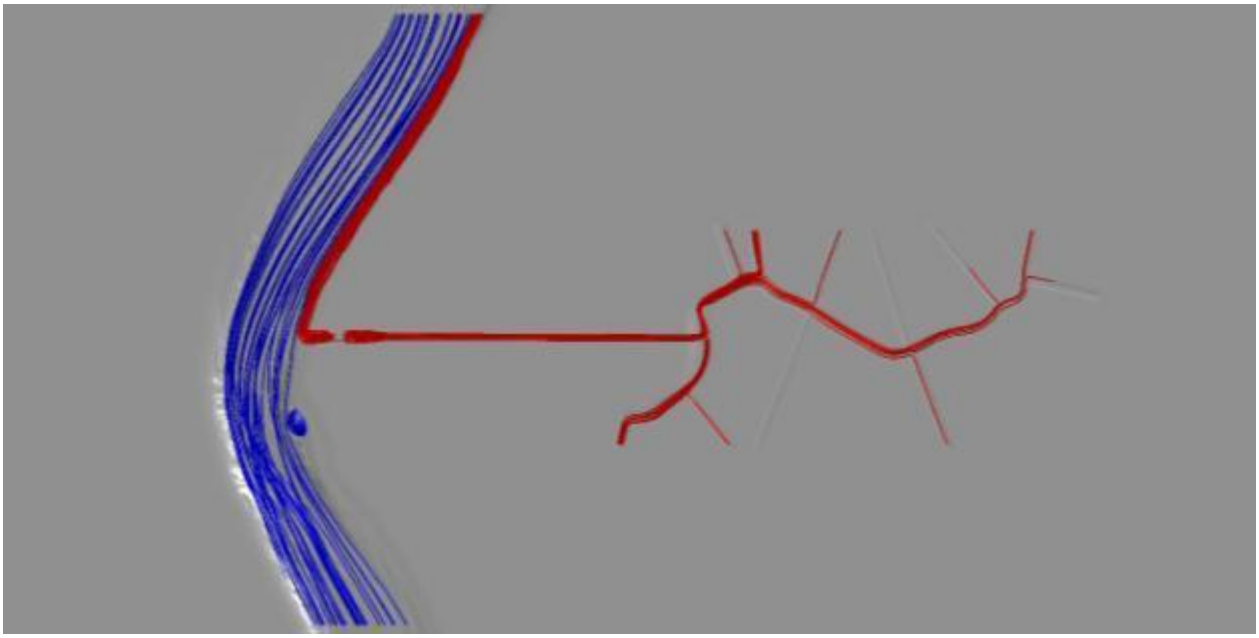

Figure A1–9. **Feasibility Study Recommended Design Analysis Model Results – Hydrodynamics: Streamlines Colored by Fate.**

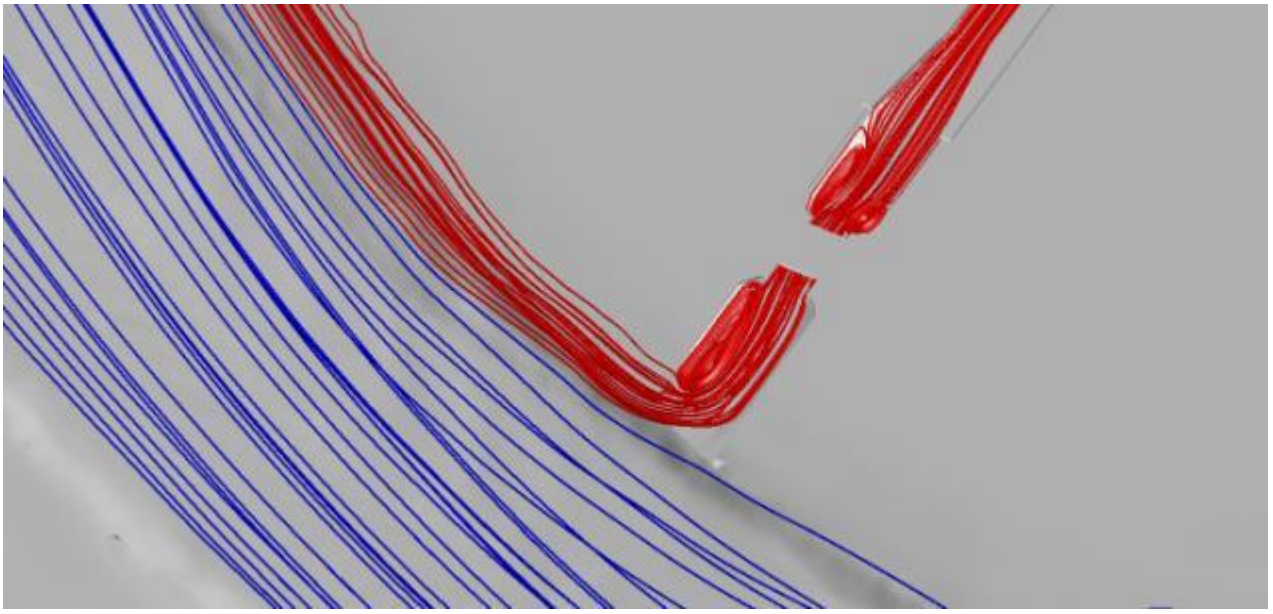

Figure A1–10. **Feasibility Study Recommended Design Model Results – Hydrodynamics: Flow Pattern at Diversion Structure (near surface, colored by fate).**

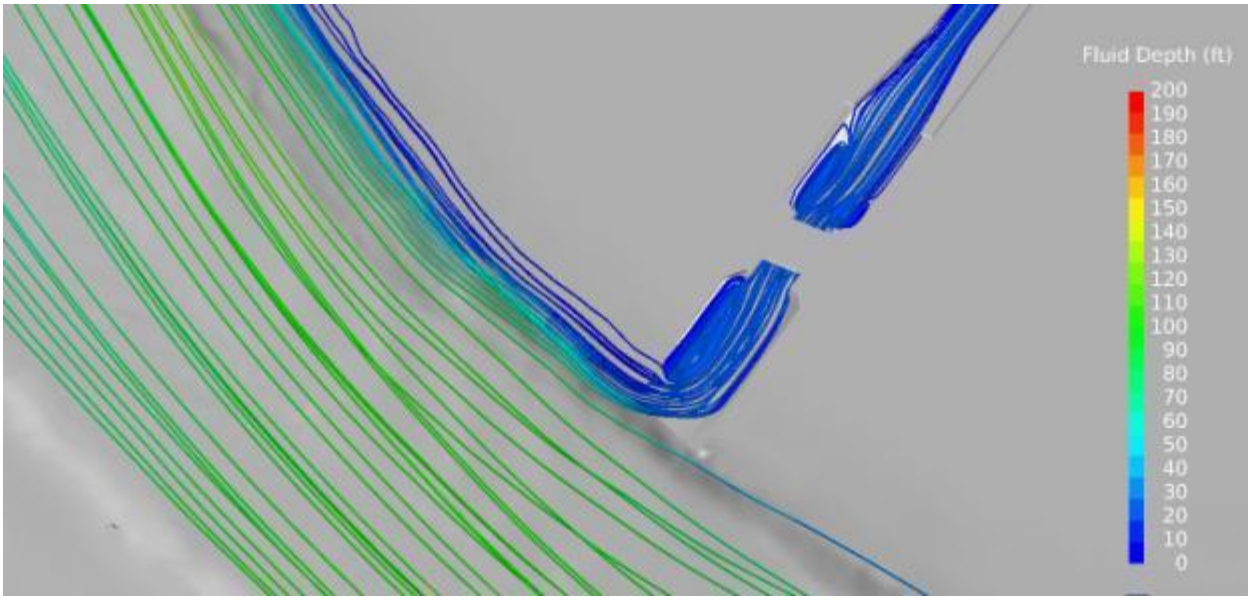

Figure A1–11. Feasibility Study Recommended Design Model Results – Hydrodynamics: Streamlines Colored by Fluid Depth.

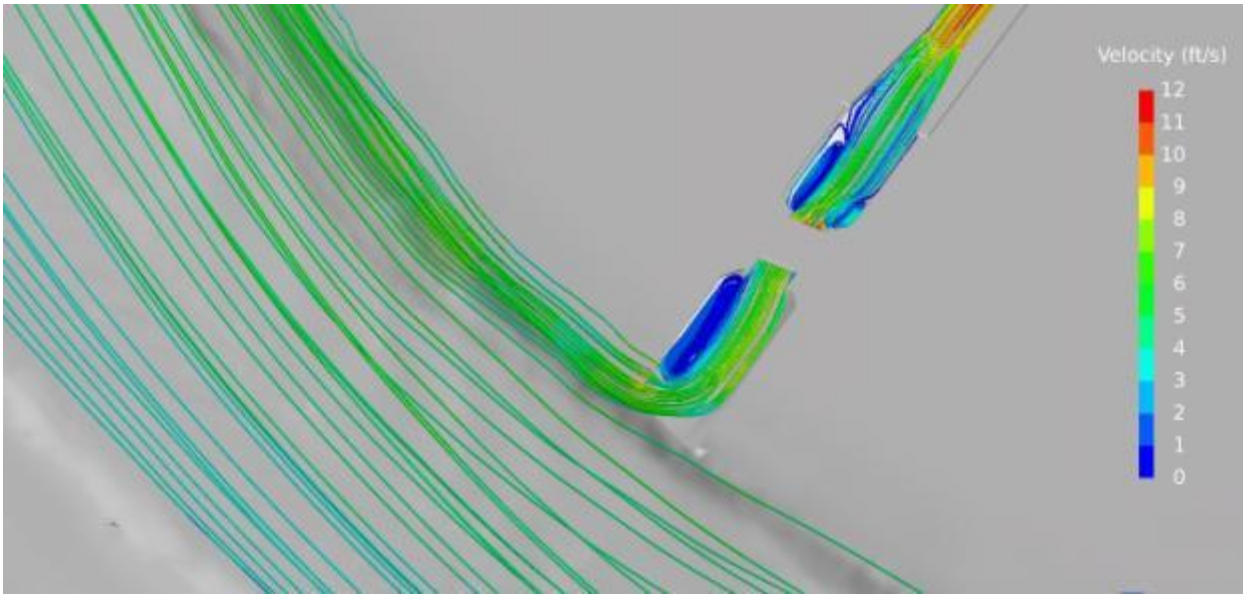

Figure A1–12. Feasibility Study Recommended Design Model Results – Hydrodynamics: Streamlines Colored by Speed.

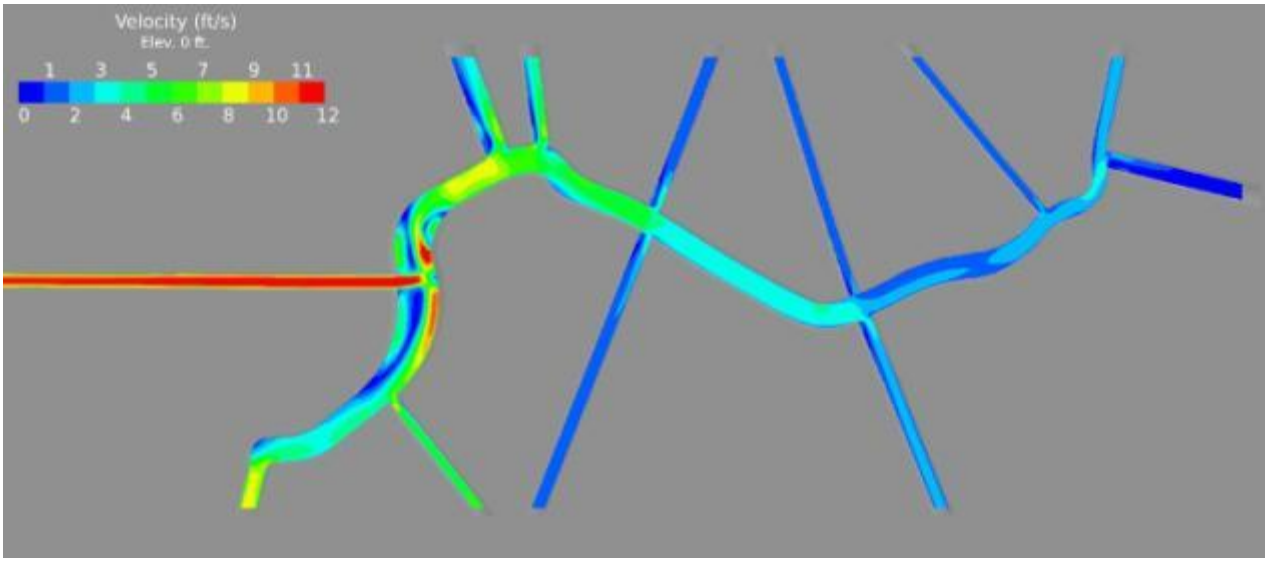

Figure A1–13. Feasibility Study Recommended Design Model Results – Hydrodynamics: Flow Pattern in Outflow Channels (near surface, colored by speed).

A.2 Design Alternative Analysis: Initial Domain Model

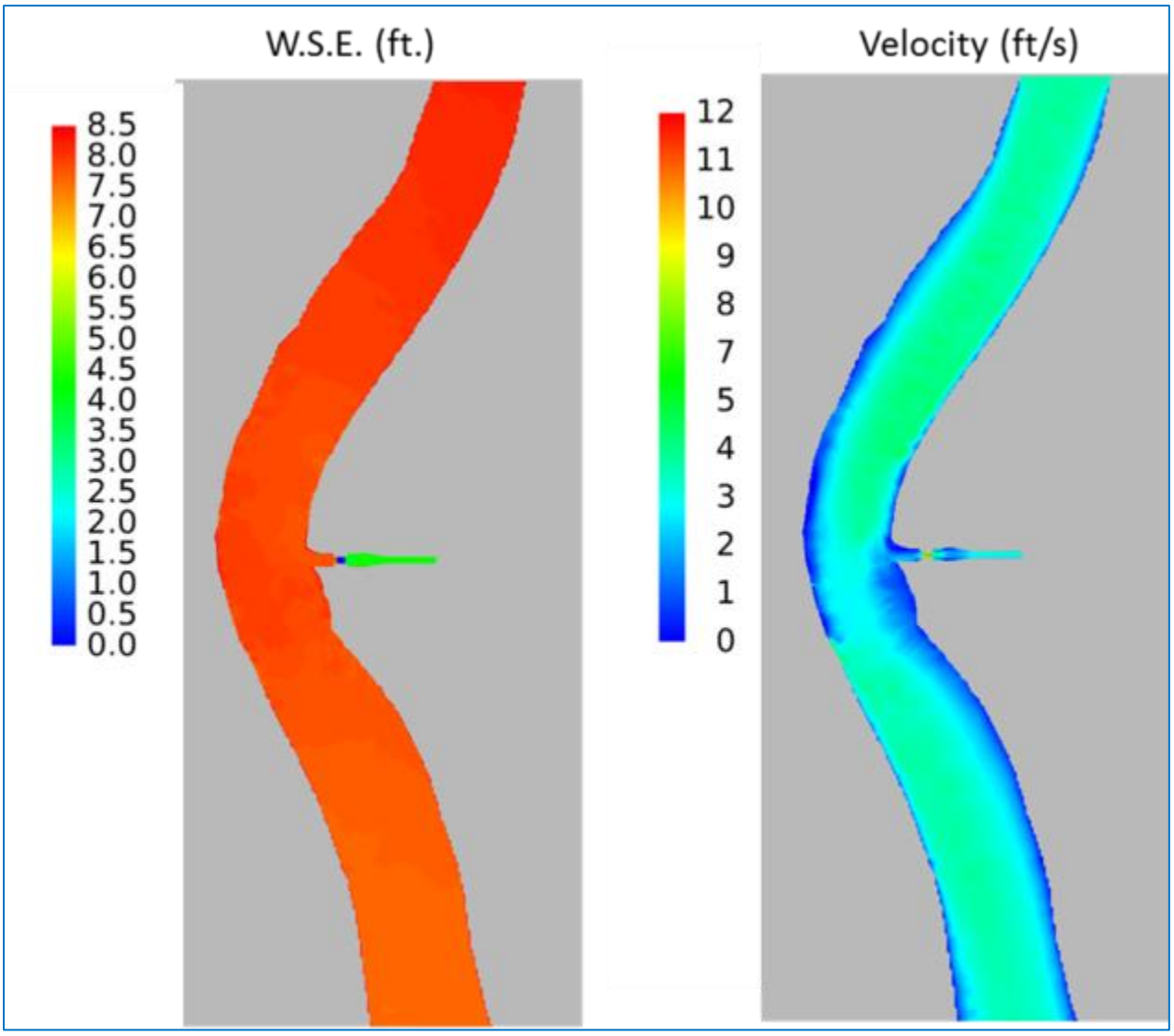

Figure A2–1. **Initial Domain Model Results, Location 3, Alternative B – Hydrodynamics: (Left) Water Surface (colored by elevation), (Right) Flow Speed Variation (near surface, colored by speed).**

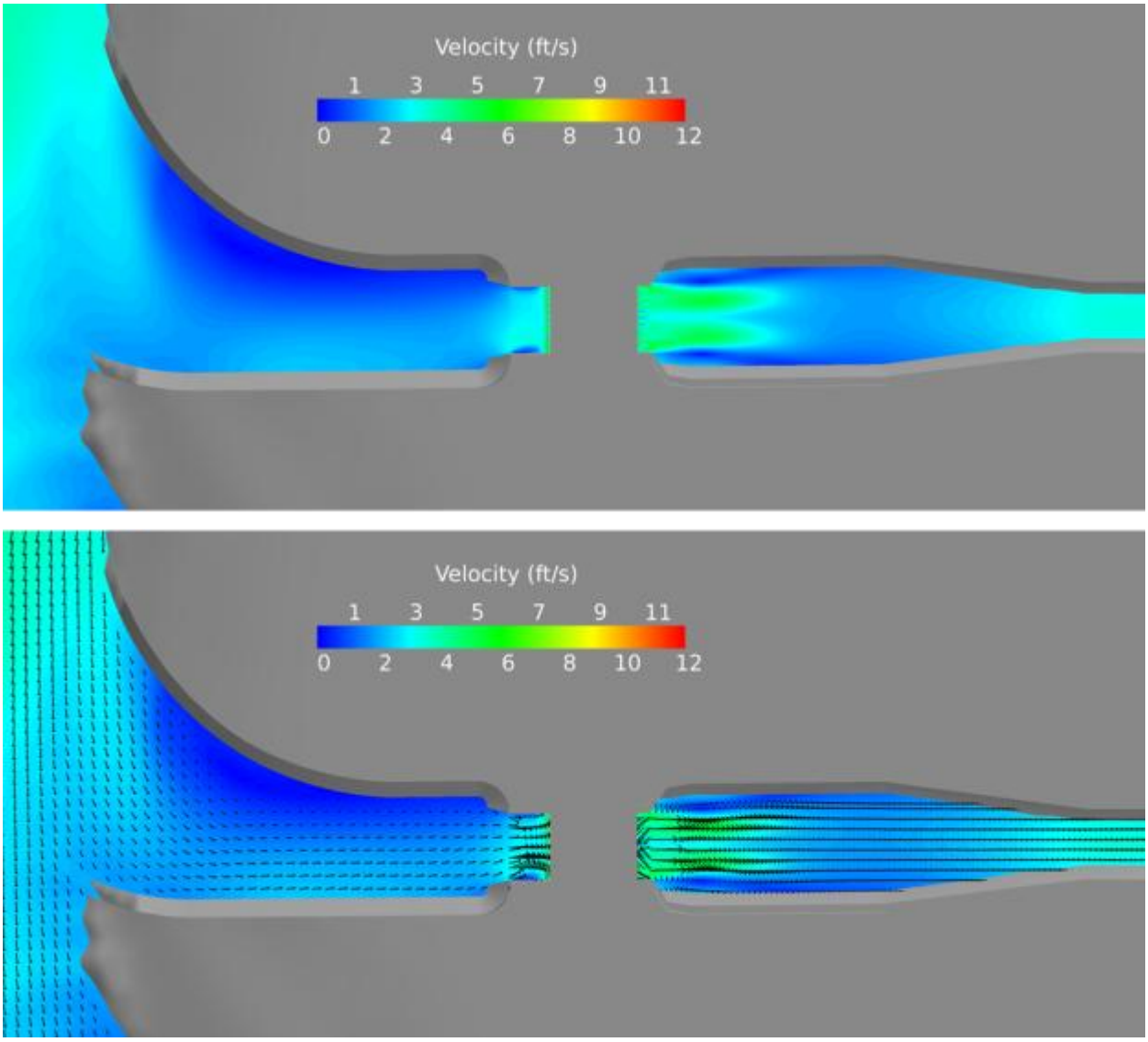

Figure A2–2. **Initial Domain Model Results, Location 3, Alternative B – Hydrodynamics: Flow Pattern at Diversion Structure (slice plane at elevation 0 foot NAVD88, colored by speed).**

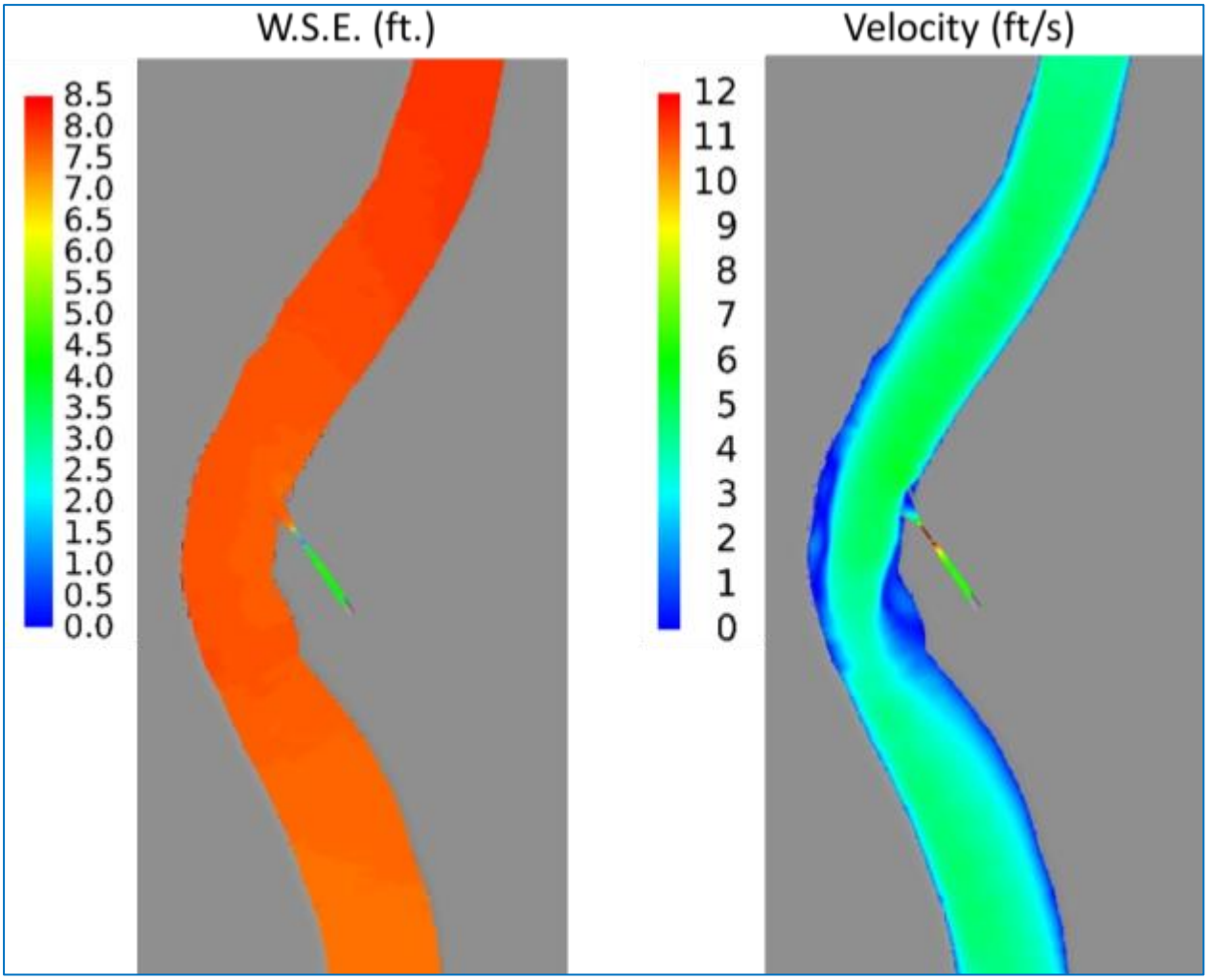

Figure A2–3. **Initial Domain Model Results, Location 3, Alternative C – Hydrodynamics: (Left) Water Surface (colored by elevation), (Right) Flow Speed Variation (near surface, colored by speed).**

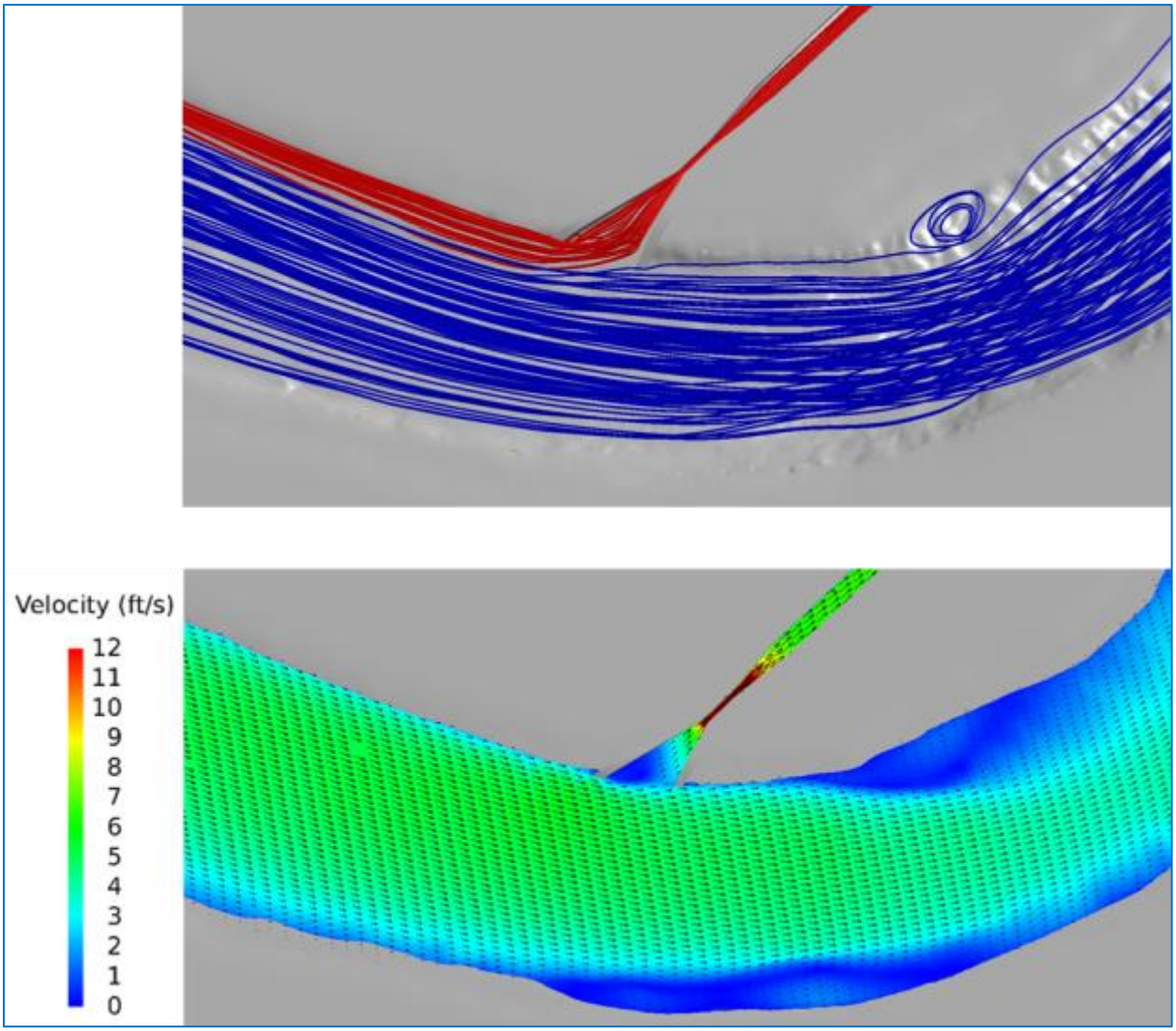

Figure A2–4. **Initial Domain Model Results, Location 3, Alternative C – Hydrodynamics: (Top) Streamlines colored by fate, (Bottom) Flow Pattern at Diversion Structure (slice plane at elevation 0 foot NAVD88, colored by speed).**

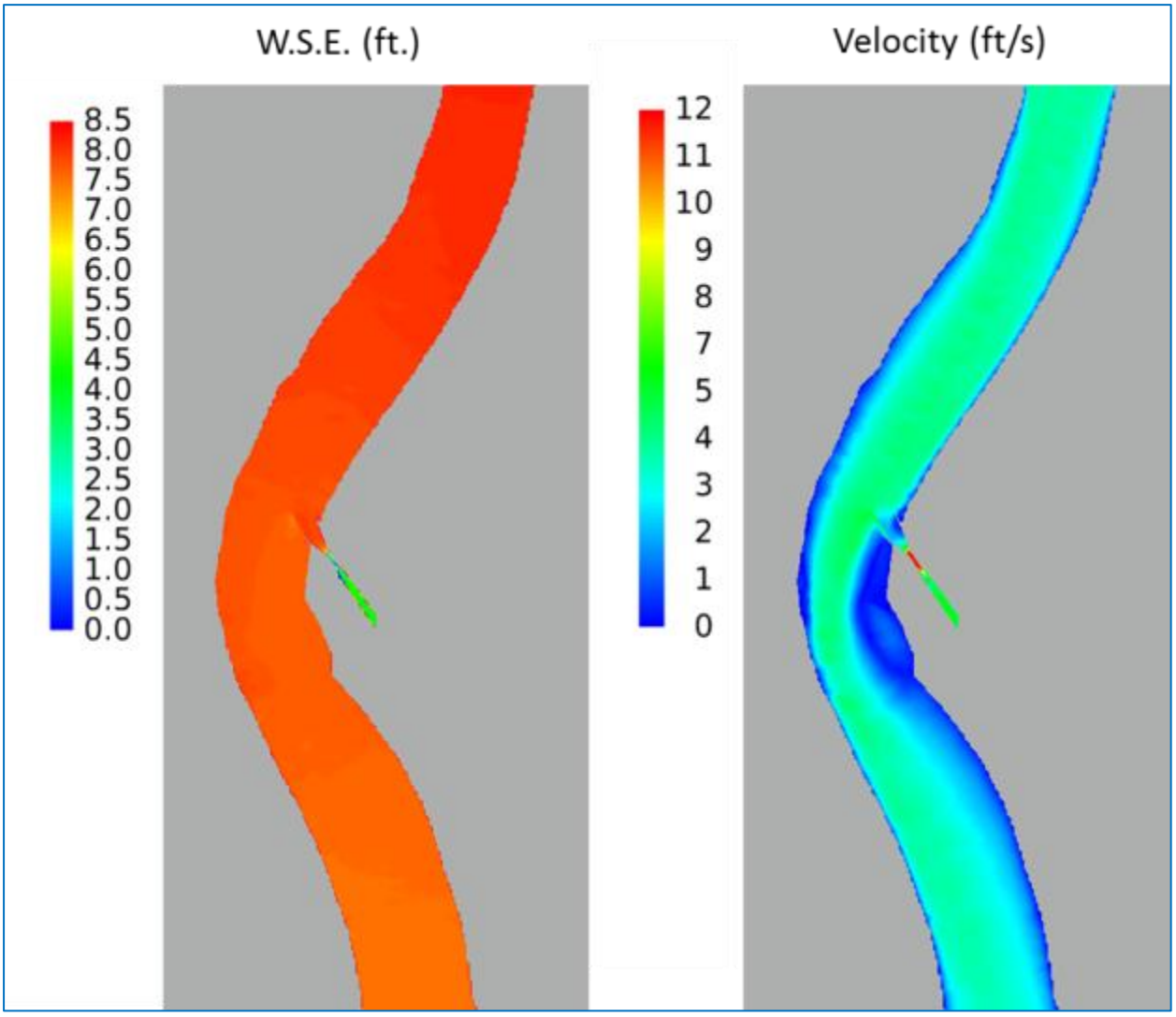

Figure A2–5. **Initial Domain Model Results, Location 3, Alternative D – Hydrodynamics: (Left) Water Surface (colored by elevation), (Right) Flow Speed Variation (near surface, colored by speed).**

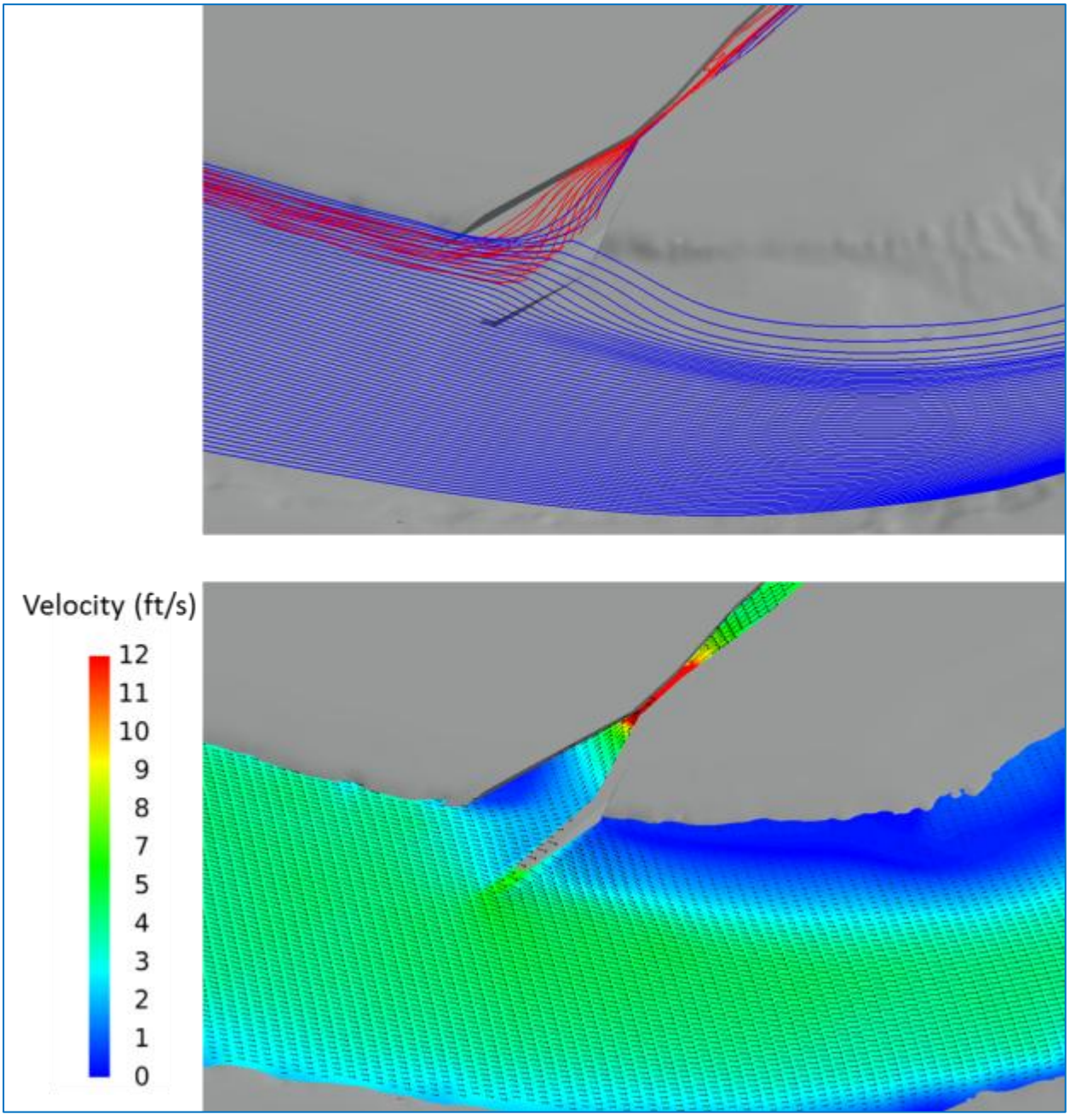

Figure A2–6. **Initial Domain Model Results, Location 3, Alternative D – Hydrodynamics: (Top) Streamlines colored by fate, (Bottom) Flow Pattern at Diversion Structure (slice plane at elevation 0 foot NAVD88, colored by speed).**

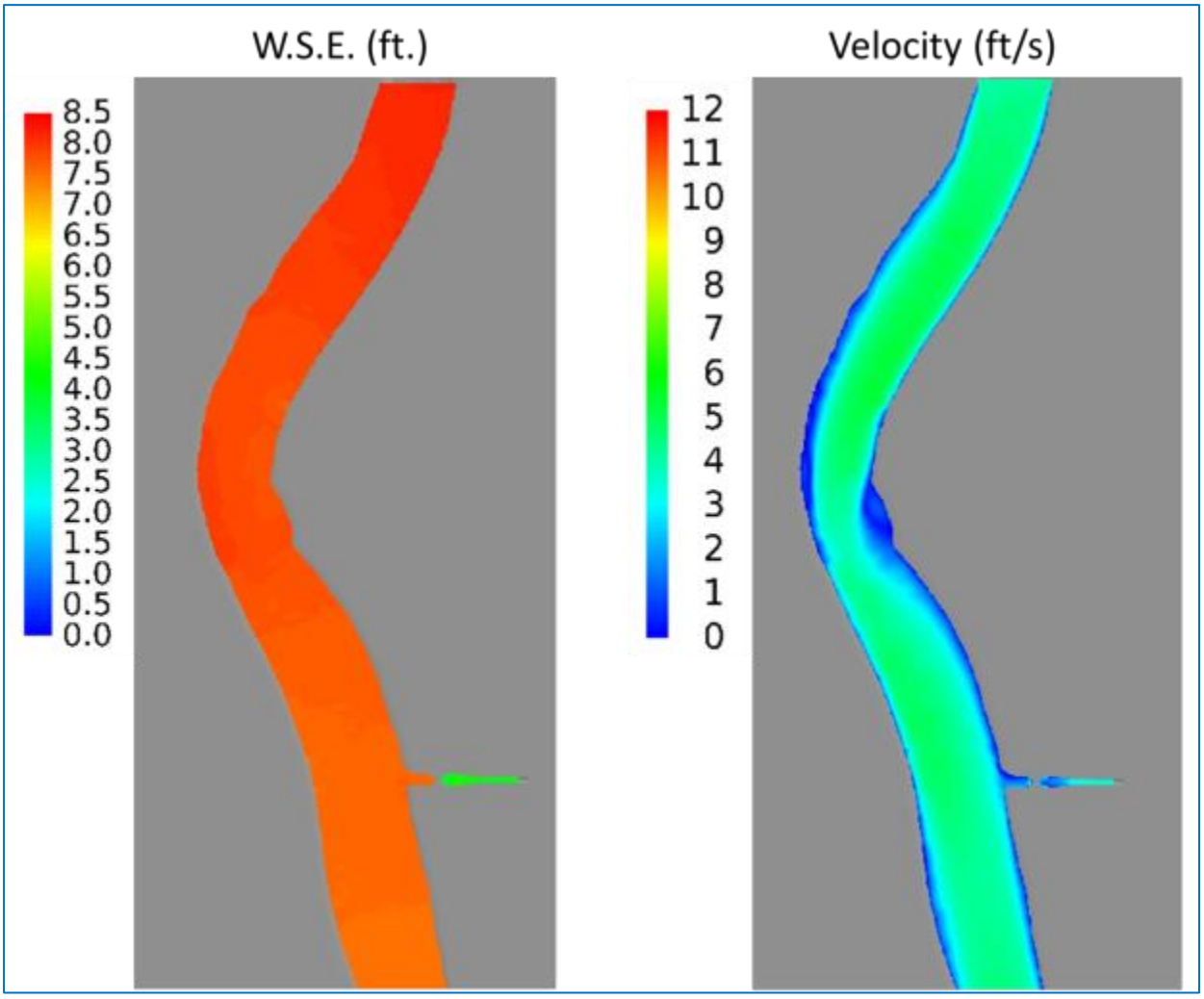

Figure A2–714. Initial Domain Model Results, Location 4, Alternative E – Hydrodynamics: (Left) Water Surface (colored by elevation), (Right) Flow Speed Variation (near surface, colored by speed).

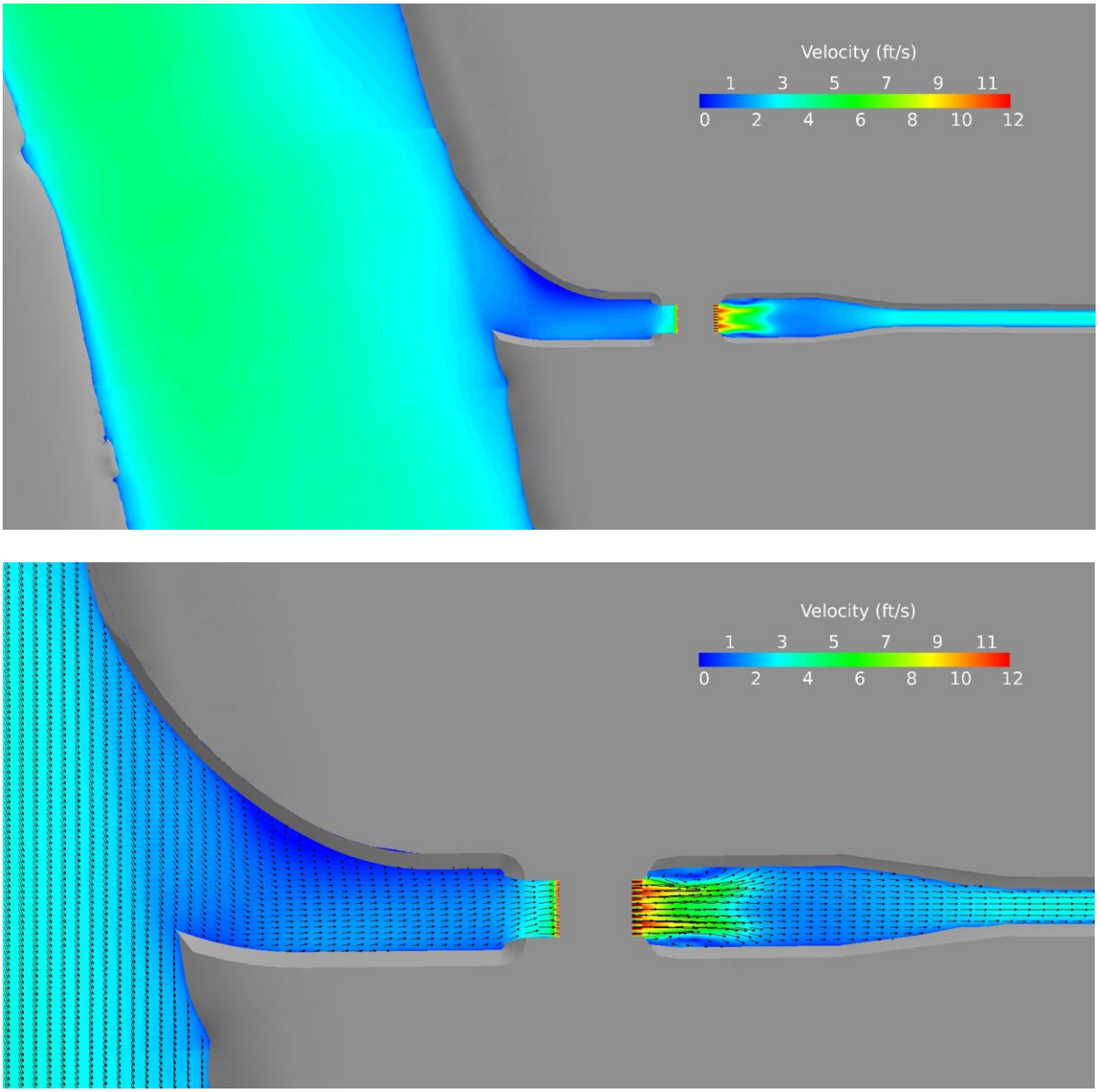

Figure A2–8. **Initial Domain Model Results, Location 4, Alternative E – Hydrodynamics: Flow Pattern at Diversion Structure (slice plane at elevation 0 foot NAVD88, colored by speed).**

A.3 Design Alternative Analysis: Extended Domain Model

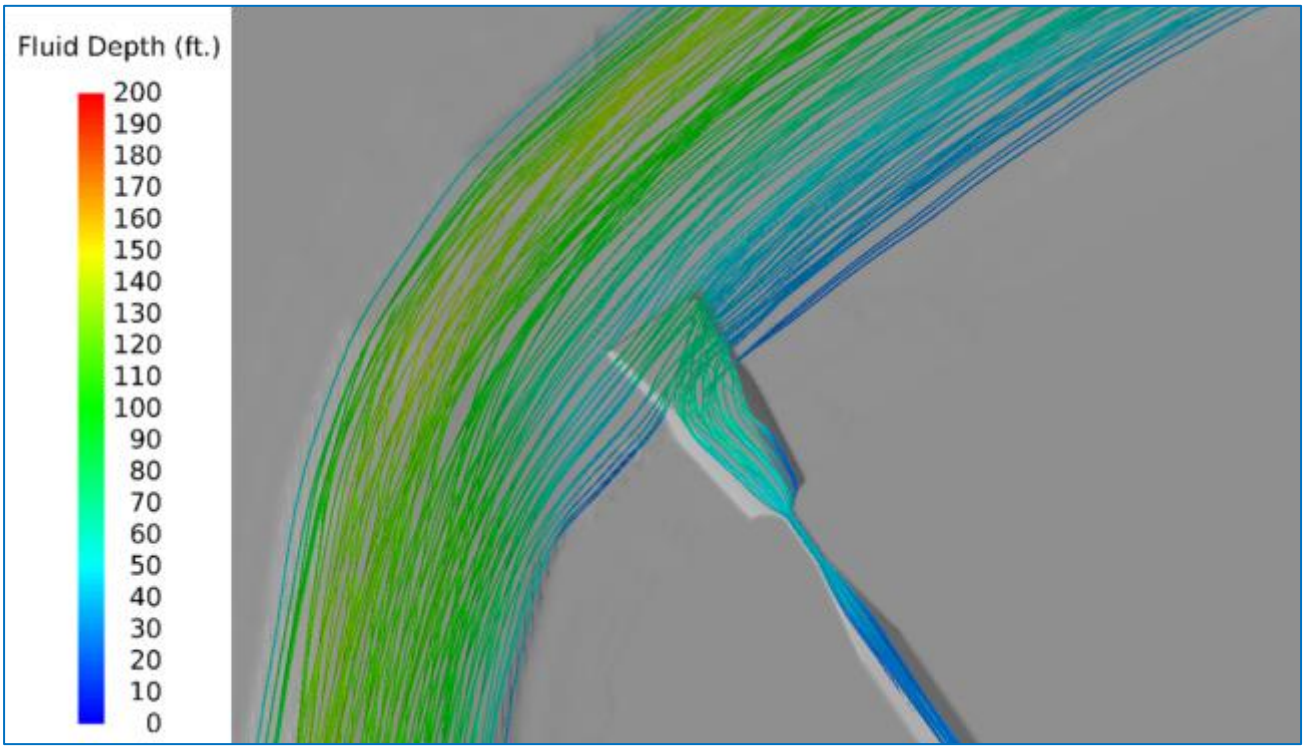

Figure A3–1. Extended Domain Model Results, Location 1, Alternative G – Hydrodynamics: Streamlines Colored by Fluid Depth.

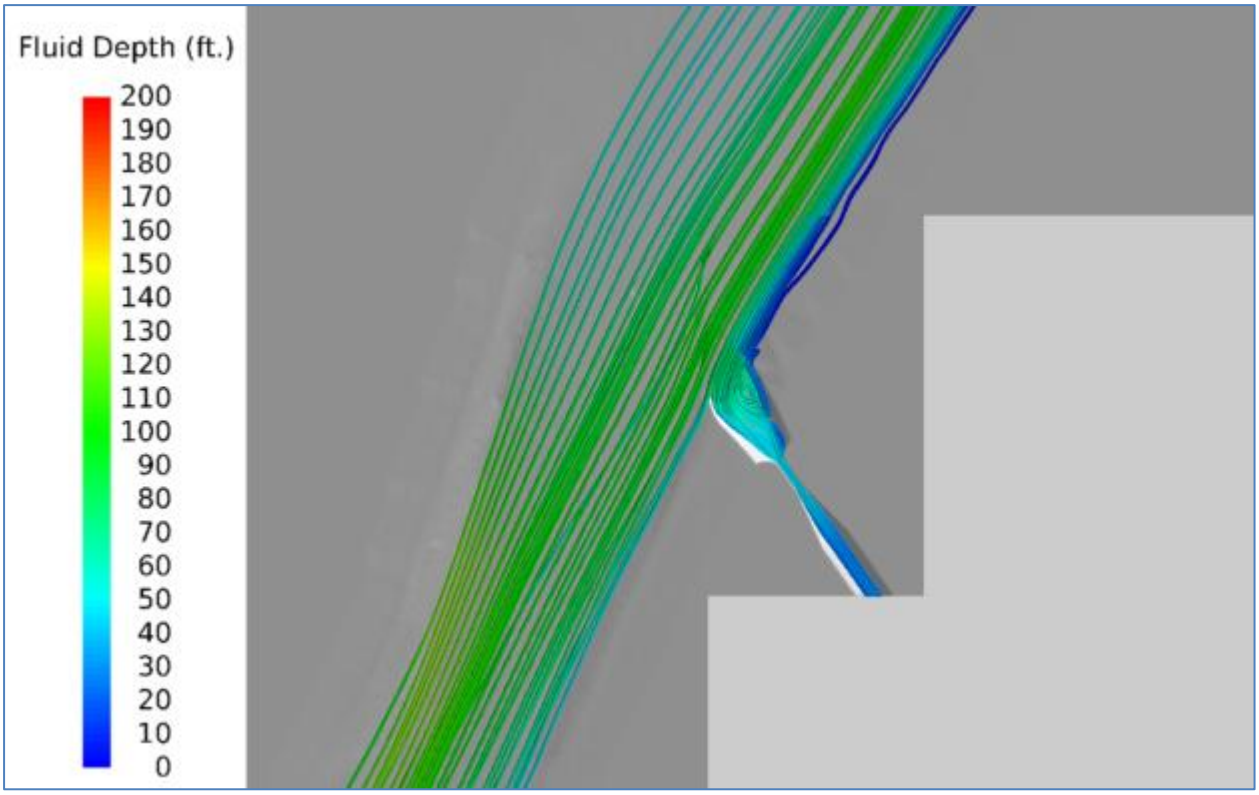

Figure A3–2. Extended Domain Model Results, Location 2, Alternative F – Hydrodynamics: Streamlines Colored by Fluid Depth.

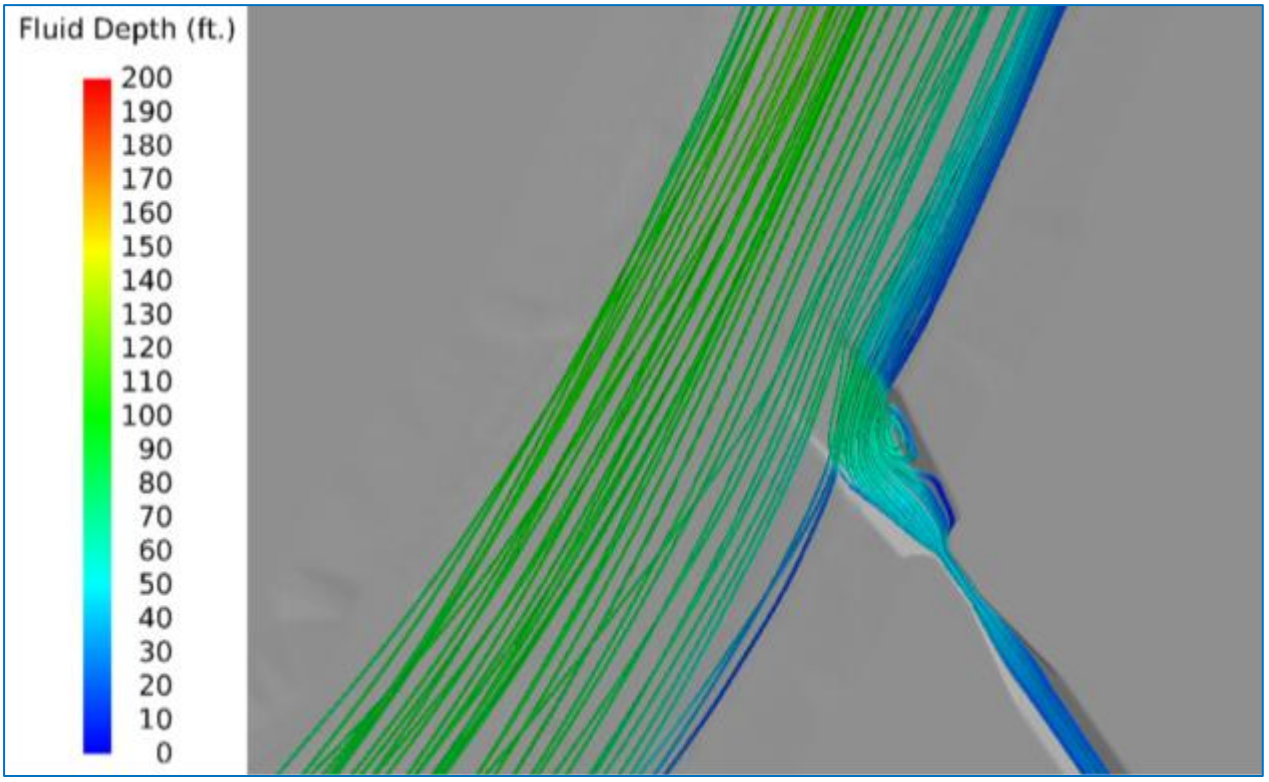

Figure A3–3. Extended Domain Model Results, Location 2.5, Alternative F – Hydrodynamics: Streamlines Colored by Fluid Depth.

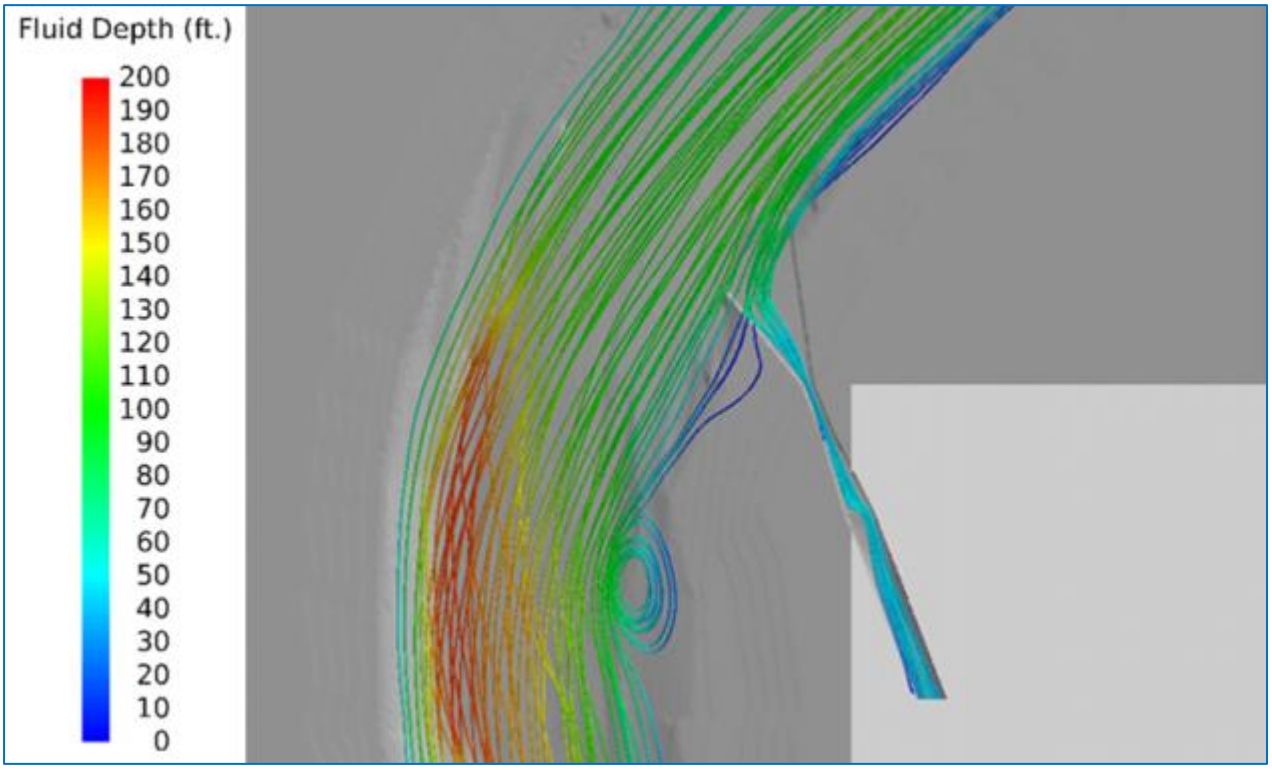

Figure A3–4. Extended Domain Model Results, Location 3, Alternative F – Hydrodynamics: Streamlines Colored by Fluid Depth.

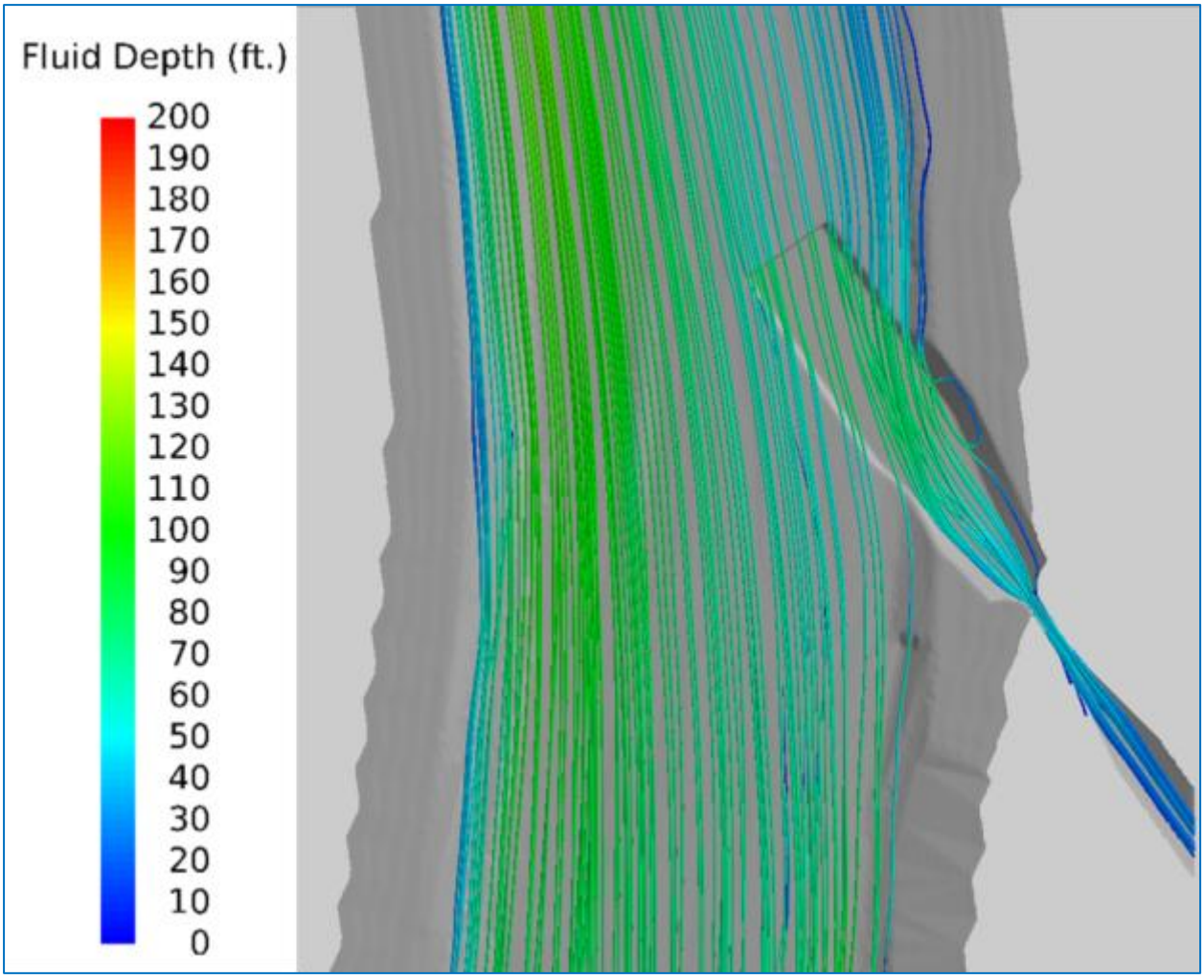

Figure A3–5. **Extended Domain Model Results, Location 4, Alternative F – Hydrodynamics: Streamlines Colored by Fluid Depth,**

A.4 Culvert Flow Calculation

Hand Calculation

In order to provide a guide for the results received from the ***FLOW-3D*** model, two different hand calculations were performed in order to gauge the results. While these calculations do not attempt to provide nearly the level of accuracy that is achieved in the ***FLOW-3D*** model, they do provide a basis for comparison to see if ***FLOW-3D*** is returning results in the correct range.

Energy Method

The first set of calculations performed involved using an energy balance method. A schematic of a single culvert is pictured in Figure A4–26. This representative culvert represents one of ten which are represented in the ***FLOW-3D*** model and, for the purposes of this calculation, all culverts are assumed to have identical flow through them.

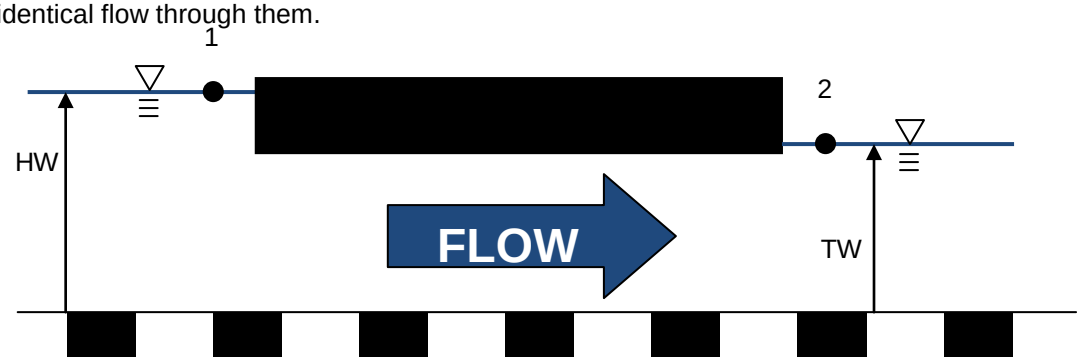

Figure A4–1. Diagram of the Idealized Setup

The known values are summarized below, along with a description of each and the value applied in this calculation.

Parameter	Description
HW	Head Water – elevation of water at entrance to culvert (6.73ft)
TW	Tail Water – elevation of water at exit of culvert (5.41ft)
H_L	Head loss
W	Width of culvert (15.0)
L	Length of culvert (230.42ft)
E	Height of culvert (15.0)
n	Manning's *n* (0.012-0.015)
K_e	Coefficient of entrance loss (0.7)
R_h	Hydraulic Radius
v_e	Velocity at entrance
v_o	Velocity at exit

First, a representation of the relationship between head water and tail water must be derived for this case.

$$H_L = H_e + H_o + H_f$$
$$H_L = \left(\frac{K_e v_e^2}{2g}\right) + \left(\frac{v_e^2}{2g} - \frac{v_o^2}{2g}\right) + \left[\left(\frac{29n^2L}{R_h^{1.33}}\right)\left(\frac{v_e^2}{2g}\right)\right]$$

Assuming that $v_e = v_0$, and no exit losses, the equation becomes:

$$H_L = \left[K_e + \left(\frac{29n^2L}{R_h^{1.33}}\right)\right]\left(\frac{v_e^2}{2g}\right)$$
$$HW - TW = \left[K_e + \left(\frac{29n^2L}{R_h^{1.33}}\right)\right]\left(\frac{v_e^2}{2g}\right)$$

Solving for the hydraulic radius, R_h yields:

$$R_h = \frac{(W)(E)}{2W + 2E} = 3.75\ ft.$$

Finally, a representative manning's n was chosen by taking an average value from the range prescribed in Chow (1959). The value used for this calculation is 0.013. Using the information derived, the velocity is solved for:

$$HW - TW = \left[K_e + \left(\frac{29n^2L}{R\pi^{1.33}}\right)\right]\left(\frac{v_e^2}{2g}\right)$$
$$22.72 - 21.41 = \left[0.7 + \left(\frac{29(0.0135)^2(233.82)}{3.75^{1.33}}\right)\right]\left(\frac{v_e^2}{(2)(32.2)}\right)$$
$$v_e = 9.64\ {}^{ft}/_{s}$$

With the velocity known, the flow rate through a single culvert is simply computed as:

$$Q_1 = Av_e = 2{,}166\ {}^{ft^3}/_{s}$$

Therefore, the total flow rate through 10 culverts is:

$$Q_{10} = 21{,}660\ {}^{ft^3}/_{s}$$

First, a representation of the relationship between head water and tail water for 35,000 cfs must be derived for this case.

$$H_L = H_e + H_o + H_f$$

$$H_L = \left(\frac{K_e v_e^2}{2g}\right) + \left(\frac{v_e^2}{2g} - \frac{v_o^2}{2g}\right) + \left[\left(\frac{29n^2L}{R_h^{1.33}}\right)\left(\frac{v_e^2}{2g}\right)\right]$$

Assuming that $v_e = v_0$, and no exit losses, the equation becomes:

$$H_L = \left[K_e + \left(\frac{29n^2L}{R_h^{1.33}}\right)\right]\left(\frac{v_e^2}{2g}\right)$$

$$HW - TW = \left[K_e + \left(\frac{29n^2L}{R_h^{1.33}}\right)\right]\left(\frac{v_e^2}{2g}\right)$$

Solving for the hydraulic radius, R_h yields:

$$R_h = \frac{(W)(E)}{W + 2E}$$

Finally, a representative manning's n was chosen by taking an average value from the range prescribed in Chow (1959). The value used for this calculation is 0.0135. Using the information derived, the velocity is solved for:

$$HW - TW = \left[K_e + \left(\frac{29n^2L}{R_h^{1.33}}\right)\right]\left(\frac{v_e^2}{2g}\right)$$

$$22.72 - 21.41 = \left[0.7 + \left(\frac{29(0.0135)^2(230.42)}{\left(\left(\frac{WE}{W+2E}\right)^{1.33}\right)}\right)\right]\left(\frac{v_e^2}{(2)(32.2)}\right)$$

$$1.31 = \left[0.7 + \left(\frac{1.217(W+2E)^{1.33}}{W^{1.33}E^{1.33}}\right)\right]\left(\frac{v_e^2}{64.4}\right)$$

$$v_e = sqrt\left(\frac{84.364}{\left[0.7 + \left(\frac{1.217(W+2E)^{1.33}}{W^{1.33}E^{1.33}}\right)\right]}\right)$$

$$Q = Av_e = WEv_e$$

For Q= 35,000 cfs, the equation becomes

$$35000 = sqrt\left(\frac{84.364}{\left[0.7 + \left(\frac{1.217(W+2E)^{1.33}}{W^{1.33}E^{1.33}}\right)\right]}\right)WE$$

At Width (W) =52.5 feet, by trial and error, the height and velocity of the culvert are calculated as:

$$E = 56\ ft.$$

$$v_e = 12\ {}^{ft}/_{s}$$

With the velocity known, the flow rate through a single culvert is simply computed as:

$$Q_1 = Av_e = 2{,}166.90\ {}^{ft^3}/_{s}$$

Therefore, the total flow rate through ten culverts is:

$$Q_{10} = 21{,}669.0\ {}^{ft^3}/_{s}$$

HY-8 Software

HY-8 is a culvert hydraulic analysis tool developed by the Federal Highway Administration (FHWA). The software is intended to aid in the design of culverts and is primarily based upon the FHWA white papers HDS-05 (Hydraulic Design of Highway Culverts, Third Edition) and HEC-14 (Hydraulic Design of Energy Dissipators for Culverts and Channels), which are both available on the FHWA website as published documents.

Much like the previous setup, an idealized condition is considered using a single culvert instead of ten. It is assumed that each culvert receives approximately equal flow. One advantage of this software over the previously introduced calculation is that exit losses are included.

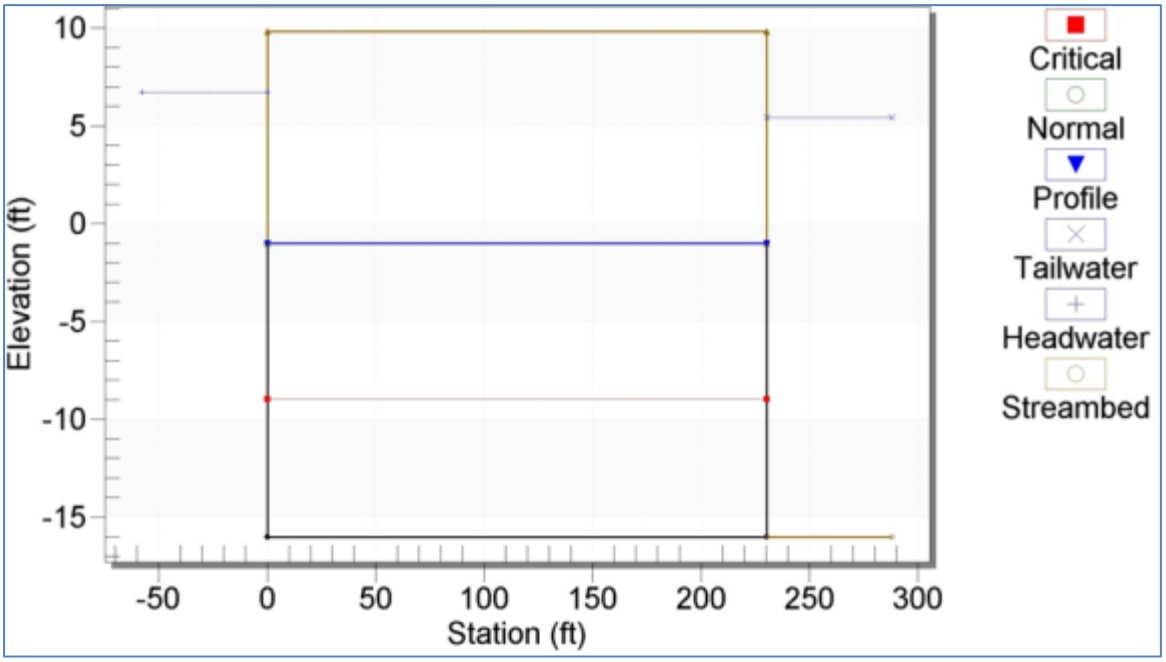

Figure A4–2. Diagram of HY-8 Representation of a Single Culvert

The assumptions made in the setup of the HY-8 calculation are:

1. The tail water elevation is approximately constant, representing a large bay/estuary
2. The tail water velocity is approximately zero, again, representing emptying into a large body of water
3. The culvert is calculated approximating a rectangular box culvert
4. There culvert cannot be overtopped under these flow conditions
5. The culvert is specified with a square edge (90 degree) headwall, assuming that the culvert specified is in the middle of the modeled culverts
6. There is no change in stream bed elevation between the inlet and outlet

In this case, the headwater elevation and tail water elevations are forced to match the ***FLOW-3D*** model data at the inlet and outlet of the culverts. The calculation is summarized in the table below.

Total Discharge (cfs)	Headwater Elevation (ft)	Outlet Depth (ft)	Outlet Velocity (ft/s)	Tail Water Velocity (ft/s)
1,589.16	6.73	5.41	7.07	0.00

Therefore, the HY-8 calculation yields an approximate discharge of 15,891.60 cfs for the ten culverts included in the ***FLOW-3D*** model.